GENETIC REGULATION OF CELL FATE DECISIONS IN THE DEVELOPING RETINA

by

Zixuan Li

A thesis submitted in partial fulfillment of the requirements for the degree of

Master of Science

Medical Sciences - Medical Genetics

University of Alberta

Abstract

Rationale: The *Dlx1/Dlx2* double knockout (DKO) mouse demonstrates major defects during retina development including significantly reduced number of retinal ganglion cells (RGCs) due to enhanced apoptosis of RGCs and consequently thinning of the optic nerve. In addition, the *Dlx1/Dlx2* DKO mouse has increased expression of *Otx2* and ectopic expression of *Crx* in the ganglion cell layer (GCL). *Crx*, the cone and rod photoreceptor homeobox gene, is a gene required for photoreceptor development. *Otx2*, the orthodenticle homeobox2 gene, belongs to the same transcription factor family as *Crx* and is a major determinant of photoreceptor specification. *Otx2* has been shown to be bound by DLX2 *in vivo*. The *Dlx1/Dlx2* DKO retina phenotype indicates that the cell fate of uncommitted retina progenitor cells (RPCs) may be altered. This suggests that *Dlx* genes may play a role in mediating cell fate decisions between retinal ganglion cells and photoreceptor cells in the developing retina.

Hypothesis: We hypothesize that OTX2 represses the acquisition of retinal ganglion cell fate in retinal progenitor cells by directly repressing *Dlx1/Dlx2* transcription, which is essential for retinal ganglion cell differentiation. The goal is to determine whether OTX2 represses retinal ganglion cell fate by repressing *Dlx2* expression.

Methods: Electrophoretic mobility shift assays were conducted to determine if OTX2 directly binds candidate regulatory subregions *in vitro*. Chromatin immunoprecipitation with a polyclonal OTX2 antibody was performed on chromatin isolated from E18.5 mouse retinal tissues to determine whether OTX2 occupied candidate EMSA-positive candidate regulatory subregions *in vivo*. Luciferase reporter assays were performed to determine whether OTX2 binding to candidate *Dlx1/Dlx2* regulatory subregions affects reporter gene transcriptional

expression *in vitro*. Histology and immunofluorescence using polyclonal DLX2 antibody was performed to compare retina morphology and DLX2 protein expression in *Otx2* heterozygous mutant ($Otx2^{+/GFP}$) and wildtype P100 retina.

Results: We discovered that 10kb upstream of the *Dlx2* and *Dlx1* promoter region and the *Dlx1/Dlx2* intergenic region contain multiple candidate homeodomain binding sites for OTX2. Electrophoretic mobility shift assays demonstrated that recombinant OTX2 specifically and directly bound multiple binding sites upstream the *Dlx2* promoter, in the *Dlx1/Dlx2* intergenic region, and upstream the *Dlx1* promoter *in vitro*. OTX2 also occupied several of these regulatory subregions upstream the *Dlx2* promoter, as well as the *Dlx1/Dlx2* intergenic enhancer, *I12a in vivo*. Luciferase reporter assays demonstrated that co-expression of OTX2 and *Dlx2* regulatory subregions regulates reporter transcription both positively and negatively *in vitro*. Luciferase reporter assays demonstrated that OTX2 activates reporter gene transcription via the *I12a* intergenic enhancer and a proximal regulatory subregion upstream the *Dlx2* promoter. OTX2 may also repress reporter gene transcription via a distal regulatory subregion upstream the *Dlx2* promoter. The heterozygous *Otx2* mutant retina may have an expansion of the retinal ganglion cell layer and a thinning of the inner nuclear layer. We also observed that DLX2 expression-domain may expand in the heterozygous *Otx2* mutant retina.

*Conclusions: T*hese results suggest that OTX2 may regulate *Dlx2* both positively and negatively during retina development which is partially consistent with our hypothesis that OTX2 represses retinal ganglion cell differentiation genes such as *Dlx2* to promote the acquisition of photoreceptor cell fate. Furthermore, OTX2 may also activate *Dlx2* to facilitate developmental programing in other cell type precursors.

Preface

This thesis is an original work by Zixuan (Christie) Li. Chapter 1 contains some material that has been drafted in a manuscript for publication.

All animal experiments received ethics approval from the University's Animal Care and Use Committee (ACUC): protocol number AUP 0001115.

Some E13.5 frozen cryosections used for immunofluorescence experiments were prepared by Dr. Jamie Zagozewski, a former graduate student in the Eisenstat laboratory.

Recombinant OTX2 protein and *Otx2*$^{+/GFP}$ mouse eye tissues were kindly provided by Dr. Kenneth Moya. OTX2 expression vector for *in vitro* experiments was kindly provided by Dr. Thomas Lamonerie.

The research conducted in the Appendix is one portion of a collaboration project with Dr. Maryam Hejazi, a former graduate student in the Eisenstat laboratory and Dr. Pranidhi Baddam, a former graduate student in Dr. Daniel Graf's lab at the University of Alberta. qPCR gene expression studies and analysis were performed by Zixuan Li with the help of Dr. Pranidhi Baddam and Dr. Maryam Hejazi.

Acknowledgements

I thank my supervisors Dr. David Eisenstat and Dr. Fred Berry and my committee members Dr. Daniel Graf and Dr. Roseline Godbout for their patience and tireless support, guidance, and directions for my research.

I thank my lab mates, Mikaela Nevin and Maryam Hejazi for their technical assistance and proof-reading my thesis.

Mikaela: you are such a talented scientist! Thank you for all your help and explanation with my experiments and proofreading my thesis. Thank you so much for making all the delicious treats for the lab.

Maryam: you are one of the kindest and most caring people I have ever met. Thank you for helping me with the experiments in the lab and making me very welcomed when I first joined.

I want to thank my friends in the department and throughout graduate school. My graduate school experience would not be the same without you guys!

Asra: you are the big sister I never had. The care and love you have given to your friends are truly unique. I am lucky to have you as my friend. Thank you so much for all your advice. You are so hard-working!

Tamara: you are such a wonderful human being and one of the most hard-working and talented scientists I have ever met. Big sister, I am so grateful to have met you at the beginning of my MatCH rotation. I am thrilled to discover our shared love for Korean TV shows. Thank you so much for all your support and advice. Our dancing sessions were most unforgettable!

Pranidhi: you are a wonderful scientist. Thank you so much for your help with my experiments and suggestions for my projects. Thank you for your humor. Our get-togethers at FoMD TGIFs were the highlight of my graduate school experience.

Tejal: you are so lovely. I love that you are always keeping me updated with your adventures and dance moves. Watching your videos gave me a lot of joy! Thank you for your care!

Priyanka: although we have not as much time to hang out but I am very grateful for your support in the form of food always and I love hearing your stories from your various volunteer jobs

To all my other church friends and fellow Graduate Student Fellowship friends: Linda and Jacob, Lang Erin, Cherry, Jared and Alan. I am so grateful to have met such strong Christian scholars and friends. Thank you for the in-depth Bible studies, philosophical discussions, and fellowship over food and good company. I learnt so much from you guys.

I deeply thank my mom for her unconditional love and support. I also thank my mom's family in Qingdao, China, my aunts and uncle and my cousins who are always there to video-chat whenever needed.

I also want to thank my church family in Edmonton, my college roommate in Montreal and church family abroad in France and Taiwan for their guidance and support.

I thank our collaborators from France, Dr. Thomas Lamonerie and Dr. Kenneth Moya for providing me with reagents to carry out my experiments.

Table of Contents

List of Tables

List of Figures

List of Abbreviations and Symbols

µM, microliter

µM, micromolar

°C, degrees Celsius

BMP, bone morphogenic protein

cDNA, complementary deoxyribonucleic acid

ChIP, chromatin immunoprecipitation

CKO, conditional knockout

Crx, cone-rod homeobox (gene)

CRX, cone-rod homeobox (protein)

DAPI, 4', 6-diamidine-2-phenylindole

DKO, double knockout

Dlx2, Distal-less homeobox (gene)

DLX2, Distal-less homeobox (protein)

DMEM, Dulbecco's Modified Eagle Medium

dNTP, deoxyribonucleoside triphosphate

dATP, deoxyadenosine triphosphate

DTT, Dithiothreitol

E, embryonic day

EDTA, ethylenediaminetetraacetic acid

EFTF, eye field transcription factor

EMSA, electrophoretic mobility shift assay

ERG, electroretinogram

FBS, fetal bovine serum

FGF, fibroblast growth factor

GCL, ganglion cell layer

gDNA, genomic DNA

GFP, green fluorescent protein

H&E, haematoxylin and eosin

IF, immunofluorescence

iNBL, inner neuroblastic layer

INL, inner nuclear layer

IPL, inner plexiform layer

LB, lysogeny broth

NBL, neuroblastic layer

Nrp2, Neuropilin-2

OCT compound, optimal cutting temperature compound

OCT, optical coherence tomography

oNBL, outer neuroblastic layer

ONL, outer nuclear layer

OPL, outer plexiform player

Otx2, Orthodenticle homeobox 2 (gene)

OTX2, Orthodenticle homeobox2 (protein)

P, postnatal day

PBS, phosphate-buffered saline

PCR, polymerase chain reaction

PIC, protease inhibitor cocktail

PKC, protein kinase C

PMSF, phenylmethylsulfonyl fluoride

qRT-PCR, quantitative real-time polymerase chain reaction

R, subregion

RGC, retinal ganglion cell

RNA, ribonucleic acid

rOTX2, recombinant OTX2 protein

RPC, retinal progenitor cell

RPE, retinal pigmented epithelium

RPM, revolutions per minute

Shh, sonic hedgehog

SDS, sodium dodecyl sulfate

SKO, single knockout

TEMED, tetramethylethylenediamine

TGFβ, transforming growth factor beta

TSS, transcription start site

Wnt, wingless/int

WT, wildtype

Chapter 1: Introduction

1.1 Anatomy of the retina

The eye has multiple layers and the innermost layer that is responsible for detecting light and relaying those signals to the brain is called the retina, also referred to as the neural retina (**Figure 1.1**). The retina is also composed of multiple layers and multiple cell types. There are two plexiform layers where retinal neurons make connections. The outer plexiform layer (OPL) is where the photoreceptors make connections with bipolar cells and horizontal cells. The inner plexiform layer (IPL) is where the amacrine cells/bipolar cells make connections with retinal ganglion cells. The outer nuclear layer (ONL) is where cell bodies of the photoreceptors (rods and cones) are localized. The inner nuclear layer (INL) is composed of bipolar cells, horizontal cells and amacrine cells. The Müller glial cell bodies are also situated in the INL, and they extend their processes in either direction between the GCL and the ONL to support retinal neurons. The ganglion cell layer (GCL) is the innermost layer composed of ganglion cells and displaced amacrine cells.

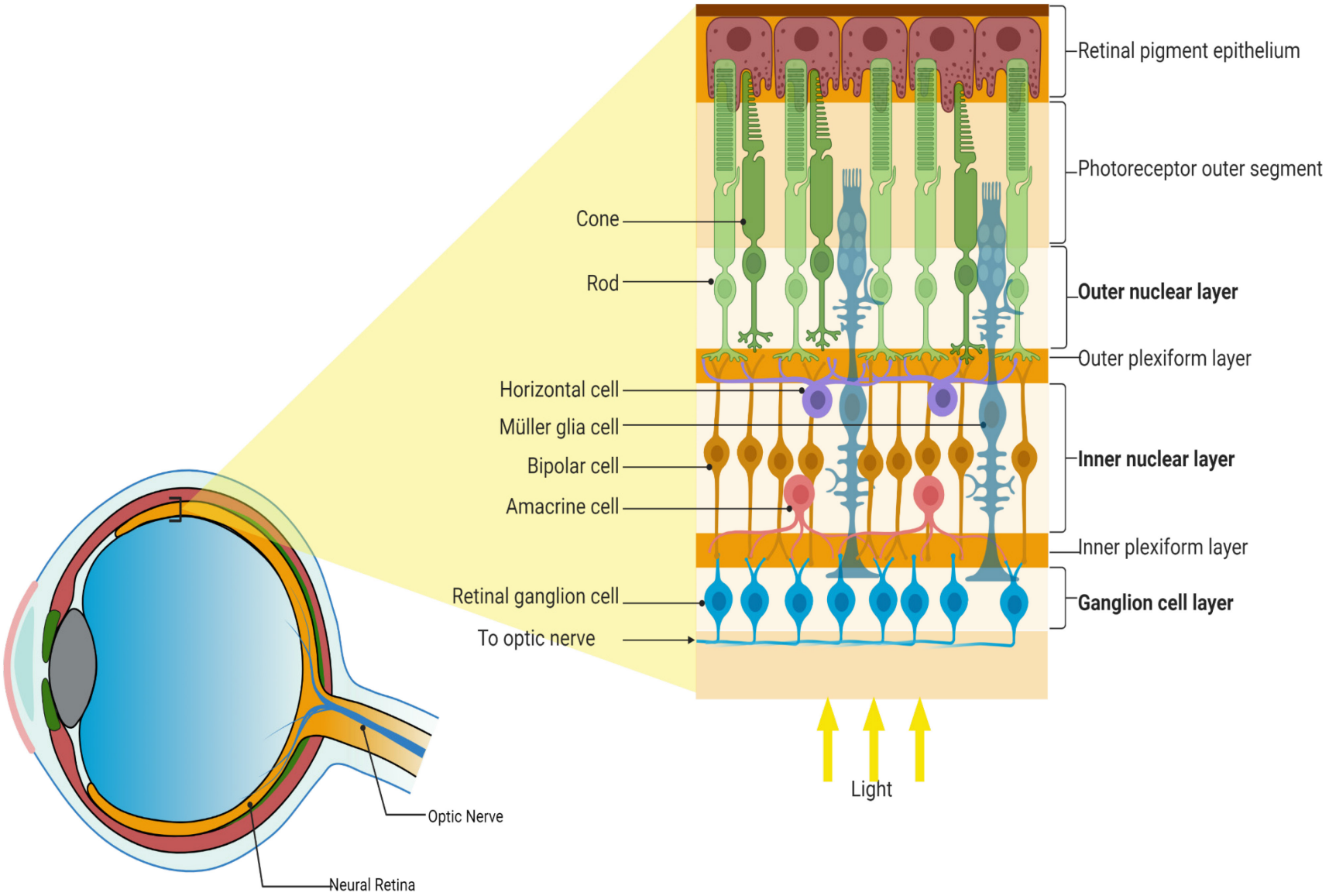
Retinal pigment epithelium
Photoreceptor outer segment
Cone
Rod
Outer nuclear layer
Outer plexiform layer
Horizontal cell
Müller glia cell
Bipolar cell
Amacrine cell
Inner nuclear layer
Inner plexiform layer
Retinal ganglion cell
To optic nerve
Ganglion cell layer
Light
Optic Nerve
Neural Retina

Figure 1.1

Laminar organization and cellular anatomy of the mature retina

The mature retina contains six layers including the innermost ganglion cell layer (GCL), inner plexiform layer (IPL), inner nuclear layer (INL), outer plexiform layer (OPL), outer nuclear layer (ONL), and retinal pigmented epithelium (RPE). The GCL contains retinal ganglion cells (RGCs) and displaced amacrine cells. The axons of RGCs form the optic nerve. The INL contains amacrine cells, bipolar cells and horizontal cells. The INL also contains the nuclei of the Müller glia cells while their cell bodies span between the ONL and the GCL. The IPL consists of synaptic connections made between the amacrine and bipolar cells to the RGCs. The OPL consists of synaptic connections made between the bipolar and horizontal cells to the photoreceptors. The ONL contains nuclei and cell bodies of the rod and cone photoreceptors. This figure was created with Biorender.com

1.2 Origin of the retina

The retina/retinal pigmented epithelium, and the lens are derived from two major embryonic sources: the neural ectoderm and the surface ectoderm respectively. The retina and the optic nerve are a part of the forebrain or the most rostral part of the brain. The retina arises from an early eye field which was derived from the anterior neural plate. Murine eye development initiates when the lateral walls (neural ectoderm) of the diencephalon begin to protrude at embryonic day (E) 8.5 (Graw, 2010) (**Figure 1.2**). They continue to enlarge to form the optic vesicles which extend laterally toward the overlying surface ectoderm and eventually give rise to the two eyes. The two optic vesicles are still connected to the forebrain via the optic stalk, which eventually becomes the optic nerve. Simultaneously, a part of the overlying surface ectoderm thickens to produce the lens placode at around E9.5(Graw, 2010). At around E10.5, the lens placode pushes into the underlying optic vesicles such that the optic vesicle folds into itself creating two nested cup shaped structure with two layers called the optic cup (Heavner & Pevny, 2012). The inner layer of the optic cup becomes the neural retina. The outer layer becomes the retinal pigment epithelium (RPE). From E10.5 onwards, the eye gradually forms, and the neural retina starts to differentiate. At E11.5, the lens pit eventually fully closes and detaches to form the lens vesicle (Raymond & Jackson, 1995).

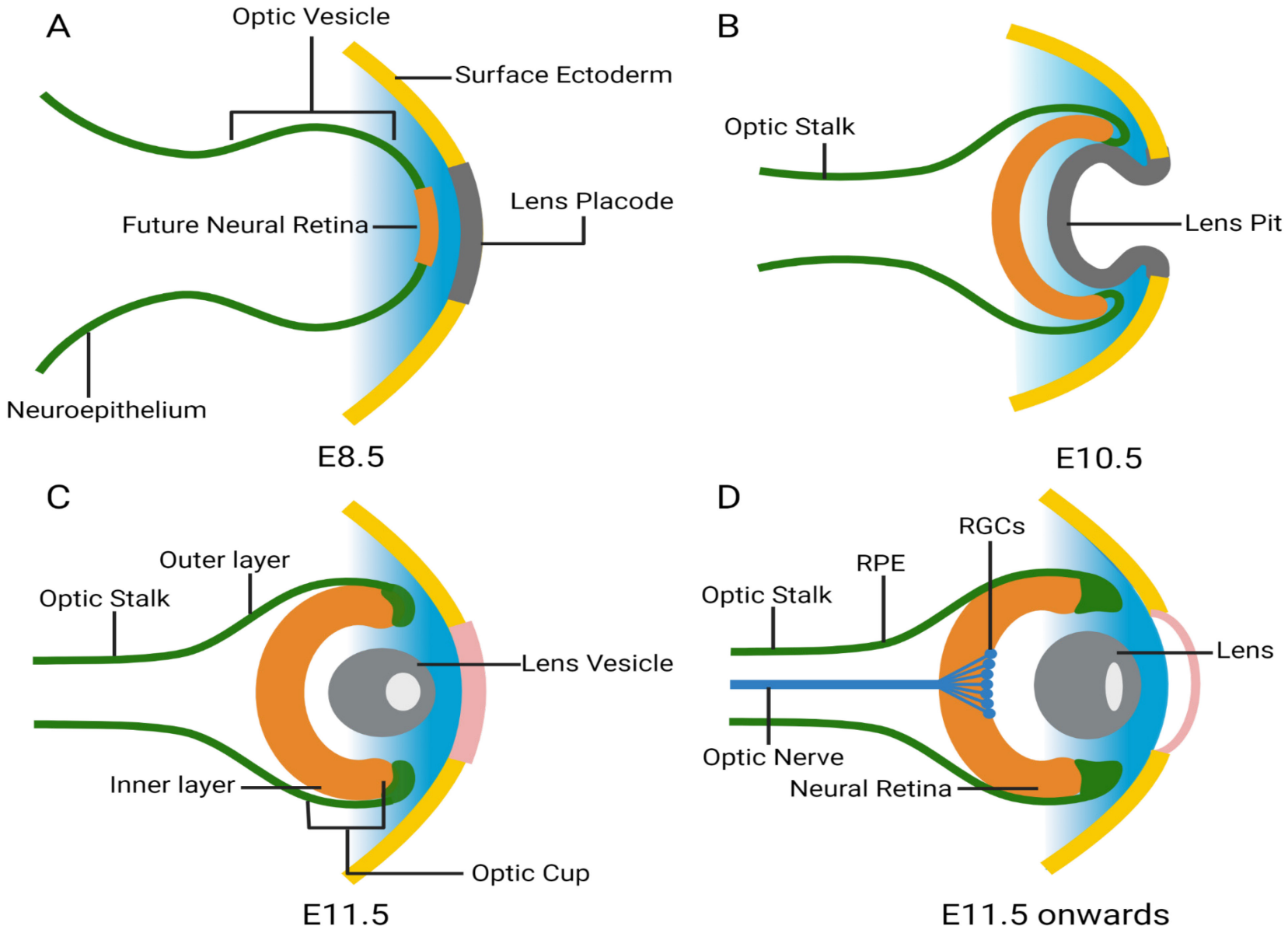
A
Optic Vesicle
Surface Ectoderm
Future Neural Retina
Lens Placode
Neuroepithelium
E8.5
B
Optic Stalk
Lens Pit
E10.5
C
Outer layer
Optic Stalk
Lens Vesicle
Inner layer
Optic Cup
E11.5
D
RGCs
RPE
Optic Stalk
Lens
Optic Nerve
Neural Retina
E11.5 onwards

Figure 1.2

Vertebrate retina development

A. During development, the eye is derived from the neuroepithelium of the forebrain and surface ectoderm. At around E8-8.5, the forebrain protrudes to become the optic vesicles. Overlying and surrounding the optic vesicles is the surface ectoderm. The surface ectoderm becomes thickened to form the lens placode at around E9.5 (Graw, 2010).

B. The optic vesicles continue to grow outwardly and eventually comes in close contact with the lens placode. At around E10.5, the lens placode starts to invaginate into the optic vesicles underneath to become the lens pit (Graw, 2010). As a result of the invagination by the lens, the optic vesicles folds into itself creating two nested cup shaped structure with two layers called the optic cup (Heavner & Pevny, 2012).

C. At E11.5, the lens pit eventually fully closes and detaches to form the lens vesicle (Graw, 2010; Raymond & Jackson, 1995). At this time, the optic cup retains connected to the forebrain (diencephalon) through the optic stalk, which contains the optic nerve. The optic cup is separated into two layers. The outer/posterior layer of the optic cup will form the retinal pigmented epithelium (RPE). The inner/anterior layer of the optic cup will form the neural retina (NR).

D. From E10.5 onwards, the eye gradually forms, and the neural retina starts to differentiate. The retinal ganglion cells (RGCs) are the first neuronal cell type to differentiate in the retina (Heavner & Pevny, 2012). At around E11.5, the axons of the RGCs enter the optic stalk and project to the superior colliculus (Heavner & Pevny, 2012).

This figure was created based on Figure 27.1 of Hufnagel & Brown. Patterning and Cell Type Specification in the Developing CNS and PNS. 2013 (Hufnagel & Brown, 2013). License Number: 5154650389671. This figure was created with Biorender.com

1.2.1 Specifying the eye field

The first step of ocular development is to establish the eye field, which indicates that a region of the medial-anterior neural plate (i.e. the presumptive forebrain) is specified and patterned. The eye field will eventually develop into the eyes. In the mouse, eye field development begins at E8.0 as indentations within the forebrain ("optic pits") (Heavner & Pevny, 2012). The eye field is specified in the neural plate stage several hours before the optic vesicle forms (Beby & Lamonerie, 2013).

This region contains a field of eye precursor cells (i.e., eye primordia) among the neuroectodermal cells. The eye field consists of all the progenitor cells necessary for neural-derived eye structures to form. The eye field is specified by inhibition of canonical *Wnt* signaling, which specifies posterior neural fates (Sabine Fuhrmann, 2008). Concomitantly, formation of the eye field is also facilitated by the action of eye field transcription factors (EFTF) within the forebrain. The eye field transcription factors include *Tbx3*, *Pax6*, *Rax/Rx1*, *Six3*, *Optx2(Six6)*, *Lhx2* and *Tlx(Nr2e1)* and they function in a coordinated cascade to control eye field specification in the anterior neural plate (Zuber, Gestri, Viczian, Barsacchi, & Harris, 2003). These transcription factors are important for the development of retinal progenitor cells. When *Pax6*, *Rax*, *Six3* and *Optx2* are individually mutated, animals have abnormal or no eye development (Zuber et al., 2003). In mice where *Lhx2* is knocked out, eye development stops at the optic vesicle stage and the optic cup does not form. *Six3* directly regulates *Shh* in bifurcating the eye field. Mice with heterozygous *Six3* mutations develop holoprosencephaly and some of those individuals affected will develop cyclopia (Geng et al., 2008). Another important transcription factor that plays an indirect but permissive role in the establishment of the eye field is *Otx2* which is essential for forebrain formation by inducing forebrain-specific genes to specify the anterior neuroectoderm, which in turn allow the EFTFs to specify the eye field.

1.2.2 Production of the neural retina and the retinal pigmented epithelium from the optic cup

After the eye field is formed, eye field transcription factors then coordinate the specification and patterning of the eye field. At E10.5, the optic vesicle invaginates creating the optic cup which is composed of two nested layers, the outer retinal pigmented epithelium (RPE) layer and the inner neural retina layer (Graw, 2010). FGF, a cell-extrinsic growth factor that is highly expressed in the surface ectoderm, is believed to induce neural retina specification and organize the two layers of the optic cup when the lens placode contacts the optic vesicles (Yang, 2004). The neural retina now expresses *Vsx2* (*Chx10*) (I. S. Liu et al., 1994). The presumptive RPE expresses the microphthalmia associated transcription factor, *Mitf*. TGFβ, WNT, FGF and BMP signaling molecules from the ocular mesenchyme surrounding the optic cup, which facilitates RPE specification by promoting the expression of RPE-specific genes such as *Mitf* and *Otx2*, while inhibiting neural retina-specific genes (S. Fuhrmann, Levine, & Reh, 2000)

Mitf and *Vsx2* are also crucial to establishing the boundary between the prospective neural retina and RPE. In *Mitf* mutants, RPE is converted to the neural retina. A similar phenotype is observed in mice that lack both *Otx1* and *Otx2*, which are also important transcription factors for RPE differentiation (Martinez-Morales, Signore, Acampora, Simeone, & Bovolenta, 2001). On the contrary, *Vsx2* loss of function mutations result in ectopic expression of *Mitf* target genes in the neural retina suggesting that the neural retina is converted to RPE as a result of *Vsx2* mutation (Heavner & Pevny, 2012; Horsford et al., 2005)

The presumptive optic stalk expresses *Pax2*. *Pax2* and *Pax6* are expressed in opposite gradients to establish the boundary between the optic stalk and the neural retina (Heavner & Pevny, 2012). Patients with *Pax2* mutation, have optic nerve coloboma because the ventral optic

fissure fails to close properly (Torres, Gómez-Pardo, & Gruss, 1996). *Pax2* and *Pax6* are also important to drive *Mitf* expression in the RPE (Bäumer et al., 2003).

1.2.3 Retinal progenitor cells and competence

Early during retinogenesis, retinal progenitor cells (RPCs), which are neuroepithelial cells in the optic cup, acquire multipotency and the competence (ability to adopt a certain cell fate) to become various retinal cell types. At the beginning, RPCs proliferate to expand and replenish a continuous pool of retinal progenitors. This multipotency is maintained by several transcription factors including *Pax6*, *Vsx2* and *Rax* (Oron-Karni et al., 2008; Xiang, 2013). In the conditional knockout of *Pax6* in mouse RPCs, all retinal cell types are lost except for GABAergic amacrine cells, suggesting that *Pax6* is required to maintain RPC multipotency. When *Rax* is ablated, there is a decrease in RPC proliferation and RPC multipotency from reduced expression of *Pax6*. In *Vsx2* knockout mutants, there is dramatically reduced proliferation of RPCs and consequently a reduction in eye size (Burmeister et al., 1996). Notch signaling and its downstream targets *Hes1* and *Hes5* is another important mechanism for maintaining the RPC population (Ohsawa & Kageyama, 2008). In the mouse eye, ablating *Hes1* results in premature RPCs existing the cell cycle and differentiating into early retinal cell types which consequently reduces optic cup size (Hufnagel & Brown, 2013).

As development progresses, the competency of RPCs becomes gradually diminished enabling sequential differentiation of early to late retinal fates (Cepko, 2014). Thus, the various retinal cell types essentially arise from this common pool of multipotent retinal progenitor cells in overlapping order. During the initial stages of retinogenesis, early gene expression upregulates to steer RPCs to produce early born cell types such as RGCs, cone photoreceptors, amacrine and horizontal cells. As retinogenesis progresses, RPCs gradually change their competence states as

newly committed precursor cells restrict RPCs from adopting the same fate (Brzezinski & Reh, 2015). The newly differentiated retinal cells also express genes that restrict RPCs from adopting the same fate. Later during development, RPCs acquire different competence states to produce late-born cell types such as bipolar cells, Müller glia and rod photoreceptors. Newly generated retinal cells then move vertically to their future layer within the retina.

The big mystery is how these retinal progenitors change their competence states over time. A variety of conditions and extrinsic factors are involved in the transformation of the multipotent RPC such as growth factors, hormones, signaling molecules and more importantly transcription factors. Evidence points to intrinsic cues (sets of transcription factors) as the primary determinants of RPC competence and retinal cell fate progression over time. Differentiating retinal precursors express certain transcription factors which bias RPCs to produce certain retinal cell types and prevent them from differentiating into the same or other retinal cell types (Cepko, 2014). For example, *Ikaros* (*Ikzf1*) is both necessary and sufficient to confer RPC competence to generate early-born retinal cell types such as amacrine, horizontal and retinal ganglion cells (Elliott, Jolicoeur, Ramamurthy, & Cayouette, 2008; Javed & Cayouette, 2017). *Casz1*, a zinc finger transcription factor, makes RPCs generate late-born cell types such as rod photoreceptors and bipolar cells (Javed & Cayouette, 2017). Early RPCs express IKAROS to repress *Casz1*. IKAROS could make certain regions of the RPC chromatin less accessible (i.e. closed conformation) to prevent genes involved in late-born cell production from being expressed. In late RPCs, IKAROS expression is lost, so *Casz1* becomes de-repressed. Other transcription factors also play an important role in "pushing" retinal progenitor cells toward distinct cell fates. The fact that Müller glia cells can be reprogrammed into retinal-neuron-producing RPCs by manipulating these intrinsic factors strongly supports that multipotent RPCs

have an intrinsic program to regulate their differentiation during retinogenesis (Fischer & Reh, 2003; S. Wu, Chang, & Goldberg, 2018). However, the mechanism that regulates these cell fate changes, and which exact genetic program to execute for each retinal cell type remains unclear.

1.3 Overview of transcriptional control of retinal cell type development

The vertebrate retina is composed of seven cell types, six neuronal cell types and one glial cell type. In the mouse, these cells arise from RPCs in an overlapping but highly conserved manner in the following order: retinal ganglion cell, horizontal cell, cone photoreceptor, amacrine cell, bipolar cells, rod photoreceptor and Müller glia cells. The key transcription factors necessary for the specification and differentiation of the various retinal cell types during the process of retinogenesis will be discussed below.

1.3.1 Retinal ganglion cell development

Retinal ganglion cells (RGCs) relay visual signals from photoreceptors via bipolar cells and amacrine cells (retinal interneurons). The axons of RGCs converge to form the optic nerve. The first cells to be born in the developing retina are the RGCs. In the murine retina, RGCs form at E11.5. RGCs are first overproduced but at postnatal (P) day 1 (P1), they begin to undergo apoptosis with the overproduced RGC lost by postnatal week 2.

Various transcription factors are important for the development of RGCs. *Atoh7 (Math5)* is necessary but not sufficient to induce RGC. If RPCs express both *Pax6* and *Atoh7*, then RGCs can be produced. If *Atoh 7* is absent in the developing mouse retina, there is a loss of ~95% RGCs and no optic nerve formation. Early on, RPCs transiently and selectively express *Atoh7*, which biases them towards a RGC fate. *Atoh7* also prevents the differentiation of other retinal cell types by repressing genes such as *Neurod1*, *Neurog2*, *Math3* (*Neurod4*/*Bhlha4*), *Bhlhb5* and

Rxrγ. During this transient period of *Atoh7* expression, *Brn3b* and *Isl1* are activated to promote RGC differentiation in a portion of *Atoh7*+ precursors (Feng et al., 2010). When *Atoh7* is downregulated, the remainder of the *Atoh7*+ precursors, which can no longer produce RGCs, start to express other transcription factors and generate horizontal cells, or continue as non-*Atoh7* lineage progenitors to produce amacrine cells and photoreceptors (Feng et al., 2010).

Another important transcription factor for specifying RGC fate is *Pou4f2* (*Brn3b*). In *Pou4f2* conditional knockout mouse retina, there are significantly reduced RGCs with very thin optic nerve and abnormal innervation to the brain (Badea, Cahill, Ecker, Hattar, & Nathans, 2009). *Pou4f2* also activates downstream RGC genes such as *Pou4f1 (Brn3a)*, *Eomes*, *Bcl2*, *Barhl2*, *Ebf104*, morphogens such as *Shh*, and cell surface protein such as *Ablim1*. *Pou4f2* also indirectly regulates *Dlx1* and *Dlx2* which are crucial for the differentiation of late-born RGCs. *Atoh7* regulates another gene, *Isl1*, in a parallel yet distinct pathway to *Brn3b*, to promote RGC genesis. When *Isl1* is deleted in the retina, 95% of RGCs are lost. Another class of transcription factors important for specifying RGCs are members of the SoxC family (SRY-related HMG box transcription factors), *Sox4* and *Sox11*. In *Sox4*/*Sox11* double knockout mutant retina, there are no RGCs although *Atoh7* and *Brn3b* are unaffected (Jiang et al., 2013).

1.3.2 Amacrine and horizontal cells development

Amacrine cells (AC) relay information between bipolar cells and RGCs in the INL. Evidence points to amacrine cells as the default retinal neuronal cell fate (Bosze, Hufnagel, & Brown, 2020; Marquardt et al., 2001). This is because *Pax6* maintains RPC multipotency and impedes retinal cell type differentiation, and in *Pax6* conditional knockout mutant retina, only amacrine cells are produced (Marquardt et al., 2001). Amacrine cells and horizontal cells arise

from the same progenitor pool and require many of the same transcription factors for their specification.

Foxn4 over-expression promotes amacrine cell differentiation (Li et al., 2004). *Foxn4* specifies amacrine cell fate by activating downstream bHLH transcription factors such as *Neurod1*, *eurod4* (*Math3*) and *Ptf1a*. *Foxn4* may inhibit RPCs from producing RGCs by activating *Neurod1*, *Neurod4* and *Ptf1a*, which can repress *Atoh7* and *Brn3b* expression (S. Liu et al., 2020). In *Foxn4*-expressing RPCs, there are distinct and parallel pathways downstream of *Neurod1*/*Neurod4* and *Ptf1a* that regulate amacrine cell differentiation. *Neurod1* is involved in the determination of bipolar cells, amacrine cells, horizontal cells, specification of M-cones, and the terminal differentiation and survival of photoreceptors (Xiang, 2013). Loss of both *Neurod1* and *Neurod4* results in complete loss of amacrine cells, and RPCs switching to RGCs and Müller glia cells (Inoue et al., 2002). *Neurod1* and *Neurod4* are functionally redundant for specifying amacrine cell fate, as single knockout of either transcription factor does not affect amacrine cell development.

Ptf1a is necessary but not sufficient for amacrine cell differentiation (Fujitani et al., 2006). *Ptf1a* represses RGC formation by repressing *Atoh7* (Fujitani et al., 2006). In *Ptf1a* knockout mouse retina, there is a cell fate switch from amacrine cells to RGCs (Inoue et al., 2002). There are other transcription factors required for amacrine cell genesis and differentiation. *Tfap2a* and *Tfap2b*, which encode AP2 transcription factors, act downstream of *Ptf1a* and are necessary for amacrine cell, in particular glycinergic and GABAergic subtypes, differentiation as well (Jin et al., 2015). In addition, several other transcription factors such as *Barhl2*, *Nr4a2* (*Nurr1*), *Isl1*, *Ebf*, *Sox2* and *Neurod2* are important for AC subtype specification (Xiang, 2013)

Horizontal cells modulate and integrate visual signals between photoreceptors and bipolar cells in the OPL. Horizontal cells form early at E11 peaking at E14.5. As mentioned previously, horizontal cells and amacrine cells share similar intrinsic programming for their cell fate specification. *Foxn4* is also necessary for horizontal cell development. Ablating *Foxn4* in RPCs results in a complete loss of horizontal cells and few amacrine cells are generated.

Foxn4 activates *Ptf1a* and *Onecut* transcription factors to regulate horizontal cell differentiation. *Ptf1a* is also important for specifying horizontal cells, as the loss of *Ptf1a* abolishes horizontal cells completely and nearly all amacrine cells (Fujitani et al., 2006) Since expressing *Ptf1a* alone only specifies the default amacrine cell fate, to specify horizontal cell fate, *Foxn4* must cooperate with *Pax6* upstream to activate *Onecut1* and *Onecut2* expression in horizontal cell precursors (Klimova, Antosova, Kuzelova, Strnad, & Kozmik, 2015). Approximately 80% of horizontal cells are lost in the absence of *Onecut1* expression (F. Wu et al., 2013). In addition to promoting RPC commitment to horizontal cell fate, *Onecut* transcription factors also regulates RPC migration inward to the boundary with the ganglion cell layer, where they will activate mature horizontal cell marker expression (F. Wu et al., 2013).

Ptf1a also regulates *Prox1* and *Lhx1* expression during the initial horizontal cell differentiation programming which is independent of *Onecut* transcription factors. At later stages of horizontal cell development, *Onecut* genes are necessary for regulating *Lhx1* and *Prox1* expression (Klimova et al., 2015). Interestingly, *Prox1* is the only transcription factor necessary and sufficient for determining horizontal cell fate (Dyer, Livesey, Cepko, & Oliver, 2003). Loss of *Prox1* results in significant horizontal cell loss, and failure of early RPCs to exit the cell cycle which results in cell fate switches to rod photoreceptors and Müller glia cells (Dyer et al., 2003). Over-expressing *Prox1* enhanced horizontal cell fate (Dyer et al., 2003). The *Lim* homeodomain

transcription factor, *Lhx1*, acts downstream of *Ptf1a* and is regulated by *Prox1*. *Lhx1* is important for horizontal cells to acquire proper laminar position. Ablating *Lhx1* or its partner gene *Sall3*, which encodes a C2H2 zinc finger transcription factor, results in mutant horizontal cell phenotypes and reduced horizontal cell differentiation marker expression (Poché et al., 2007). Although insufficient to specify horizontal cell fate, the Spalt-like zinc finger transcription factor *Sall3* is another transcription factor that promotes a partial horizontal cell phenotype that is independent of *Lhx1*. *Sall3* knockout retinas have dramatic reduction in horizontal cells, ectopic horizontal cell localization to the inner portions of the INL similar to *Lhx1* mutants (de Melo, Peng, Chen, & Blackshaw, 2011).

Neurod1, *Neurod4*, and *Neurog2*, which function downstream of *Foxn4*, may also specify horizontal cell fate in a distinct and parallel manner as *Ptf1a* (Xiang, 2013). Forced expression of *Pax6* with *Neurod4* steered more horizontal cells to be produced over amacrine cells (Ohsawa & Kageyama, 2008). In triple knockout mice of *Neurod4*/*Ascl1*(*Mash1*)/*Neurog2*, *Neurod1*/*Ascl1*/*Neurod4*, as well as *Neurod1*/*Neurod4*/*Neurog2*, there is a complete loss of horizontal cells (Bosze et al., 2020).

1.3.3 Photoreceptor development

Photoreceptors sense light stimuli and relay that information to subsequent retinal neurons through phototransduction. There are two kinds of photoreceptors: rods and cones. Cones are needed for bright-light and colour vision whereas rods function in low-light vision. Humans have one type of rods and three types of cones which detect blue, green, and red light. Mice have one type of rods and two types of cones, S-cones and M-cones, which detect UV and green light, respectively (Szatko et al., 2020).

Nuclei of photoreceptors localize to the ONL, which is derived from the neuroblastic layer (NBL) of embryonic retina and their cell bodies extend towards the back of the retina to the RPE. Cones and rods arise at different times during retinogenesis. In the mouse, cones begin to be generated at E11, one day after RGCs are specified; this is complete at around birth (E18). Rods begin to form right before birth (E18), and they become fully differentiated by P7.

The development of photoreceptors is dependent on both extrinsic and intrinsic cues. Photoreceptor differentiation begins with an extrinsic signal from the downregulation of *Notch1* signaling (Jadhav, Mason, & Cepko, 2006). *Notch1* expression in proliferating and undifferentiated cells as well as glial cells, is important to suppress differentiation. In mutants where *Notch1* was deleted early during retinogenesis, there is an increase in cones. Deleting *Notch1* late during retinogenesis after the window of cone production, results in only rod photoreceptors being produced (Jadhav et al., 2006).

Crx (cone-rod homeobox) and *Otx2* (*Orthodenticle* homeobox 2), which are members of the bicoid subclass homeodomain transcription factor family, are important regulators of photoreceptor fate. After *Notch1* is downregulated, *Otx2* is upregulated in RPCs that will differentiate into either photoreceptors or bipolar cells. When *Otx2* is lost, amacrine cells develop at the expense of photoreceptors, bipolar cells or horizontal cells (Nishida et al., 2003). *Otx2* knockout mutants also lack bipolar cells. Photoreceptor gene expression, such as *Crx*, *Nr2e3* and *Nrl*, is decreased in *Otx2* conditional knockout retinas (Omori et al., 2011). Retinal cell fate decisions and cell survival are also dependent on *Otx2* dosage. High levels of *Otx2* induces photoreceptor cell fate specification and low levels of *Otx2* expression are required for rod photoreceptor survival (Yamamoto, Kon, Omori, & Furukawa, 2020). OTX2 activates *Crx* after RPCs exit the cell cycle. *Crx* functions as a direct downstream target of OTX2 and is

crucial for photoreceptor differentiation and maintenance. In *Crx*-null mouse retinas, photoreceptor specification is normal, however terminal differentiation and survival of photoreceptors is severely impaired (Yamamoto et al., 2020)

Whether a photoreceptor precursor becomes a cone or a rod is of great interest to the developmental neuroscience community and the consensus is that this decision is regulated by various downstream transcription factors, namely the basic-motif neural retina leucine zipper *Nrl* and the nuclear receptor *Nr2e3*. Evidence supports that the default photoreceptor fate is cones because blocking the *Notch* signaling pathway in early RPCs resulted in a dramatic increase in cones (Jadhav et al., 2006). Specifically, it has been hypothesized that photoreceptor precursors maintain a default S-cone state, and then *Nrl* is expressed to drive rod production by cooperating with *Crx* and other transcription factors. *Nrl* is sufficient to determine the fate of a photoreceptor precursor into a cone or later retinal cell types such as a rod or Müller glia. In the absence of *Nrl*, rods become S-cones.

RPCs fated to develop into cones express *Rxrγ* (*Nr2b3*) and thyroid hormone nuclear receptor *Trβ2* (Swaroop, Kim, & Forrest, 2010). *Rxrγ* (*Nr2b3*) and *Trβ2* form heterodimers to regulate which of the two cone opsin genes a cone will express. *Trβ2* expression promotes M-cone development over the default S-cone fate (Swaroop et al., 2010). In *Trβ2* mutant mice, *M-opsin* expression is lost and cones only express *S-opsin*. By increasing thyroid hormone levels, *Trβ2* influences cone opsin patterning (Roberts, Hendrickson, McGuire, & Reh, 2005). Deleting *Rxrγ* causes all cones to express *S-opsin* (Roberts et al., 2005).

Furthermore, *Sall3* is important in regulating cone development (de Melo et al., 2011). In *Sall3* mutants, there is loss of multiple cone-specific genes. *Sall3* is necessary and sufficient to induce blue-sensitive cone specific genes such as the E3 ubiquitin ligase *Sop* and *Arrestin 3* (de

Melo et al., 2011). *Neurod1* is required for cone subtype specification, and mice that lack *Neurod1* display cone subtype defects and increased rod genesis (H. Liu et al., 2008).

Rod photoreceptors are much more abundant in the mouse and human retina than cones. Rods which are born late during development are maintained in an undifferentiated state by STAT3 activation. By P0, STAT3 is inactivated due to its ligand CNTF (ciliary neurotrophic factor) being downregulated and increased SOCS3 (suppressor of cytokine signaling 3) (Ozawa et al., 2008). As a result of STAT3 being inactivated, rhodopsin becomes expressed. This initiates the differentiation programming for rod photoreceptors. Some transcription factors involved in cone development are important for rod development as well. For example, *Otx2* is a key transcription in specifying cone and rod photoreceptors. In order for photoreceptor genes (ie *Opsin* genes), which determine whether a rod or cone photoreceptor is produced, to be expressed, *Crx* and *Otx2* are required. How these two transcription factors are regulated, and their complete regulatory network remains to be elucidated. A major determinant of that decision is *Blimp1* (Brzezinski, Uoon Park, & Reh, 2013).

Nrl is also an important determinant of rod differentiation as it is preferentially expressed in rod precursors and rod photoreceptors. In the absence of *Nrl*, mouse retinas display rod loss and take up a cone-like morphology (Mears et al., 2001). *Nrl* directly targets *Nr2e3* to drive *Nrl*+ precursors to become rods by repressing cone genes (Cheng et al., 2006). *Nr2e3* also acts as a co-activator of *Nrl* and *Crx* to further activate rod-specific gene expression (Swaroop et al., 2010). In human and mouse *Nr2e3* mutants, hybrid cones develop which express both rod and cone opsins.

Casz1 encodes a nuclear protein that promotes rod photoreceptor production. Cone production is increased when *Casz1* is inactivated in the developing mouse retina. Expressing

Casz1 early (ectopic expression) results in decreased cone genesis (Javed & Cayouette, 2017). These factors are important because they have the potential to stop RPCs at certain stages in order to produce desired retinal cell types (Javed & Cayouette, 2017). Changing chromatin accessibility is one important way for these temporally expressed transcription factors to target downstream genes that are necessary for functional cones, without forcing the RPCs to exit the cell cycle (Javed & Cayouette, 2017).

1.3.4 Bipolar cell development

Bipolar cells facilitate the transmission of visual signals from photoreceptors to RGCs. Bipolar cells are localized to the inner nuclear layer, with axons extending into the inner plexiform layer and outer plexiform layer. There are multiple bipolar cell subtypes, such as the ON-center or OFF-center subtypes. *Vsx2 (Chx10)* is critical for the specification of bipolar cells, as bipolar cells are absent in the *Vsx2*-null retina (Burmeister et al., 1996). *Vsx2* favors bipolar cell fate by repressing photoreceptor gene expression (Barbieri et al., 1999). *Vsx1* is also involved in bipolar cell development, in particular in the differentiation of bipolar cell subtypes by activating genes necessary for the differentiation and maintenance of bipolar cells such as *Recoverin*, *Neto1*, *Nk3r* and *CaB5* (Chow et al., 2004).

Otx2 is another important transcription factor for bipolar cell development. *Otx2*+ precursor cells specify bipolar cells in the absence of photoreceptor-specific gene expression (ie *Prdm1*) (Brzezinski, Lamba, & Reh, 2010). The dosage of *Otx2* expressed in RPCs is important in regulating cell fate decisions between rod photoreceptors and bipolar cells (Bernard et al., 2014; C. S. Y. Chan et al., 2020). Over-expressing *Otx2* in newborn mouse retina, increased bipolar cells at the expense of rod photoreceptors (Wang, Sengel, Emerson, & Cepko, 2014). Postnatal conditional ablation of *Otx2* results in reduced Protein Kinase C (*PKC*) expression,

which is a mature bipolar cell marker. The expression of other mature bipolar cell markers such as *Vsx2*, *Bhlhb4*, *Cabp5* and *Pcp2* is also reduced (Omori et al., 2011).

Whether *Otx2*-expressing progenitors become photoreceptor or bipolar cells depends on the gene dosage of *Otx2* as well as *Blimp1*. Conditional knockout of *Blimp1* (also *Prdm1*) in the retina results in profound reduction in photoreceptors and increased bipolar cell-like cells and proliferating RPCs (Katoh et al., 2010). Forced expression of *Blimp1* reduced the number of bipolar cells (Katoh et al., 2010). These data suggest that *Blimp1* represses bipolar cell fate by inhibiting *Vsx2* expression (Brzezinski et al., 2010, 2013).

Ascl1 (*Mash1*) and *Neurod4* (*Math3*) are also critical for bipolar cell differentiation. In *Ascl1*(*Mash1*)/*Neurod4*(*Math3*) double knockout retina, bipolar cells are completely lost with significant increase in Müller glia cell number. The increased Müller glia does not occur in *Vsx2* mutant retina (Tomita, Moriyoshi, Nakanishi, Guillemot, & Kageyama, 2000).

1.3.5 Müller glia cell development

Müller glia cells are the only glia cell type in the retina derived from RPC. They are produced late during development from E18 to P21. Spanning across the entire thickness of the retina from the GCL to the ONL, Müller glia cells provide structural and functional support to the retina such as by contributing to neuronal function and signaling, maintaining homeostasis, and providing nutritional and metabolic support (Bringmann et al., 2006). In the mature retina, Müller glia cells can respond to injury and protect retinal neurons by releasing neuroprotective factors in a process called reactive gliosis (Bringmann et al., 2006). However, in mammalian retina, Müller glia cells cannot regenerate retinal neurons after injury. Interestingly, teleost retina can reprogram Müller glia cells into multipotent RPCs and thus regenerate retinal neurons to repair vision (Goldman, 2014).

Factors that are important for maintaining RPCs are also required for Müller glia cell development. The *Notch-Hes* pathway is critical for Müller glia development as it is shared in RPCs as well. When *Notch1*, *Hes1* and *Hes5* are ablated, there is a significant loss of Müller glia cells and increased rod photoreceptors (Furukawa, Mukherjee, Bao, Morrow, & Cepko, 2000; Hojo et al., 2000). In contrast, forced expression of any of these genes upregulated the expression of glial markers (Furukawa et al., 2000). *Sox* family transcription factors, such as *Sox2*, *Sox8* and *Sox9*, are expressed in proliferating RPCs and Müller glia cells later during development. There is a reduction of Müller glia cells when these *Sox* transcription factors are knocked out or knocked down in the developing retina (Muto, Iida, Satoh, & Watanabe, 2009). *Sox8* and *Sox9* may specify Müller glia cells by suppressing rod photoreceptor fate in late RPCs. The relative expression of *Notch1*, *Hes1* and *Hes5* also contribute to cell fate decisions of these late RPCs. *Lhx2* appears to have an important role in Müller glia development because reintroducing several Müller glia factors in *Lhx2*-null mice cannot completely rescue Müller glia development (de Melo et al., 2016). Conditional loss of *Lhx2* in mature retinas results in glial cell hypertrophy and reactive gliosis (de Melo et al., 2012).

1.4 *Dlx* genes in development

Distal-less homeobox genes (*Dlx*) are the vertebrate orthologs of Drosophila *distal-less* (*Dll*) gene (Panganiban & Rubenstein, 2002). *Dll* genes are important for distal limb development. *Dll* is expressed in the adult optic lobes in Drosophila. *Dll*, in combination with other transcription factors, is also important for antenna determination (Casares & Mann, 1998). However, whether *Dll* plays a role in Drosophila ocular development remains unknown. *Dlx* and *Dll* genes share a conserved homeodomain (Merlo et al., 2000).

Dlx genes encode homeobox transcription factors which bind DNA and regulate transcription. The third α-helix of the homeobox binds ATTA/TAAT motifs to activate or repress target genes. The vertebrate *Dlx* genes play a critical role during the development of the central nervous system, craniofacial structures and the retina (de Melo et al., 2005; Panganiban & Rubenstein, 2002).

The human and mouse *Dlx* genes are found in three oppositely transcribed (i.e., gene 1 transcribed 5' to 3', gene 2 transcribed 3' to 5') bigene clusters, *Dlx1/2*; *Dlx3/4*; and *Dlx5/6*. Mouse *Dlx1/2*; *Dlx5/6* are partially redundant. Each pair is linked to a *Hox* gene cluster, *HoxD*, *HoxB*, *HoxA* respectively. Each *Dlx* gene has three exons and two introns. The homeodomain is encoded between exon 2 and exon 3 (**Figure 1.3**). The primitive chordate amphioxus species has a single *Dlx* gene, whereas more advanced species possesses more *Dlx* genes. It has been proposed that the mammalian *Dlx* bigenic clusters arose from adjacent duplication of an ancestral *Dlx* gene followed by two rounds of genome duplication and a subsequent loss of the *Dlx* pair linked to *HoxC* (Panganiban & Rubenstein, 2002). The intergenic region of each pair contain enhancer elements. *Dlx* genes cross-regulate other *Dlx* genes via these enhancer elements. For example, DLX1 and DLX2 bind the *Dlx5/6* intergenic enhancer *I56i in vivo* to upregulate *Dlx5/Dlx6* expression in the forebrain (Zhou et al., 2004). The *Dlx1*/*Dlx2* intergenic region also contains enhancer elements that are important for regulating *Dlx* expression in subpopulations of interneurons that migrate to the dorsal cortex and the olfactory bulb (Ghanem et al., 2007). There are also upstream regulatory elements (UREs) located upstream of the *Dlx1/Dlx2* genes that regulate *Dlx1* and *Dlx2* expression to specify interneuron subtypes (Ghanem et al., 2007). Retinoblastoma protein, pRb, regulates *Dlx1* and *Dlx2* expression through sites in the *Dlx1* and *Dlx2* proximal promoters and in the *Dlx1/2* intergenic enhancer (Ghanem et

al., 2012). *Dlx* genes have been found to repress *Notch* signaling in the nervous system (Panganiban & Rubenstein, 2002).

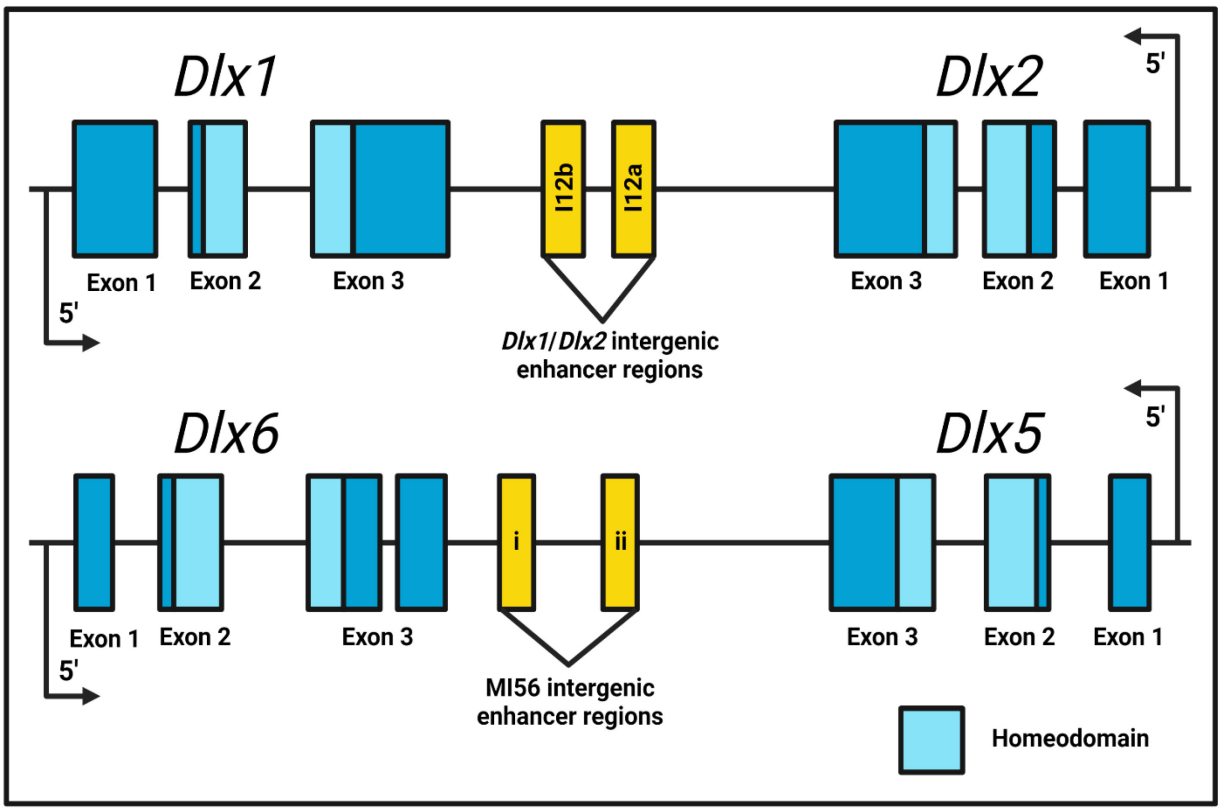

Figure 1.3
Dlx1/Dlx2 and Dlx5/Dlx6 gene pair structure

Dlx genes share similar genomic structure. They are arranged in bigenic pairs. For each pair, they are transcribed in the opposite direction. The homeodomain (light blue) is encoded by exons 2 and 3. The intergenic regions contain regulatory elements, such as the *I12a*/*I12b* and *MI56i*/*MI56ii* intergenic enhancers. *MI56i* and *MI56ii* enhancers regulate *Dlx5/Dlx6* expression. This figure was adapted and created based on Figure 3 of Q.P. Zhou et al. Nucleic Acids Research. 2004 (Zhou et al., 2004). License Number 5154640648272. This figure was created with Biorender.com

1.4.1 General expression of *Dlx* genes

In the mouse, *Dlx* genes, such as *Dlx1/Dlx2*; *Dlx5/Dlx6*, are expressed in the central nervous system (Panganiban & Rubenstein, 2002). They especially localize to the forebrain in diencephalic and telencephalic regions. Their expression follows a temporal order, first *Dlx2*, then *Dlx1*, *Dlx5* and lastly *Dlx6* in the forebrain (Panganiban & Rubenstein, 2002). *Dlx* genes are also expressed in the branchial arches and neural crest derivatives, which develop into craniofacial skin and connective tissues. *Dlx* genes are also expressed in some sensory organs. For instance, *Dlx* genes are also expressed in the otic placode, olfactory bulb and the developing retina. *Dlx* genes are also expressed in certain domains of the limb buds and genital eminence.

1.4.2 *Dlx1/Dlx2* expression in the developing retina

Dlx1 and *Dlx2* are transcription factors, thus are primarily expressed in the nucleus. In the retina, *Dlx1* and *Dlx2* are expressed in neuronal precursors and in certain groups of neurons ((D. D. Eisenstat et al., 1999; Panganiban & Rubenstein, 2002). At E11.5, *Dlx2* begins to be expressed in the central retina (de Melo et al., 2008) while the earliest documented expression of *Dlx1* is at E12.5. At E13.5, *Dlx1* and *Dlx2* are expressed throughout the retinal neuroepithelium (de Melo, Qiu, Du, Cristante, & Eisenstat, 2003). At this time, *Dlx2* is expressed in the highest proportions of early differentiating retinal neuroblasts (de Melo et al., 2003). *Dlx2*-expressing cells also co-localize with *Vsx2*/*Chx10* (marker of RPC), *Brn3b* (marker of retinal ganglion cells) and *Pax6* (marker of amacrine cells) at this time.

At E16.5, both DLX1 and DLX2 remain restricted to the retinal neuroepithelial cells where they continue to co-localize with BRN3B and PAX6 (de Melo et al., 2003). At E16, *Dlx2* continues to co-express with bipolar cell marker *Vsx2* (*Chx10*), although there are some *Dlx*-expressing cells that do not express *Vsx2 (Chx10)* (de Melo et al., 2003).

At P0, both *Dlx1* and *Dlx2* expression is now restricted to the inner layer of the retina (de Melo et al., 2003). *Dlx1* expression is reduced compared to *Dlx2* and is only expressed in the ganglion cell layer (GCL) which is where the RGCs and displaced amacrine cells are localized. *Dlx2* is primarily expressed in the ganglion cell layer and the inner neuroblastic layer (iNBL), where newborn neurons such as retinal ganglion cells and amacrine cells are. A small number of *Dlx2*-expressing cells are also present in the differentiating outer retina. DLX2 also co-localizes with *Gad65, Gad67* and GABA-expressing neurons in the retina at birth and in adults.

Postnatally, *Dlx1* is no longer detected after P0. However, unlike *Dlx1*, *Dlx2* expression increases in completely differentiated adult retina and is maintained in the nuclei of the ganglion cell layer (GCL) and the differentiated inner nuclear layer (INL). DLX2 co-localizes with the amacrine cell marker, *Syntaxin* at P0 and in adulthood. In the adult, only some *Chx10*-expressing cells co-express *Dlx2* in the INL (de Melo et al., 2003). DLX2 also co-localizes with *Calbindin*-expressing horizontal cells in the adult (de Melo et al., 2003).

Dlx5 is expressed in the retina at E16, P0 and throughout adulthood where it co-localizes with *Dlx2*-expressing cells in the GCL and the INL (Zhou et al., 2004). The functional significance of *Dlx5/Dlx6* in retinal development remains unknown.

1.4.3 *Dlx1*/*Dlx2* functions and mutations in the retina

Dlx1 and *Dlx2* expression overlaps in the forebrain, the ganglion cell layer and the inner nuclear layer of the retina. The phenotype in the *Dlx1*/*Dlx2* double knockout (DKO) mice is more severe than the *Dlx1*/*Dlx2* single knockouts (SKO). This suggests some functional redundancy between *Dlx1* and *Dlx2*, because when one member of this bigene cluster is mutated or ablated, this results in a smaller phenotypic effect than expected by the function of each gene. Hence, one gene can compensate for the loss of function of the other gene to some degree. When

both *Dlx1/Dlx2* are ablated, the effect is much more severe. The functional redundancy is explained partially by the temporal and spatial overlap in *Dlx1* and *Dlx2* expression. The redundant functions of the *Dlx* genes may also be explained by their nearly identical homeodomains (J. K. Liu, Ghattas, Liu, Chen, & Rubenstein, 1997; Zhou et al., 2004). However, *Dlx1* and *Dlx2* can have unique functions due to the divergence of their amino acid sequences in domains other than the homeodomain.

In the absence of *Dlx1* and *Dlx2*, retinal ganglion cell numbers decrease by ~1/3 at E13.5 and E16.5. The optic nerve, which is composed of RGC axons, decreases in thickness by 23% in the DKO mutant (de Melo et al., 2005). Unfortunately, due to the embryonic lethality of the *Dlx1/Dlx2* mutants (*Dlx1* and *Dlx2* SKO die on P0; *Dlx1/2* DKO mice also die just after birth), we cannot study the function of these genes postnatally or in the adult mouse retina.

DLX transcription factors may regulate cell fate decisions by regulating other genes by occupying their regulatory regions *in vivo*. Interestingly, in the *Dlx1/Dlx2* DKO mutants, in addition to the loss of RGCs, there was also ectopic expression of *Crx*, the cone and rod photoreceptor homeobox gene, in the ganglion cell layer and increased *Crx* expression in the outer neuroblastic layer (oNBL). *Crx* is expressed in developing photoreceptors in the outer retina (de Melo et al., 2005). This suggests that upon loss of *Dlx1*/*Dlx2*, some retinal ganglion cell progenitors may adopt photoreceptor cell fate. Therefore, *Dlx1*/*Dlx2* may play a role in cell fate decisions between retinal ganglion cells and cone photoreceptors. Unfortunately, also due to embryonic lethality of the *Dlx1*/*Dlx2* DKO mice at P0, we cannot eliminate the possibility that rod photoreceptors may also be affected, as rods are primarily produced postnatally (Jamie Lauren Zagozewski, 2017).

1.5 *Otx* genes in development

Orthodenticle-like homeobox (*Otx*) genes are the mammalian version of the Drosophila *orthodenticle* (*Otd*) family. The *Otx* genes and the related *Crx* encode homeodomain transcription factors. Specifically, they are bicoid-related homeodomain transcription factors. *Otx2,* in particular, is one of the key regulators of nervous system development. It is important for early specification of the brain and embryonic development of sensory organs, including the pituitary gland, pineal gland, inner part of the ear, eyes, and optic nerve. In later developmental stages, they are important for maintaining the retina and brain function.

The human *OTX2* gene consists of five exons, of which the last three are coding (Beby & Lamonerie, 2013). The mouse *Otx2* gene uses various promoters at various timepoints and cellular types to generate various OTX2 isoforms (Beby & Lamonerie, 2013). The human OTX2 protein contains a homeodomain for DNA binding, SGQFTP and SIWSPA motifs for protein-protein interactions, and two C-terminal tandem OTX-tail motifs which accounts for the transactivation activity of the protein (Markitantova & Simirskii, 2020) (**Figure 1.4**). The mouse OTX2 shares 100% amino acid composition with the human OTX2 protein (Beby & Lamonerie, 2013). The OTX2 homeodomain will bind bicoid-like *cis*-elements TAATCC (Lamba, Khivansara, D'Alessio, Santos, & Bernard, 2008). They can also bind related motifs such as TAACCC or TAAGCC (Beby & Lamonerie, 2013).

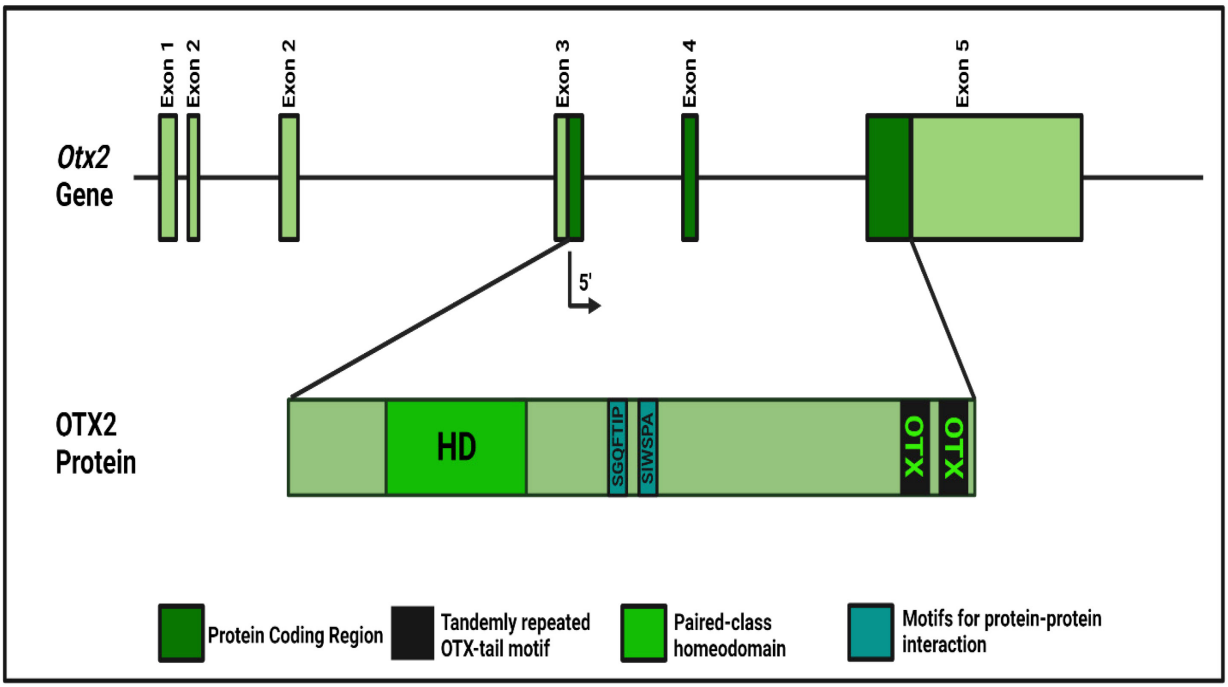

Figure 1.4

Human and mouse OTX2 gene and OTX2 protein structure

The human *OTX2* gene contains 5 exons. The OTX2 protein is encoded by exons 3, 4 and 5. The mouse *Otx2* gene structure is similar to its human homolog . The mouse OTX2 protein shares the same amino acid composition as the human OTX2 protein (Beby & Lamonerie, 2013). OTX2 protein contains a homeodomain for DNA binding; SGQFTP and SIWSPA motifs for protein-protein interactions; and two C-terminal tandem OTX-tail motifs which accounts for the transactivation activity of the protein. This figure was adapted and created from Figure 1 of Beby & Lamonerie. Experimental Eye Research. 2013 (License Number: 5154640848763), and Figure 2 of Deml et al. European Journal of Human Genetics. 2016 (Creative Common Attribution-Non Commercial-Share Alike 4.0 International License, CC-BY-NC-SA 4.0) (Beby & Lamonerie, 2013; Deml et al., 2016). This figure was created with Biorender.com

1.5.1 General expression of *Otx1/Otx2* in the developing nervous system

Otx2 is an essential gene for the development of the nervous system and in particular it is important for forebrain and midbrain induction. Before the onset of gastrulation, *Otx2* is first expressed at E6.5 in the epiblast and visceral endoderm (VE) (Boyl et al., 2001). During gastrulation, *Otx2* is expressed in the anterior neuroectoderm and anterior mesendoderm (AME) (Boyl et al., 2001). Then it is expressed in the anterior part of the hindbrain (rhombomere 1). *Otx1* is first expressed at E8.5 in the presumptive forebrain and midbrain neuroepithelium At E11.5, *Otx1* is then expressed in the dorsal telencephalon which will become the deep layers of the brain cortex (Acampora, Gulisano, & Simeone, 2000).

Late during embryonic development, *Otx2* is expressed in several regions of the basal telencephalon such as the anterior ganglionic eminence, the septum adjacent to the diencephalon, the diencephalon, mesencephalon, choroid plexus, pineal gland and cerebellum (Beby & Lamonerie, 2013). *Otx2* is also expressed in sensory organs associated with olfaction, eyesight and hearing such as the inner ear, retina and olfactory epithelium (Acampora et al., 2000; Beby & Lamonerie, 2013). Postnatally, *Otx2* is expressed in the thalamus, the superior colliculus, the choroid plexus and the hypothalamus (Pensieri, 2019).

1.5.2 *Otx2* expression in the developing retina

Otx2 is required for the development of sensory organs such as the eye. As development progresses, *Otx2* is expressed in various retinal progenitors and retinal cell types. First *Otx2* cooperates with *Rax*, *Hes1* and *Six3* to regulate the contact between the optic vesicles and the surface ectoderm to form the optic cup (Ghinia Tegla et al., 2020). Later when the neural retina and RPE regions are being specified, *Otx2* is highly expressed in the RPE and in a group of RPCs that primarily generate cones and horizontal cells. Subsequently during the specification of

retinal cell types, *Otx2* is expressed in photoreceptors. In the mature retina, *Otx2* is expressed in photoreceptors and bipolar cells, as well as in a group of Müller glia cells. Interestingly *Otx2* is transiently expressed in the differentiating RGCs in chicks which suggests a role of *Otx2* in retinal neurogenesis (Bovolenta, Mallamaci, Briata, Corte, & Boncinelli, 1997).

Early during eye development, *Otx2* is expressed in neuroepithelial cells of the early optic vesicle regulating its formation and expansion. At E9.5, *Otx1* and *Otx2* are expressed in the presumptive RPE (Pensieri, 2019). At this stage, *Otx2* promotes RPE specification by inhibiting *Sox2* and *Fgf8*, which are factors that induce neural retina differentiation (Nishihara et al., 2012).

At E10.5, *Otx2* is strongly expressed in retinal progenitor cells of the outer neuroblastic layer (oNBL), which is the presumptive photoreceptor layer, and weakly expressed in the inner NBL (iNBL), which is the presumptive INL (Pensieri, 2019) (Muranishi et al., 2011). At E11.5, *Otx2* is expressed primarily in the RPE and weakly in the neural retina.

At E12.5, *Otx2* expression in the neural retina upregulates reflecting a second wave of *Otx2* expression. At E17.5, *Otx2* is primarily expressed in the outer portions of the NBL which includes the prospective photoreceptor layer of the mature retina. *Otx2* is also weakly detected in the inner portion of the NBL. These neuroblasts can become both neuronal and glia cell types (Martinez-Morales et al., 2001). At P6, *Otx2* expression in the RPE downregulates and its expression in the INL upregulates. Postnatally, *Otx2* is expressed in the nuclei of bipolar cells and RPE cells, as well as in the surrounding nuclei of photoreceptors (Beby & Lamonerie, 2013).

Crx is first expressed at E12.5 and its expression is maintained throughout adulthood (Furukawa, Morrow, & Cepko, 1997). *Crx* is also expressed in the pineal gland which contains cells that have photosensitive opsins, and is important for the circadian cycle (S. Chen et al., 1997; Furukawa, Morrow, Li, Davis, & Cepko, 1999).

1.5.3 *Otx1*/*Otx2* functions and mutations in the developing nervous system

Very early during embryonic development, the primary function of *Otx2* is to specify the forebrain, because it is only expressed in the most anterior part of the embryo. Also since *Otx2* is expressed in pre-committed anterior visceral endoderm (AVE) cells, it is important for specifying anterior-posterior polarity by regulating the migration of these cells (Kimura-Yoshida et al., 2005). Next in the anterior mesendoderm (AME), *Otx2* regulates *Dkk1* and *Lhx1*, which are important for head formation (Ip, Fossat, Jones, Lamonerie, & Tam, 2014).

Later during development, *Otx2* is expressed throughout the forebrain and midbrain neuroepithelium, as well as dorsally in an area anterior to the midbrain/hindbrain boundary and will induce this region to become the future cerebellum (Beby & Lamonerie, 2013; Di Giovannantonio et al., 2014). Hence, *Otx2* is important for rostro-caudal compartmentalization and patterning of the brain to ensure that the midbrain-hindbrain boundary is correctly positioned so that the midbrain and hindbrain regions can then be correctly induced.

In mice, complete deletion of *Otx2* causes the anterior neuroectoderm (future forebrain) to be absent, which results in embryonic lethality (Acampora et al., 1995). Various loss-of-function *Otx2* mutations (heterozygous knockout mice) display a range of phenotypes from acephaly, holoprosencephaly, short nose, anophthalmia/microphthalmia, agnathia/micrognathia, to normal (Beby & Lamonerie, 2013; Matsuo, Kuratani, Kimura, Takeda, & Aizawa, 1995). In mice where *Otx2* is conditionally ablated, they lack pinealocytes in the pineal gland, which is the organ involved in melanogenesis and the sleep-wake cycle (Nishida et al., 2003). In contrast, *Otx1*-null mice are viable and have subtle brain abnormalities which cause them to develop spontaneous epilepsy (Mark, Rijli, & Chambon, 1997).

Patients with *OTX2* mutations can also have variable neurological phenotypes ranging from severe developmental delay to normal cognitive development (Ragge et al., 2005). *OTX2* is

also required for anterior pituitary development by regulating *Hesx1* and *Pit1* genes (Dateki et al., 2008). Heterozygous *OTX2* loss-of-function patients can have growth hormone deficiency and short stature possibly from reduced transactivation of *HESX1* and *PIT1* genes. Furthermore, patients with heterozygous *OTX2* mutations develop various pituitary phenotypes possibly related to the fact that *OTX2* is also important for regulating gonadotropin-releasing hormone (GnRH) secretion in the hypothalamus as *OTX2* transactivates the *GnRH1* promoter (Dateki et al., 2010).

1.5.4 *Otx2* functions and mutations in the retina

The functions of OTX2 differ in the prenatal and mature adult retina. Very early during ocular development, *Otx2* plays a role in the formation of the eye field by cooperating with *Rax* and *Pax6*. *Otx2* is also co-expressed in the neuroepithelial cells of the early optic vesicle with *Rax*, *Pax6*, *Hes1*, *Lhx2*, *Six3* and *Six9* and has been shown to play a role in the patterning of the optic vesicle and regulating the contact between the optic vesicle and the overlying surface ectoderm (Ghinia Tegla et al., 2020). In the early embryonic mouse retina, *Otx2* is expressed in the presumptive RPE. Thus, *Otx2* is essential for RPE specification (~E9.5). *Otx2* inhibits pro-neural factors such as *Sox2* and *Fgf8* to specify the RPE (Nishihara et al., 2012; Pensieri, 2019). In mice that lack *Otx2*, the optic vesicle malforms, and the RPE is converted to the neural retina and optic stalk (Martinez-Morales et al., 2001). In mice that lack either *Otx2* or *Mitf*, the RPE develops abnormally and there is reduced expression of genes important for the process of producing melanin (Beby & Lamonerie, 2013)..

Subsequently, *Otx2* is expressed in retinal progenitor cells in the neuroblastic layer (~E10.5) to regulate photoreceptor specification and differentiation. *Otx2* is expressed at high levels in the layer that is fated to become the photoreceptor layer. *Otx2* is also expressed weakly

in progenitor cells that are fated to become the inner nuclear layer cells (ie. horizontal, amacrine, bipolar cells). Around E12.5, *Otx2* begins to specify photoreceptors by activating photoreceptor genes, such as *Crx* which is required for terminal differentiation of photoreceptors and a normal sleep-wake cycle. When *Otx2* is conditionally ablated in *Crx*-expressing cells in the developing retina, it leads to the loss of *Crx* and loss of rod and cone photoreceptors, bipolar cells and horizontal cells, and the photoreceptors are converted to amacrine-like neurons (Nishida et al., 2003). Misexpression of *Otx2* drove retinal progenitor cells to a photoreceptor cell fate (Nishida et al., 2003).

Later during embryonic development (from E14.5 on), *Otx2* is primarily expressed in the outer NBL, which is the future photoreceptor layer, to regulate photoreceptor terminal differentiation. When both *Otx2* and *Crx* are deleted in the retina (*Otx2*+/-;*Crx*-/-), there is profound downregulation of photoreceptor specific genes, which supports that *Otx2* functions with *Crx* to regulate photoreceptor differentiation (Koike et al., 2007). There is also a loss of key genes for photoreceptor development and survival such as *Crx*, *Nrl*, *Nr2e3* and *Neurod1* in the *Otx2* conditional knockout (Omori et al., 2011). Ectopic expression of *Otx2* in non-retinal cells such as ciliary or iris derived cells can induce ectopic expression of photoreceptor genes such as rod *Opsin* or *Recoverin*, and photoreceptor-like phenotypes (Akagi et al., 2004) (Beby & Lamonerie, 2013).

During late embryonic development, in the outer retina, *Otx2* is expressed in both photoreceptor and bipolar cell progenitors, thus playing a role in both photoreceptor and bipolar cell development (Beby & Lamonerie, 2013). *Otx2* can regulate photoreceptor versus bipolar cell fate by directly targeting *Blimp1*, which represses bipolar cell fate. When *Blimp1* is expressed, it pushes *Otx2*-expressing precursors towards the photoreceptor cell fate (Brzezinski et al., 2010).

Otx2 also represses other retinal lineages. When *Otx2* is ablated in embryonic chick eye via *in ovo* electroporation utilizing CRISPR/*Cas9* mediated gene editing, the mutants demonstrated microphthalmia, optic nerve enlargement, and patches of depigmentation in the RPE. The mutants also demonstrated reduced photoreceptors and bipolar cells which was demonstrated previously (Nishida et al., 2003). Interestingly, this study discovered that in the mutants, the number of *Pou4f2/Pou4f3* positive retinal ganglion cells with similar morphology to the retinal ganglion cells (large soma, dendritic-like neural projections and a long axonal-like neurite) and Lhx1-positive horizontal cells were upregulated significantly. These results suggest that increased horizontal cell and retinal ganglion cell subtypes arise from the *Otx2*+ retinal progenitor cells targeted in the mutants (Ghinia Tegla et al., 2020). This study indicates that OTX2 plays a role in repressing the gene regulatory mechanisms associated with retinal ganglion cell fate and horizontal cell fate (Ghinia Tegla et al., 2020).

Shortly after birth, *Otx2* continues to regulate the long-term maintenance of photoreceptors, and plays a role in bipolar cell terminal maturation (Markitantova & Simirskii, 2020). In postnatal mice where *Otx2* is specifically ablated in bipolar cells, both bipolar cell number and function are diminished (Koike et al., 2007).

In the mature retina, *Otx2* continues to be expressed in the RPE, photoreceptors and bipolar cells and continues to regulate the long-term maintenance of photoreceptors. When *Otx2* loss is induced in the retina by tamoxifen in adult CreERT conditional knockout mouse, slow degeneration of photoreceptor cells develops due to a profoundly disrupted RPE (reduced melanin content, extensive vacuolization, loss of RPE contact with disc-containing photoreceptor outer segments) (Béby et al., 2010; Pensieri, 2019). Furthermore, when *Otx2* is deleted in the adult, *Crx* remains expressed, which suggests *Otx2* functions differently, perhaps by only

regulating RPE genes as opposed to photoreceptor genes in the mature retina (Béby et al., 2010; Pensieri, 2019). Heterozygous *Otx2* mutants survive and demonstrate abnormalities in RPE and retina development. They also display a wide range of eye phenotypes from anophthalmia/microphthalmia to normal (Markitantova & Simirskii, 2020; Ragge et al., 2005).

Similarly in humans, *OTX2* mutations are associated with severe blinding eye phenotypes in addition to brain abnormalities. In humans, various loss-of-function *OTX2* mutations result in various phenotypes such as optic-nerve aplasia, sclerocornea, anophthalmia, microphthalmia, coloboma and Leber congenital amaurosis (LCA), possibly from disrupted *OTX2* regulation of *CRX* function (Ragge et al., 2005). All in all, it is interesting that the mutations of the same *OTX2* gene can result in varying severity of phenotypes between different affected individuals. This suggests a complex system with multiple levels of regulation (Gat-Yablonski, 2011).

Chapter 2: Rationale and Hypothesis

2.1 Rationale

In the developing retina, there exists a group of retinal progenitor cells which, under the regulation of key transcription factors, may commit to either retinal ganglion cell differentiation programming or photoreceptor differentiation pathways (Brown, Patel, Brzezinski, & Glaser, 2001; Dorsky, Chang, Rapaport, & Harris, 1997). For instance, in *Atoh7/Math5* knockout mutant retinas, there is a complete loss of RGCs and increase in photoreceptors (Brown et al., 2001). Interestingly, in the *Dlx1/Dlx2* DKO retina, there is a reduction in RGCs due to enhanced apoptosis, and we also observed an ectopic and increased expression of *Crx* in the ganglion cell layer and neuroblastic layer (de Melo et al., 2005). Although *Crx* is not required for specifying photoreceptors (cell fate determination), it is essential for the development and maintenance of photoreceptors by activating photoreceptor specific genes such as *Rhodopsin* and cone *Opsins* (Jamie L. Zagozewski, Zhang, Pinto, Wigle, & Eisenstat, 2014). This result supports that analogously in the *Dlx1/Dlx2* DKO mutant retina, *Crx* expression is upregulated in certain progenitor cells, which suggests they converted from a retinal ganglion cell fate to a photoreceptor cell fate (de Melo et al., 2005). Hence, *Dlx1*/*Dlx2* may be implicated as being a part of a complex gene regulatory network together with photoreceptor fate determinants such as *Crx* to regulate photoreceptor versus RGC cell fate decisions.

In addition to *Crx*, we also observed increased mRNA expression of *Otx2* in the *Dlx1/Dlx2* DKO retina (Pinto, 2010). *Otx2* is required for photoreceptor specification. Therefore, it is imperative to investigate the role that *Otx2*, the master photoreceptor fate determinant, plays in this gene regulatory network. Transcriptional control of genes in a gene regulatory network largely relies on specific transcription factors binding specific DNA binding sites. We observed that DLX2 occupies both the *Crx* and *Otx2* promoter regions *in vivo* (Pinto, 2010), which

suggests that DLX2 interacts with photoreceptor-fate-determinants such as *Otx2* and *Crx* in a gene regulatory network to regulate cell fate decisions. Reciprocal regulation or cross-regulation of transcription factors to suppress transcription factors responsible for other retinal cell fates has been observed in gene regulatory networks to fine-tune their functions or exert other regulatory effects on cell fate decisions (Hennig, Peng, & Chen, 2008; Yoshida et al., 2004; Zanotti, Smerdel-Ramoya, & Canalis, 2011). For instance, it is previously established that OTX2 activates *Crx* expression to promote photoreceptor development (Hennig et al., 2008; Nishida et al., 2003). CRX also regulates its upstream inducer *Otx2* (Hennig et al., 2008). Both OTX2 and CRX auto-regulates itself through feedback mechanisms (Hennig et al., 2008). We have also observed that DLX1/DLX2 may repress *Otx2* and *Crx* expression in cells destined to become retinal ganglion cells (Pinto, 2010). The role that OTX2 plays in regulating *Dlx2* in this gene regulatory network is not yet understood.

Currently, the cell fates and the gene regulatory networks that are affected by the loss of *Otx2* are not completely understood. *Otx2* ablation in the retina leads to a loss of photoreceptors, and ectopic and abnormal production of amacrine cells (Nishida et al., 2003; Sato et al., 2007). These studies focused on characterizing the mutant phenotype postnatally thus the effects of ablating *Otx2* early during embryonic retinogenesis remains unclear (Ghinia Tegla et al., 2020). In knockout animal models of *Otx2*, *Dlx1/Dlx2* and other retinal ganglion cell markers including *Pou4f2/Brn3b* are upregulated (Ghinia Tegla et al., 2020; Omori et al., 2011), which suggests that OTX2 may suppress other retinal cell fates. We propose that OTX2 restricts retinal progenitor cells from adopting RGC fate by suppressing *Dlx1/Dlx2* genes, which are critical for RGC differentiation, to promote photoreceptor cell fate. We hypothesize that upstream photoreceptor-lineage transcription factor OTX2 regulates *Dlx1/Dlx2* by directly binding and

interacting with the regulatory regions of the *Dlx1/Dlx2* bigene cluster including distal promoter regions upstream *Dlx1* and *Dlx2,* and the *Dx1/Dlx2* intergenic region.

2.2 Hypotheses and Research Aims

Objective: Characterize OTX2 transcriptional regulation of *Dlx2*

Hypothesis: OTX2 restricts RPCs from adopting retinal ganglion cell fate by directly binding and interacting with the regulatory regions of the *Dlx1/Dlx2* bigene cluster to suppress the expression of these genes, which are critical for retinal ganglion cell differentiation, during retina development.

Specific Aim 1: Determine the expression of OTX2 and DLX2 during normal retina development

The expression patterns of OTX2 and DLX2 during early (E13.5) and late (E18.5) embryonic retinogenesis will be characterized by conducting immunofluorescence on wildtype mouse retina sections using OTX2 and DLX2 antibodies.

Specific Aim 2: Determine if OTX2 directly and specifically binds regulatory regions upstream the *Dlx1* and/or the *Dlx2* promoter as well as in the *Dlx1/Dlx2* intergenic region *in vitro*

To determine if OTX2 can directly bind regulatory subregions identified upstream the *Dlx1* and *Dlx2* promoters as well as in the *Dlx1/Dlx2* intergenic region, electrophoretic mobility shift assays will be conducted using recombinant OTX2 protein and radiolabeled oligonucleotide probes corresponding to each subregion.

Specific Aim 3: Determine if OTX2 occupies regulatory regions upstream the *Dlx1* and/or the *Dlx2* promoter as well as in the *Dlx1/Dlx2* intergenic region *in vivo*.

Should we observe that OTX2 is able to directly bind potential regulatory subregions upstream the *Dlx1* and/or *Dlx2* promoters as well as in the *Dlx1/Dlx2* intergenic region *in vitro*, it does not necessarily mean that OTX2 binds these putative regulatory subregions in the relevant biological context at the corresponding developmental time point. Therefore, to determine if OTX2 occupies these potential regulatory subregions *in vivo*, chromatin immunoprecipitation will be conducted on chromatin obtained from E18.5 wildtype retina using OTX2 antibody.

Specific Aim 4: Determine if OTX2 binding of *Dlx1/Dlx2* regulatory regions elicits transcriptional responses *in vitro*

Transcription factor binding does not always affect transcriptional activity or result in any functional response. To determine if OTX2 binding of regulatory subregions affects *Dlx2* transcription, luciferase reporter assays will be performed. EMSA-and-ChIP-identified regulatory subregions bound by OTX2 will be cloned into a luciferase reporter vector. Reporter construct plasmids will be co-transfected with an *Otx2* expression plasmid in HEK293 cells. Reporter gene activity will be assessed by luciferase reporter assays *in vitro*.

Specific Aim 5: Determine the effect of ablating one *Otx2* allele on retina morphology *in situ*

To determine the function of *Otx2* in the developing retina, the retina of a loss of function *Otx2* mouse model will be examined. However, homozygous *Otx2* mutants die embryonically (Acampora et al., 1995). In contrast, heterozygous *Otx2* mice with one *Otx2* allele replaced by GFP were generated to circumvent this issue (Bernard et al., 2014). To assess the effect of ablating a single *Otx2* allele on retina morphology, assessment of histology will be conducted in

wildtype and heterozygous *Otx2* mouse retina sections using haematoxylin and eosin staining (Bernard et al., 2014).

Specific Aim 6: Determine if DLX2 expression is upregulated in the absence of one *Otx2* allele *in situ*

To assess DLX2 protein expression changes in the loss of function heterozygous *Otx2* mouse retina where one allele of *Otx2* is replaced with GFP (Bernard et al., 2014), immunofluorescence on wildtype and heterozygous $Otx2^{+/GFP}$ retina sections will be performed using DLX2 antibody.

Chapter 3: Materials and Methods

3.1 Animals and genotyping

All animal experiments were carried out in accordance with the guidelines set by the Canadian Council on Animal Care and the University of Alberta under Protocol Number 0001115. All routine colony maintenance, tasks, breeding, and biopsy collection was provided by the Health Sciences Laboratory Animal Services at the University of Alberta

Nrp2 knockout mice were provided by Dr. Marc Tessier-Lavigne (The Rockefeller University, NY, USA) and they have a CD-1 background. Homozygous mutant mice are viable and fertile (Chen et al. 2000). Heterozygous and mutant animals were used for breeding and colony maintenance. Juvenile CD-1 mice for the purposes of colony out-crossing the *Nrp2* single knockout colony were also ordered and received from Charles River Laboratories.

Genotyping of the *Nrp2* single knockout colony was performed using RNA extraction as described in Chen et al., 2000 (H. Chen et al., 2000) because the *Nrp2* single knockout colony was generated using a gene trap technology. Tail biopsies are first stored in RNALater, followed by total RNA extraction. The tail biopsies were first homogenized using 1.5mL tube-sized blue pestles in 200µL of Trizol (Invitrogen). The phases were then separated using 40µL chloroform. Next, the samples were precipitated using100µL of 100% isopropanol. The RNA pellet was washed two times with 75% Ethanol and resuspended in RNAse-free H_2O. RNA concentration and purity was determined using the RNA setting on a NanoDrop instrument. 500µg of RNA was used for complementary DNA (cDNA) synthesis according to the First Strand cDNA synthesis protocol of SuperScript III Reverse Transcriptase kit (Invitrogen) using *Nrp2* gene-specific primers RC and RV (**Table 3.1**). Once cDNA was generated, the cDNA was then used as template for PCR amplification using *Nrp2* gene-specific primers RC, RV and F, using the

Hotstar Polymerase kit (Qiagen) to determine genotype. The primer sequences used for *Nrp2* colony genotyping are listed in **Table 3.1**.

For chromatin immunoprecipitation (ChIP) and immunofluorescence experiments, timed-pregnant WT CD-1 mice were ordered and received from Charles River Laboratories. Embryonic age was determined by the day of appearance of the vaginal plug, which is designated to be E0.5.

Table 3.1: List of primers used for genotyping the Nrp2 single knockout mice

Primer Name	**Primer Sequence (5'-3')**
RC	CTGCCCTGGTCCTCACGGATGAC
RV	CTTGAGCCTCTGGAGCTGCTCAGC
F	AGACTACCACCCCATATCCCATGG

3.2 Tissue preparation and cryopreservation

Retinal tissues (eyes/retinas) for chromatin immunoprecipitation experiments were dissected from timed-pregnant CD-1 mice obtained from Charles River Laboratory. For investigating OTX2 occupancy of *Dlx1/2* regulatory regions, E18.5 retina and spinal cord (negative tissue control that does not express OTX2) tissues were dissected using a Leica dissecting microscope. Processing of the dissected tissues will be discussed under the Chromatin Immunoprecipitation section.

Tissues for immunofluorescence experiments were dissected from timed-pregnant CD-1 mice obtained from Charles River Laboratory at E13.5 and E18.5. An earlier time point (E13.5) was also chosen for the immunofluorescence experiments because this is the peak of DLX2 expression; therefore, I sought to examine expression of both OTX2 and DLX2 transcription factors at this time point. Pregnant dams were sacrificed by cervical dislocation at the desired

time point. Embryos were isolated, decapitated and dissected. Eye nuclei and/or heads were dissected for immunofluorescence experiments. For the E13.5 sections, the E13.5 embryos were decapitated, and the head was collected leaving the eyes in place. For the E18.5 sections, the eyes were dissected from E18.5 embryos.

Tissues were then fixed with freshly prepared 4% paraformaldehyde (PFA) for 30 minutes for the E18.5 eyes and 3 hours for the E13.5 eyes with rotation at 4℃ for fixation. Following fixation, tissue was washed with cold 1XPBS and equilibrated using a sucrose gradient (5%, 10%, 15%, 20% to 30%). Tissue was then embedded in an Optimal Cutting Temperature Compound (VWR) filled cryoblock mold placed in a container filled with dry ice. The orientation of the tissue was labelled on the sides of the cryoblock mold and the frozen cryoblocks were then stored at -80℃ prior to sectioning. Cryoblocks were equilibrated for 30 minutes at -20℃ in the Leica CM 1900 Cryostat prior to sectioning. Cryoblocks were sectioned at 10-12µm thickness on the cryostat, and tissues sections were mounted on Superfrost Plus Microscope slides (Fisher Scientific). Slides were stored in slide boxes sealed in Ziploc bags at -20℃ for short-term and at -80℃ for long term prior to immunofluorescence experiments.

For investigation into differential gene expression in the absence of *Nrp2* function, we euthanized the pups at the desired time point postnatally by either decapitation at P7 or by carbon dioxide at P28. The retina was then dissected from P7 and P28 pups. The dissected retina tissues were flash-frozen in liquid nitrogen and stored at -80℃ for subsequent experiments.

3.2 Tissue immunofluorescence

Cryosections were first encircled with hydrophobic pens. Next they were first fixed onto the slides with acetone. Then cryosections were blocked for 2 hours at room temperature with 5% serum blocking solution (0.1% bovine serum albumin (BSA), 0.2% Triton-X-100, 5% serum

in 1XPBS). Following the blocking step, primary antibodies were diluted in the same blocking solution to the desired concentration (see **Table 3.6**). Cryosections were then incubated with the primary antibody dilution solution overnight at 4°C. After overnight incubation, tissues were washed 3 times for 5 minutes using 0.05% Triton-X-100 in 1XPBS solution. Secondary antibodies were diluted to 1:200 in blocking solution. The cryosections were then incubated with secondary solution for 1-2 hours in the dark at room temperature. Slides were then washed again 3 times for 5 minutes each with 0.05% Triton-X-100 in 1XPBS solution. Slides were mounted with VectaShield Mounting Medium containing DAPI (Vector). Coverslips were then applied and sealed using a clear lacquer. Fluorescent images were captured with a Nikon Eclipse TE2000U platform and NIS Elements software.

Dual immunofluorescence with both OTX2 and DLX2 antibodies was also conducted. Procedures for the first primary antibody was the same as previously described. However after incubation of the first secondary antibody and subsequent 3 washes for 5 minutes each, the second primary antibody was applied. The second primary antibody was diluted in blocking buffer to the desired concentration and applied to the same sections and incubated overnight at 4°C. After overnight incubation, tissues were washed 3 times for 5 minutes using 0.05% Triton-X-100 in 1XPBS solution. The appropriate second secondary antibody was diluted to 1:200 in blocking solution. The second secondary antibody solution was applied to the cryosection and incubated in the dark for 1-2 hours at room temperature. Slides were then washed again 3 times for 5 minutes each with 0.05% Triton-X-100 in 1XPBS solution. Slides were then mounted with VectaShield Mounting Medium containing DAPI (Vector). Coverslips were then applied and sealed using a clear lacquer. Fluorescent images were captured with a Nikon Eclipse TE2000U platform and NIS Elements software.

3.4 Electrophoretic mobility shift assay

To investigate whether OTX2 binds to specific DNA regulatory elements, electrophoretic mobility shift assays (EMSA) were conducted. First, complementary oligonucleotides of previously identified regulatory subregions were synthesized by IDT (see **Table 3.2**) Next to anneal the oligonucleotides, forward and complementary oligonucleotides were diluted in one tube to a final concentration of 20pmol/µL each in 1X Annealing Buffer (10mM Tris-HCl pH 7, 1mM EDTA, 50mM NaCl).

Diluted oligonucleotides were then incubated in a heat block that had been heated to 100℃, then immediately switched off after reaching this temperature. Oligonucleotides were then slowly allowed to cool to room temperature to anneal. Annealed oligonucleotides were then labelled using the T4 Polynucleotide Kinase system (Invitrogen) and ɣ-32P-dATP (Perkin Elmer) according to the manufacturer's 5' labelling protocol. The reaction mixture composed of 5pmol of oligonucleotides, 2.5µL 10X reaction buffer B, 1µL (10 units) of T4 Polynucleotide Kinase and ɣ-32P-dATP and nuclease free dH_2O were incubated at 37℃ for 30 minutes. The labelling reaction was then terminated with 1µL 0.5M EDTA (pH 8.0) and 20µL 1X TE (pH 8.0). Labelled probes were then purified to separate unincorporated labels using GE Healthcare Illustra Microspin G-25 Columns (GE Life Sciences).

Probe radioactivity levels were measured using a Beckman Coulter LS 6500 series scintillation counter and subsequently diluted in 1X TE to 80, 000 counts per million (CPM)/µL for all probes corresponding to each binding motif.

Each binding reaction was then performed with labelled probes. First 5X binding buffer (Promega), poly(dI-dC)(Thermofisher Scientific), and 300ng of recombinant OTX2 protein and 600ng of OTX2 antibody for their respective treatment groups were incubated for 30 minutes at

RT. After 30 minutes, radiolabeled probes were added to each binding reaction and incubated for another 30 minutes. There were four binding reaction mixtures corresponding to the four treatment groups for each candidate subregion. The first treatment group was free radiolabeled probes only. The next treatment group was the binding reaction in which radiolabeled probes were added to OTX2 recombinant protein. Next, in the "cold competition" treatment, the radiolabeled probes were added to a reaction mixture containing 30 fold excess of unlabelled probes (10μL) and OTX2 recombinant protein. Next, in the "supershift" treatment, the radiolabeled probes were added to a reaction mixture containing OTX2 recombinant protein and an anti-OTX2 antibody.

The reaction mixtures were then resolved on a non-denaturing vertical 4% acrylamide gel at 300V for approximately one hour and 15 minutes in 0.5X TBE running buffer using a Hoefer SE 600 standard dual cooled gel electrophoresis unit. Resolved gels were then dried onto filter paper wrapped with plastic wrap using Biorad Gel dryer and HydraTech vacuum pump system (BioRad) for 1 hour at 80°C. Dried gels were then exposed to BioMax X-ray film (Kodak Carestream) in a Kodak BioMax cassette with a photo intensifying screen at -80°C for 2 hours or overnight. Films were developed in a dark room using an AFP Imaging Mini-Medical 90 film developer.

Table 3.2: Oligonucleotide probes used for electrophoretic mobility shift assays

Oligonucleotide name	**Oligonucleotide sequence (5'-3')**
EMSA_Dlx2_R1_Sense	TGCACGCCTTTAATCCCAGCACTCAG
EMSA_Dlx2_R1_Antiense_RC	CTGAGTGCTGGGATTAAAGGCGTGCA
EMSA_Dlx2_R2.2_Sense	TGGCACATGCCTTTAATCCCAGCACTTGGGAG

EMSA_Dlx2_R2.2_Antisense_RC	CTCCCAAGTGCTGGGATTAAAGGCATGTGCCA
EMSA_Dlx2_R3_Sense	GGTCCACCAGCGCTAACCCGCCTGCCCTGGG C
EMSA_Dlx2_R3_Antisense_RC	GCCCAGGGCAGGCGGGTTAGCGCTGGTGGAC C
EMSA_Dlx2_R4.1_Sense	GCATTGAGACACCTAACCCTCCTCTACTAGA
EMSA_Dlx2_R4.1_Antisense_RC	TCTAGTAGAGGAGGGTTAGGTGTCTCAATGC
EMSA_Dlx2_R4.2_Sense	TGGCTCATGCCTGTAATCCCAGCACTCAGGA
EMSA_Dlx2_R4.2_Antisense_RC	TCCTGAGTGCTGGGATTACAGGCATGAGCCA
EMSA_IG_R5_Sense	TAAATCTTCATTGTAATCCCCTTCCATTTACT
EMSA_IG_R5_Antisense_RC	AGTAAATGGAAGGGGATTACAATGAAGATTT A
EMSA_IG_R6.1_Sense	TTTCAGGAAGTGTTAATCCCTCAAGATTTGGG
EMSA_IG_R6.1_Antisense_RC	CCCAAATCTTGAGGGATTAACACTTCC TGA AA
EMSA_IG_R6.2_Sense	TTTCAAGGGTCTTTAACCCCAGGTGAGAGGA A
EMSA_IG_R6.2_Antisense_RC	TTCCTCTCACCTGGGGTTAAAGACCCTTGAAA
EMSA_IG_R9.1_Sense	ATAATTTTCCCAAAGATTACCAAGATCTCGAG T
EMSA_IG_R9.1_Antisense_RC	ACTCGAGATCTTGGTAATCTTTGGGAAAATTA T
EMSA_IG_R9.2_Sense	ACATTTATGCTAATAATCTGCAATTTTTTTCA
EMSA_IG_R9.2_Antisense_RC	TGAAAAAAATTGCAGATTATTAGCATAAATG T
EMSA_Dlx1_R7_Sense	AGACACTACATGCTAATCTGATTGCTCTAGAA

EMSA_Dlx1_R7_Antisense_RC	TTCTAGAGCAATCAGATTAGCATGTAGTGTCT
EMSA_Dlx1_R8.1_Sense	ATGGATATCTGGATAAGCCCACAGGGTTAAAC
EMSA_Dlx1_R8.1_Antisense_RC	GTTTAACCCTGTGGGCTTATCCAGATATCCAT
EMSA_Dlx1_R8.2_Sense	TTGCTTCCTACCTTAACCCAAATCCTCCCACC
EMSA_Dlx1_R8.2_Antisense_RC	GGTGGGAGGATTTGGGTTAAGGTAGGAAGCAA

3.5 Chromatin immunoprecipitation

E18.5 embryonic retinal/eye tissues were collected and dissected for chromatin immunoprecipitation (ChIP) experiments from timed-pregnant WT CD-1 mice obtained from the Charles River Laboratories. E18.5 embryonic spinal cords were also collected as a negative tissue control since *Otx2* is not expressed in the spinal cord.

After the tissues were collected, tissues were then washed with ice-cold 1XPBS two times. Tissues were mechanically dissociated into a single cell suspension by triturating with a pipette tip and needle. The cell suspension was then pelleted at 2000rpm at 4°C for 5 minutes to remove the supernatant. Cells were then cross-linked with a freshly prepared solution of 1% paraformaldehyde, 1X protease inhibitor cocktail (1XPIC, Roche), 1mM phenylmethylsulfonyl fluoride (PMSF) for 30 minutes at room temperature. The cell suspension was then centrifuged at 2000rpm at 4°C for 5 minutes and the cell pellet was washed with ice-cold 1X PBS two times to remove paraformaldehyde.

Cross-linked cells were then resuspended in freshly prepared lysis buffer (1%SDS, 10mM Tris-HCl (pH 8.1), 10mM EDTA, 1XPIC, 1mM PMSF) for sonication. In order to generate soluble chromatin complexes, the chromatin was sheared into small pieces between

300-500 base pairs (bp) in size. This is achieved by sonicating the cells on an ice bath using a 60 Sonic Dismembrator probe sonicator (Fisher Scientific). Cells were sonicated at an output power of 40%, for 30 cycles of 15 seconds sonication ON, 30 seconds OFF. To ensure the right fragment size was obtained from the sonication, 3µl of sonicated chromatin was run on a 1% agarose gel. The sonicated chromatin was then centrifuged at maximum speed (14000Xg) for 15 minutes at 4°C to remove insoluble chromatin and cell debris. Sonicated chromatin was then flash-frozen in liquid nitrogen and stored in -80°C for subsequent chromatin immunoprecipitation experiments.

First, at the beginning of the ChIP experiment, two sets of Pierce Ultralink protein A/G beads (60µl beads/sample) were washed two times in 1 mL Dilution Buffer (0.01% SDS, 1.1% Triton-X-100, 1.2mM EDTA, 16.7mM Tris-HCl (pH 8.1), 167mM NaCl, 1X PIC).

One set of beads was used for preclearing. Preclearing beads are first diluted in Dilution Buffer, 1X PIC, 1mM PMSF to a 50% slurry of beads. 60µl of preclearing beads are added to each sample tube each containing 100µl of chromatin sample and rotated at 4°C for 2 hours to reduce nonspecific binding of the antibody to background IgG and other factors that stick to the beads. Samples were then centrifuged and transferred to fresh tubes. The preclearing beads were then discarded. After preclearing was finished, BSA and yeast tRNA (Invitrogen) were added to each sample tube to a final concentration of 0.5mg/mL BSA, 0.5mg/mL yeast tRNA. The precleared samples were then stored at 4°C with rotation until use.

The second set of beads are the actual immunoprecipitation beads (IP beads). The IP beads were first diluted in Dilution Buffer, 1X PIC, 1mM PMSF, 0.5mg/mL BSA, 0.5mg/mL yeast tRNA (Invitrogen) to a 50% slurry of beads. The IP beads alone were then incubated with rotation at 4°C until use.

Next, 3ug of goat OTX2 antibody and 3 µg of goat IgG were added to the respective precleared sample tubes. Next 60µl of primed IP beads were added to each sample tube to precipitate out individual antibody-chromatin-antibody complexes. The samples were incubated with rotation overnight at 4°C.

The following day, beads were pelleted by centrifugation at 2500rpm for 5 minutes at 4°C. The beads were saved. The supernatant which includes the unbound chromatin was removed. Next the beads were subjected to a series of washes with increasingly stringent wash buffers to remove chromatin and proteins that were non-specifically bound to the beads.

1. First washed with Low Salt Wash Buffer (0.1%SDS, 1% Triton-X-100, 2mM EDTA, 20mM Tris-HCl (pH 8.1), 150 mM NaCl) for 5 minutes at 4°C with rotation.
2. Next washed with High Salt Wash Buffer (0.1% SDS, 1% Triton-X-100, 2mM EDTA, 20mM Tris-HCl (pH 8.1), 500mM NaCl) for 30 minutes at 4°C with rotation.
3. Next washed with LiCl Wash Buffer (0.25M LiCl, 1% sodium deoxycholate, 1mM EDTA, 10mM Tris-HCl, 1% NP-40) for 30 minutes at 4°C with rotation.
4. Lastly, chromatin-OTX2-bound beads were then briefly washed two times for 5 minutes each with 1XTris-EDTA (pH 8.0) at 4°C with rotation.

Bead bound antibody-chromatin-protein complexes were eluted from the beads using freshly prepared 100µl of Elution Buffer (1% SDS, 0.1M NaHCO3) preheated to 65°C. Elution was conducted by incubating the samples for 15 minutes at 65°C with agitation (vortexed vigorously) every 2 minutes. Eluted chromatin was then collected by centrifugation at 3000rpm for 5 minutes and transferred to fresh tubes. This elution step was repeated again with another 100µl of Elution Buffer and eluted chromatin from both elution steps were combined into the

same tube. Subsequently, cross-linking was reversed at 65℃ overnight by addition of 25µl of 5M NaCl and 2µl of 5mg/mL RNase A to remove RNA contamination.

Finally, the next morning, 10µl of 0.5M EDTA (pH 8.0), 20µl of 1M Tris-HCl (pH 6.5) and 2µl of Proteinase K were added to the samples and incubated at 55℃ for 2 hours to degrade the proteins.

Lastly, chromatin was purified using QIAQuick PCR Purification Kit (QIAGEN). Purified chromatin was then PCR amplified using primers designed for the putative OTX2 binding sites identified in regulatory regions upstream the *Dlx2* promoter region and in the *Dlx1/Dlx2* intergenic region using Hotstar Polymerase kit (QIAGEN) (see **Table 3.3**). gDNA and molecular biology-grade H_2O were used as positive and negative PCR controls respectively.

Table 3.3: List of primers used in OTX2 ChIP-PCR experiments

Subregion	**Forward Primer Sequence (5'-3')**	**Reverse Primer Sequence (5'-3')**
Dlx2 promoter Subregion 1	GTGAAGGTTTGAGTCCAGAGC	GGCTGTCCTGGAACTCACTT
Dlx2 promoter Subregion 2	GAAACAAACTGGCTGGGTGT	TGGTCTGGAACTTGTGGACT
Dlx2 promoter Subregion 3	GGAGCACCTGGGAGAGAAAA	AGACCCAATCACCATCCGTT
Dlx2 promoter Subregion 4.1	GGCTGCAAACTGAGATGTGT	AGAGAAACTGGCTGCCTGAA
Dlx2 promoter Subregion 4.2	AACCTAGATTTTGGCGGGTG	CACAATCTCAGGACGCTGTG
Dlx2 promoter Subregion 4.12	GGCTGCAAACTGAGATGTGT	TGTGTAGACGAACCTGGCTT
Dlx1/2 Intergenic Subregion 5	CTAACTTGCGCTCCCCAAAG	CCTGCGCTTGTCATATCCTG

Dlx1/2 Intergenic Subregion 6.1	TTGTCAGCGATGTCAGGAGT	TTTCCCCGGGCTCAAGAAA
Dlx1/2 Intergenic Subregion 6.2	GGGTTCTGATGGCTATGGGA	CACCACCACCAATGAACCTG
Dlx1/2 Intergenic Subregion 6.12	TTGTCAGCGATGTCAGGAGT	GGTTTTGCCTTCCTCTCACC
Dlx1/2 Intergenic Subregion 9.1	GCATAACATCTTGACTCCTCGA	CGCTGATGACATTGTGCACT
Dlx1/2 Intergenic Subregion 9.2	ACCAAGATCTCGAGTGCACA	AGCCCCATCTTCCTATGCTG
Dlx1/2 Intergenic Subregion 9.12	GCATAACATCTTGACTCCTCGA	GCCTCTGTCTTTATAGCTGATGA
Dlx1 promoter Subregion 7	CGGCATCCTGTTTTCCCTTT	AGCTTGTTTGGGAAATGGGG
Dlx1 promoter Subregion 8.1	ACACTTGGCCACTTTGCTTT	CCAGGAGAGGTAGCATCAGG
Dlx1 promoter Subregion 8.2	CCATTCTTCAACAGCTGCCA	AGGAGGGGTGGGAGGATTT
Dlx1 promoter Subregion 8.12	ACACTTGGCCACTTTGCTTT	AGGAGGGGTGGGAGGATTT
OTX2 ChIP Positive Control Locus *Irbp*	CCT CAC ATC TAA CTC CCA CAT TG	CCT TGG CTC CTG GAT AAG AG

3.6 Molecular cloning

Molecular cloning of EMSA-positive-ChIP-positive regulatory subregions into the luciferase reporter vector was performed using the Gibson Assembly Cloning Kit (NEB). First, 2µg of pGL4.23 was digested with 10 units of EcoRV Fast Digest enzyme (Fermentas) in 1X Fast Digest Buffer (Fermentas). The digest was run on a 0.8% agarose 1XTBE gel, and then visualized in a Major Sciences UVDI machine. The expected 4000bp band was extracted and

purified using the MinElute Gel Extraction Kit (QIAGEN) per the manufacturer's protocol and eluted in 20µL of molecular biology-grade H_2O. DNA was quantified by Nanodrop.

EMSA-positive-ChIP-positive regulatory subregions were synthesized by IDT and diluted in molecular biology-grade H_2O to 0.1pmol/µL. A two-fold molar excess of insert to vector ratio was used in each assembly reaction. 0.1pmol of insert and 0.05pmol of linearized vector. Next the fragments were diluted to 10µL of molecular biology-grade H_2O and 10µL of 2X Gibson Assembly Master Mix to make a final 20ul assembly reaction. The assembly reaction mixture was incubated at 50℃ for 15 minutes.

Next, chemical transformation was conducted by adding 2µL of the assembly reaction mixture to a freshly thawed 50µL aliquot of NEB 5-alpha Competent *E. Coli*. The tube was flicked gently 4-5 times to gently mix the transformation reaction mixture. The mixture was then incubated on ice for 40 minutes. Next, the transformation reaction mixtures were heat-shocked at 42℃ for 30 seconds and then incubated on ice for 2 minutes. Subsequently, 950µL SOC media warmed to room temperature was added to the transformation reaction mixture and cells were recovered at 37℃ for 1 hour with shaking at 250rpm.

100µL of the recovered cells were then spread on pre-warmed LB plates supplemented with carbenicillin, which were inverted and then incubated overnight at 37℃. Colonies were then streaked out for single colonies on fresh LB plates supplemented with carbenicillin and incubated overnight. The next morning, 7-8 fresh single colonies were selected to each inoculate a 5ml LB culture supplemented with carbenicillin. These cultures were incubated overnight at 37℃ with shaking at 250rpm. Before harvest, glycerol stock was made by adding 500µL of the bacteria culture to 500 µL of 50% glycerol. The bacteria cultures were then harvested for plasmid DNA purification using QIAprep Spin Miniprep kit (QIAGEN) according to the

manufacturer's protocol. Insertion of the desired subregion into the vector was verified by single-direction Sanger sequencing (TAGC, University of Alberta).

3.7 Sequencing of Luciferase reporter constructs

Purified plasmid products were verified by single-direction Sanger sequencing of the full-length regulatory subregion using the RVprimer3. Samples were diluted to 20ng/uL. 10uL of sample and 1uL of 3.2uM (3.2pmol/uL) of RVprimer3 primer were added to 0.2mL strip tubes. Stripped tubes were submitted to TAGC for sequencing (University of Alberta).

3.8 Cell culture

HEK293 cells were acquired from the ATCC. Cells were cultured in a humidified 5% CO2, 37℃ incubator and maintained in 75cm^2 vented flasks (Corning). HEK293 cells were maintained in 15ml of Dulbecco's Modified Eagle Medium (DMEM) (Gibco), supplemented with 10% fetal bovine serum (FBS, Gibco). This cell line was propagated by subculturing every 2 days at 1:5 or every 3 days at 1:10, when cells reached 80% confluence.

Prior to subculturing, all reagents including the media, Trypsin-EDTA and 1XPBS were warmed to 37℃ in a stainless-steel sand incubator for at least 30 minutes. Subculturing was conducted by first aspirating the media. Cells were then gently washed with 1XPBS, then treated with 0.25% Trypsin-EDTA (Gibco) at 37℃ for 2 minutes. Trypsin-EDTA was then inactivated by adding 5-6mL of the DMEM media supplemented with 10% FBS. The cell suspension was then collected into a 15mL conical tube. Trypsin-EDTA was then removed by first centrifuging the cell suspension at 1500rpm for 5 minutes at room temperature and then aspirating the supernatant. The cells were then subcultured at the indicated dilutions or plated for experiments by adding an appropriate amount of DMEM media supplemented with 10% FBS.

3.9 Transfection

One day before transfection, cells were plated at a desired density of $3X10^5$ cells/mL in DMEM+10%FBS in 24 well plate (Corning). Cells were then incubated for 24 hours at 37℃, 5% CO_2 to reach 70% confluence.

The next day, cells were transfected using Lipofectamine 2000 (ThermoFisher Scientific). Transfection was done according to the manufacturer's protocol. For the transfection, 1.5ml microcentrifuge tubes were used to dilute plasmid DNA and dilute the transfection reagent. For transfecting a $10cm^2$ plate for Western Blot experiment, 24µg of total DNA was added to 1.5mL pre-warmed serum-free Opti-MEM growth medium (Gibco) and mixed by pipetting. In a separate microfuge tube, transfection reagent was then diluted by adding 60µl of Lipofectamine 2000 to 1.5mL prewarmed serum-free Opti-MEM growth medium (Gibco). Mixtures were then incubated for 5 minutes at room temperature. After the 5-minute incubation, the diluted DNA and diluted Lipofectamine 2000 were combined in a 15mL conical tube (total volume 3mL). The combined mixture was then gently mixed by inversion and incubated for 30 minutes at room temperature. 3mL of the complexes was then added dropwise to the $10cm^2$ dish containing the cells and the complete growth media. The dish was swirled to mix and returned to the incubator for 48 hours.

For multi-well plate transfection reactions were scaled down according to the Lipofectamine 2000 manufacturer's scale-down protocol as follows:

For a 24-well plate 500ul DMEM+10% FBS media; 1µg of total plasmid DNA diluted in 50µL Opti-MEM; and 2µl of Lipofectamine 2000 reaction diluted in 50µl Opti-MEM. Total transfection complex of 100µl was added to each well containing cells. Plasmids used for each well were as follows: 750ng of pGL4.23 reporter construct (with or without the subregion),

250ng protein expression vector (OTX2-pcDNA3.1+/C-(K)-DYK and 0.1ng TK-Renilla luciferase vector to 50µL of Opti-MEM media. 2µL of Lipofectamine 2000 for each 1X reaction were diluted in 50µl serum free Opti-MEM media. The final volume for each DNA-Lipofectamine 2000 complex was 110µl. Then the transfection mixture was incubated for 30 minutes. 100µL of the transfection mixture was added dropwise to each well. Plates were then gently swirled to mix and returned to the incubator for 48 hours.

3.10 Dual-Luciferase reporter assay

24 hours before transfection, HEK293 cells were plated by adding 500µL of $3X10^5$ cells/mL of cell suspension into each well of a 24-well plate. Each transfection was performed in triplicate as three technical replicates (3 wells) for each treatment condition investigated. For accuracy, transfection reactions were set up by multiplying 1.1 for the quantity of reagents needed for each well. After 24 hours, the cells were transfected as described previously. The following table shows the four co-transfection conditions for each regulatory subregion of interest (**Table 3.4**).

Table 3.4: Plasmids used in each co-transfection condition

1. Empty vector backbones	2. OTX2 alone	3. Regulatory subregion alone	4. OTX2+Regulatory subregion
Empty pGL4.23 Empty pcDNA3 TK-Renilla	Empty pGL4.2 OTX2-pcDNA3.1+FLAG TK-Renilla	pGL4.23-subregion Empty pcDNA3 TK-Renilla	pGL4.23-subregion OTX2-pcDNA3.1+FLAG TK-Renilla

48 hours after transfection, cells were harvested using the Dual-Luciferase Reporter Assay System (Promega). Before starting, kit reagents were brought to room temperature. During the actual Luciferase experiment, media was first aspirated from the wells. Cells were

then washed one time with 1XPBS for 2 minutes. Cells were then lysed with freshly diluted 1X Passive Lysis Buffer (Promega Dual-Luciferase Reporter Assay kit) in pre-warmed 1X PBS by dispensing 100µl of 1X passive lysis buffer into each well. The multi-well plate was then rocked at room temperature to facilitate cell lysis for 30 minutes.

While the multi-well plate was being rotated, 100µl of Luciferase Assay Reagent II was dispensed to individual 1.5mL microfuge tubes. After 30 minutes of cell lysis, the cell lysates were collected into fresh 1.5mL microfuge tubes. Next, the Stop-N-Glo reagent was diluted to 1X in Stop-N-Glo buffer in a non-reactive glass test tube. This was prepared right before the luminescence was measured. The process for measuring luminescence was conducted according to the manufacturer's protocol for the Dual-Luciferase Reporter Assay (Promega). Luminescence was measured using the GloMax Multi Jr Single Tube Multimode Reader (Promega) with the Luminescence Module.

The relative luciferase activity (RLU) was determined as a ratio of Firefly Luciferase to Renilla Luciferase. Average relative luciferase activity (Average RLU) was graphed for each condition. Error bars represent relative luciferase activity (RLU) of each replicate. Fold change was calculated by normalizing each condition to their respective control condition ([RLU of [OTX2+pGL4.23] was normalized to [RLU of pCDNA3+pGL4.23]; RLU of [OTX2+subregion] was normalized to [pcDNA3+subregion). Average fold change was graphed for each condition. Error bars represent standard deviation of fold change of each replicate. Statistical significance between the co-transfection conditions was calculated using the One-Way ANOVA test where $P \leq 0.05$ was considered statistically significant using Sigma Plot.

3.11 Total protein extraction

During the luciferase experiment, a separate 10cm^2 plate of HEK293 cells were transfected as described above with 24 µg of OTX2-FLAG expression vector (OTX2-pcDNA3.1+/C-(K)-DYK). 48 hours after transfection, cells were harvested for Western Blot analysis. This was performed by first aspirating the media from the dishes. Cells were then washed twice in 1XPBS (10mM PO_4^{3-}, 137mM NaCl, 2.7mM KCl, pH7.4). Next cells were collected in 1mL of 1XPBS via plastic cell lifter. Cells were then pelleted by centrifugation at 1000Xg for 5 minutes at 4°C.

For cell lysis, HEK293 cells were lysed in 150µL(per 10cm^2 dish) of Mammalian Lysis Buffer (50mM Tris-HCl (pH7.5), 150 mM NaCl, 1% Triton X-100 and 0.1% sodium deoxycholate) with freshly added 1µL PIC. PMSF was also added to a final concentration of 1mM, and DTT to a final concentration of 1mM.

Cells were then sonicated in an ice bath two times at intervals of 5 seconds sonication ON, 5 seconds sonication off at 30% amplitude using the Sonic Dismembrator ultrasonic processor (Fischer). Cell lysates were then incubated at 4°C with rocking for 30 minutes. After incubation, cell lysates were centrifuged at 12000rpm for 5 minutes at 4°C and supernatant was collected in a fresh 1.5mL Eppendorf tube. Lysates were stored at -80°C for subsequent experiments.

3.12 Protein quantification

After proteins were extracted as previously described, protein concentrations were determined using 5X BioRad Protein Assay (BioRad) reagent diluted 1: 5 in dH_2O to a final concentration of 1X. Protein standards were prepared by diluting 0-20µL of 100mg/mL BSA in 1mL of 1X BioRad Protein Assay to final concentrations of 1000µg/mL, 2000µg/mL,

5000µg/mL, 10000µg/mL, or 20000µg/mL of BSA in cuvettes. Cuvettes containing the protein standards were vortexed briefly twice to mix. We prepared one more cuvette with 1mL of dH_2O as the blank for the spectrophotometer instrument. Next samples were prepared by diluting 2µL of protein samples in 1mL 1X BioRad Protein Assay solution in cuvettes. Cuvettes containing the protein samples were vortexed briefly twice to mix.

Subsequently, light absorbance measurements of the protein standards and samples were read on a GloMax Multi Jr Single Tube Multimode Reader (Promega) with the Absorbance Module. The Photometer mode was selected. To measure the absorbance, the spectrophotometer was first blanked with the cuvette containing only 1mL of dH_2O and then absorbance was measured for each cuvette containing the protein standards first, followed by cuvettes containing the protein samples.

Protein concentrations of the samples were then calculated by interpolation on the standard curve generated from absorbance readings of the protein standards. The standard curve was separately generated for each protein quantification experiment.

3.13 Western blot

Forty-eight hours after transfection. cells were collected and lysed as previously described in the Protein Extraction section. For cell lysis, proteins from samples were extracted also as previously described in the Protein Extraction section. Next, protein concentration was determined as previously described in the Protein Quantification section. Volume for 50µg of protein was calculated for each sample from the specific standard curve.

Protein samples were then denatured by diluting 50µg of protein sample in equal part 2X SDS-PAGE sample buffer (125mM Tris-HCl (pH6.8), 4% SDS, 20% glycerol, 0.02% (v/v) β-mercaptoethanol, 0.005% bromophenol blue). Next, protein samples were denatured by boiling

at 95℃ for 5 minutes followed by incubating on ice. Protein samples were then briefly centrifuged to collect the condensates.

Denatured protein samples were separated based on molecular weight by polyacrylamide gel electrophoresis (SDS-PAGE). 50ug of protein samples were loaded per lane in a 1mm thick discontinuous 4% stacking polyacrylamide gel (125mM Tris-HCl (pH 6.8), 0.1% SDS) and 12% separating polyacrylamide gel (375mM Tris-HCL (pH 8.8), 0.1% SDS). 5µL of Prestained Page Ruler Plus protein ladder (Thermofisher) was loaded into the first well of the SDS-PAGE gel and used as a protein size maker. Next, 50ug of each protein sample in 1X SDS-PAGE sample buffer were loaded into each subsequent well. Next, the SDS-PAGE gel underwent gel electrophoresis in 1X SDS-PAGE running buffer (25mM Tris-HCl, 192mM glycine, 0.1% SDS) at 140 V for 60-75 minutes until the blue dye front reached the bottom of the gel.

Subsequently, separated proteins were transferred to a nitrocellulose membrane using the wet transfer method with pre-chilled Transfer Buffer (20% methanol, 25mM Tris, 192mM glycine, 0.1% SDS) at 110V for 1 hour at 4℃ with stirring. The transfer stack was assembled in the following stack order: red cassette side (positive electrode), one piece of sponge, one piece of thick filter paper, one piece of thin filter paper, membrane, gel, one piece of thin filter paper, one piece of thick filter paper, one piece of sponge, black cassette side (negative electrode). After the transfer was complete, the transfer apparatus was then disassembled. The membrane was then rinsed once with dH_2O to remove traces of methanol.

The membrane was then subjected to immunoblotting. The membrane was first blocked for 2 hours at room temperature in a solution of 50% Li-Cor blocking buffer in 1X PBS 0.05% Tween-20 (PBS-T). After blocking, membranes were directly incubated with primary antibody (mouse anti-FLAG) diluted to the desired concentration in a solution of 50% LI-COR blocking

buffer in 1X PBS 0.05% Tween-20 (PBS-T) overnight at 4°C with rocking. Mouse anti-FLAG antibody was diluted 1: 10,000.

The next day after primary antibody incubation, the membrane was washed four times with PBS-T for five minutes each at room temperature with rocking. Next, the membrane was incubated with anti-mouse secondary antibody (IRDYE 800) diluted 1: 5000 in 50% Li-Cor blocking buffer in PBS-T for 2 hours at room temperature with rocking. The antibody-conjugated immunoblots were then washed two times with PBS-T for five minutes each and then washed once with 1X-PBS at room temperature with rocking. After the last wash, the immunoblots were transferred to a small plastic container containing 1XPBS. The immunoblots were then scanned on the LI-COR Odyssey scanner using the 600 nm channel. The immunoblots were wrapped in plastic wrap and stored at 4°C.

3.14 Paraffin embedding and microtome sectioning

P100 adult mice eyes (received from our collaborators in France) were fixed in Davidson solution (2 parts formalin (37%), 3 parts Ethanol, 1part glacial acetic acid, 3 parts dH_20) for 1 hour and washed with 1XPBS. The eyes were processed in increasing ethanol gradient washes from 75%v/v to 95%v/v to 100%v/v and lastly Xylol prior to being embedded in paraffin as described in Baddam et al. 2021 (Baddam, Kung, Adesida, & Graf, 2021). The paraffin blocks were then sectioned using an 820 Spencer Rotary Microtome at 7µm. The section ribbons were first floated on a cold-water bath. Next, the section ribbons were heated in a 60°C-water bath before mounting on Superfrost Plus slides (Fisher Scientific). The slides were dried overnight on a slide rack.

3.15 Histology (Haematoxylin and Eosin Staining)

Paraffin embedded sections were incubated at 60℃ for 15 minutes until the wax began to melt to further fix the tissues onto the slides. Paraffin-embedded sections were placed in a slide holder. The sections were deparaffinized with two Neo-Clear (Xylene substitute) treatments for 4 minutes each. The sections were then rehydrated by incubating in the following sequence of solutions: two times for 1 minute each with 100% ethanol, 1 minute with 95% ethanol, 1 minute with 70% ethanol; 1 minute with 50% ethanol and 1 minute with distilled water.

Subsequently, the rehydrated slides were incubated in hematoxylin staining solution (Richard Allen Scientific) for 8 minutes. The slides were then rinsed in water for 10 minutes. Slides were then rinsed by dipping in 95% ethanol for 10 times (10 dips). Next the slides were submerged in Eosin staining solution (1% eosin stock dissolved in 80% ethanol and 10ml glacial acetic acid) for 1 minute.

Finally, slides were then cleared and dehydrated in 100% ethanol two times for 5 minutes each. Slides were then incubated two times in Neo-Clear solution for 5 minutes each. Following clearing and dehydration, slides were immediately mounted by adding 1 drop of Neo-Mount (Sigma Aldrich) to the sections and slowly lowering the coverslips on top of the section using a pair of forceps and running it up along to coverslips afterwards to remove any air bubbles. Slides were imaged using Zeiss Stemi 2000-C Brightfield microscope and images were captured using a Leica DM IRB microscope as well as Olympus digital camera, or a Zeiss AxioCam 208 Color microscope-camera imaging system and ZEN 3.2 software as required.

3.16 Immunofluorescence of paraffin embedded sections

Paraffin embedded sections were incubated at 40℃ for 15 minutes until the wax began to melt to fix the tissues onto the slides. The sections were further fixed with 4% paraformaldehyde

for 15 minutes. The sections were deparaffinized with two Neo-Clear (Xylene substitute) treatments for 5 minutes each. The sections were rehydrated by incubating in the following sequence of solutions: two times for 5 minutes each with 100% ethanol, 3 minutes with 95% ethanol, and 3 minutes with 70% ethanol. The sections were then rinsed with distilled water.

While the sections were being rehydrated, the antigen retrieval solution was prepared by diluting 20mL stock Citrate buffer (10mM Tri-Sodium Citrate, 0.05% Tween 20, pH 6.0) solution in 200mL dH_2O with 100µl 1XPBS added. The antigen retrieval solution was heated in a beaker in the microwave first and then a hot plate to 95-100°C. After the Citrate buffer reached its boiling point, sections were immersed and heated in the antigen retrieval solution for 20 minutes to unmask the antigens. After antigen retrieval, the sections were then cooled by placing the beaker in a container that was filled with running tap water for 10 minutes. The slides were washed two times by incubating in 1XPBS-X (1XPBS, 0.05% Triton-X-100) for 5 minutes each.

To prevent non-specific antibody binding and reduce background signal, the sections were then blocked with a 5% serum blocking buffer, which was made from the serum of the host of the secondary antibody, in a humidity chamber for two hours at room temperature.

After two-hours of blocking, the primary antibody was diluted in the same 5% serum blocking solution. After diluting the primary antibody, the blocking buffer was then removed from the sections by horizontally tapping the slide on a paper towel. The sections were incubated with the diluted primary antibody in a humidity chamber overnight at 4°C.

The next day, the primary antibody was first tapped off of the sections. The slides were then washed twice for 5 minutes each with PBS-X. The hydrophobic barriers were also reinforced with the Smear Edge pen at this time. Next the secondary antibody was diluted in the

same 5% serum blocking solution in the dark. Sections were then incubated with ~100µL of secondary antibody per section for 2 hours at room temperature in the dark.

After secondary antibody incubation, the slides were washed for 5 minutes with PBS-X followed by another 5-minute wash with 1XPBS. Finally, the slides were incubated with DAPI (Sigma Aldrich) solution diluted 1:500 in 1XPBS.

Slides were first cleaned using a Kimwipe. Mounting was performed by adding 1 drop of the Prolong Gold Anti-Fade reagent (ThermoScientific) to the sections and slowly lowering the coverslips on top of the section using a pair of forceps and running it up along to coverslips afterwards to remove any air bubbles. The mounted slides were cured overnight in the dark. The slides were imaged using the Axioplan 2 Imaging Fluorescence Microscope and images were captured using the Hamamatsu Orca Digital Camera and Micro-Manager 1.4 imaging software.

3.17 Quantitative real-time polymerase chain reaction

To assess possible changes in mRNA expression of various genes in the *Nrp2* SKO retina, quantitative real-time polymerase chain reaction was performed in P7 and P28 wild-type and *Nrp2* SKO retina.

RNA was extracted immediately after retina dissection by manually homogenizing the samples in 200 µL TRIzol (Invitrogen) with plastic blue pestles that fit into the 1.5mL Eppendorf tubes until completely homogenized. The homogenized samples were incubated for 15 minutes at room temperature. Next 40 µL of Chloroform was added to each sample. The tubes were shaken by hand for 15 seconds. Then the tubes were incubated at room temperature for 3 minutes, followed by centrifugation at 12, 000X RPM for 15 minutes at 4°C. The aqueous phase (top clear layer) of the sample was pipetted and transferred into a new and labelled Eppendorf tube. The interphase and the bottom organize phase was discarded. Next 100 µL of 100%

Isopropanol was added to the aqueous phase in the new Eppendorf tube. The samples were incubated at room temperature for 10 minutes, followed by centrifugation at 12, 000X RPM for 10 minutes at 4℃. The supernatant was removed from tube leaving only the RNA pellet. The RNA pellet was washed two times each as follows: 200 µL of 75% Ethanol was added to each sample, the samples were vortexed briefly and centrifugated at 7, 500X RPM for 5 minutes at 4℃, the supernatant was removed. The RNA pellet was air dried for 30 minutes. The RNA pellet was re-suspended in RNAse-free H_2O by gentling piepetting up and down. The concentration and purity of RNA was measured using a NanoDrop Spectrophotometer.

RNA was then reverse transcribed to cDNA using Superscript III Reverse Transcriptase kit (Invitrogen) and random Oligo(dT) primers as per the manufacturer's manual. 500ng of RNA, 1µL of Oligo(dT) and 1µL of dNTP were mixed and incubated at 65℃ for 5 minutes in the thermocycler (Bio-Rad). Next, the samples were incubated on ice for 1 minute. 4uL 5X First-Strand Buffer, 1µL DTT, 1µL RNaseOUT, and 1µL Superscript III reverse transcriptase were added to the mixture, followed by one hour incubation at 50 ℃ and 15-minute incubation at 70℃ in the thermocycler (Bio-Rad).

Quantitative real-time PCR was conducted by dispensing 1µL of sample cDNA diluted 1:5 in H_2O, 1µL of 10µM forward primer, 1µL of 10µM reverse primer for each gene, 10µL of 2X FastStart SYBR Green Master Mix (Roche Life Sciences) and 7µL H_2O in a 96 plate. The plate was sealed with tape and then the reaction was conducted using a LightCycler 96 System (Roche). The program used was the standard 3-step amplification program as follows: 1 cycle of pre-incubation at 95℃ for 600 seconds; 45 cycles of 3-step amplification with an annealing temperature of 57℃ (95℃ for 10 seconds; 57℃ for 15 seconds; 72℃ for 15 seconds); 1 cycle of melting (95℃ for 10 seconds; 65℃ for 60 seconds; 97℃ for 1 second); 1 cycle of cooling at

37℃ for 30 seconds. The data was analyzed using the ΔΔCt method. First the average Ct for each gene subtracts the average Ct for the internal control gene for both the wild type and the mutant to obtain the ΔCt value of each gene for the wildtype and mutant. For each gene, the ΔCt of the mutant subtracts the ΔCt of the wildtype to obtain the ΔΔCt value. The fold change of gene in the mutant was calculated using the formula $2^{-\Delta\Delta Ct}$. Statistical analysis (paired Student's t-test, $p<0.05$) is conducted and the graph is generated using Sigma Plot. The sequences of primers for genes investigated are listed in **Table 3.5**.

Table 3.5: List of qRT-PCR primers used for gene expression studies

Primer Name	**Primer sequence (5'-3')**
STX1_FWD_qPCR	AGAGATCCGGGGCTTTATTGA
STX1_REV_qPCR	AATGCTCTTTAGCTTGGAGCG
CALB2_FWD_qPCR	AGTACACCCAGACCATACTACG
CALB2_REV_qPCR	GGCCAAGGACATGACACTCTT
PROX1_FWD_qPCR	AGAAGGGTTGACATTGGAGTGA
PROX1_REV_qPCR	TGCGTGTTGCACCACAGAATA
RCVRN_FWD_qPCR	ACGACGTAGACGGCAATGG
RCVRN_REV_qPCR	CCGCTTTTCTGGGGTGTTTT
RHO_FWD_qPCR	CCCTTCTCCAACGTCACAGG
RHO_REV_qPCR	TGAGGAAGTTGATGGGGAAGC
MOPSIN_FWD_qPCR	ATGGCCCAAAGGCTTACAGG
MOPSIN_REV_qPCR	CCACAAGAATCATCCAGGTGC

SOPSIN_FWD_qPCR	CAGCCTTCATGGGATTTGTCT
SOPSIN_REV_qPCR	CAAAGAGGAAGTATCCGTGACAG
VSX2_FWD_qPCR	CTGAGCAAGCCCAAATCCGA
VSX2_REV_qPCR	CGCAGCTAACAAATGCCCAG
BRN3A/POU4F1_FWD_qPCR	CGCGCAGCGTGAGAAAATG
BRN3A/POU4F1_REV_qPCR	CGGGGTTGTACGGCAAAATAG
BRN3B/POU4F2_FWD_qPCR	TGGACATCGTCTCCCAGAGTA
BRN3B/POU4F2_REV_qPCR	GTGTTCATGGTGTGGTAAGTG G
36B4_FWD_qPCR	GTGTGTCTGCAGATCGGGTA
36B4_REV_qPCR	CAGATGGATCAGCCAGGAAG

Table 3.6: List of antibodies used for immunofluorescence and ChIP experiments

Antibody	Source	Dilution	Use	Catalog #
Rabbit DLX2	Dr. D. Eisenstat	1:200 (IF)	Primary antibody for immunofluorescence experiments	N/A
Alexa Fluor 488 (green)	Invitrogen	1:200	Secondary Antibody for IF	A21206(dar) A11055(dag)
Alex Fluor 594 (red)	Invitrogen	1:200	Secondary Antibody for IF	A21207(dar) A11058(dag) (dar)
Goat Polyclonal Anti-Otx2	Santa Cruz Biotechnology	1:200 for IF	ChIP IF EMSA	Sc-30659
Normal Goat IgG	Santa Cruz Biotechnology	N/A	ChIP	sc-2028
Monoclonal Anti-FLAG produced in mouse	Millipore Sigma	1:10,000	Western Blot	F1804-50UG
IRDYE Anti-mouse IgG 800 (green) Secondary Antibody	LI-COR	1: 5,000	Secondary antibody for Western Blot	926-32210

Chapter 4: Results

4.1 DLX2 and OTX2 expression at E13.5 and E18.5 in wild-type mouse retina

Since *Otx2* activates photoreceptor genes, whereas *Dlx2* activates RGC genes, we hypothesize that OTX2 represses retinal ganglion cell gene expression to promote photoreceptor cell fate. Therefore, if OTX2 represses *Dlx2*, then we expect *Otx2*-expressing cells to not express *Dlx2*. Expression patterns of *Otx2* and *Dlx2* were characterized by single immunofluorescence and double immunofluorescence with OTX2 and DLX2 antibodies on E13.5 and E18.5 mouse retina tissue sections. These time points were assessed because E13.5 corresponds to the window when cone photoreceptors are actively being produced (Emerson, Surzenko, Goetz, Trimarchi, & Cepko, 2013). *Otx2* is expressed in a group of early retinal progenitor cells before photoreceptors are formed. The role that *Otx2* plays in regulating these retinal progenitor cells is unknown (Buenaventura, Ghinia-Tegla, & Emerson, 2018; Ghinia Tegla et al., 2020). E18.5 was also assessed because it corresponds to the window when rod photoreceptors are produced.

Figure 4.1A demonstrates that at E13.5, DLX2 is expressed throughout the retina and primarily in the central and inner retina. At E13.5, OTX2 is expressed throughout the neuroblastic layer, primarily in the outer neuroblastic layer (oNBL), and in the retinal pigmented epithelium (RPE) (**Figure 4.1B**). At E13.5, there are a few OTX2/DLX2 co-expressing cells localized primarily in the central and inner portions of the NBL (**Figure 4.1C**). At E18.5, DLX2 is expressed in the ganglion cell layer and the inner retina (inner neuroblastic layer, iNBL) (**Figure 4.1D**). At this time point, OTX2 is expressed primarily in the outer retina (outer neuroblastic layer, oNBL) and the RPE (**Figure 4.1E**). Evidently, at this stage, OTX2 and DLX2 expression domains become more distinct (**Figure 4.1F**). OTX2-expressing cells become restricted to the outer retina (presumptive photoreceptor layer), whereas DLX2-expressing cells become restricted to the inner retina (presumptive retinal ganglion cell layer) respectively. At

this stage, there are only some OTX2/DLX2 co-expressing cells localized in the inner portions of the NBL (**Figure 4.1F**).

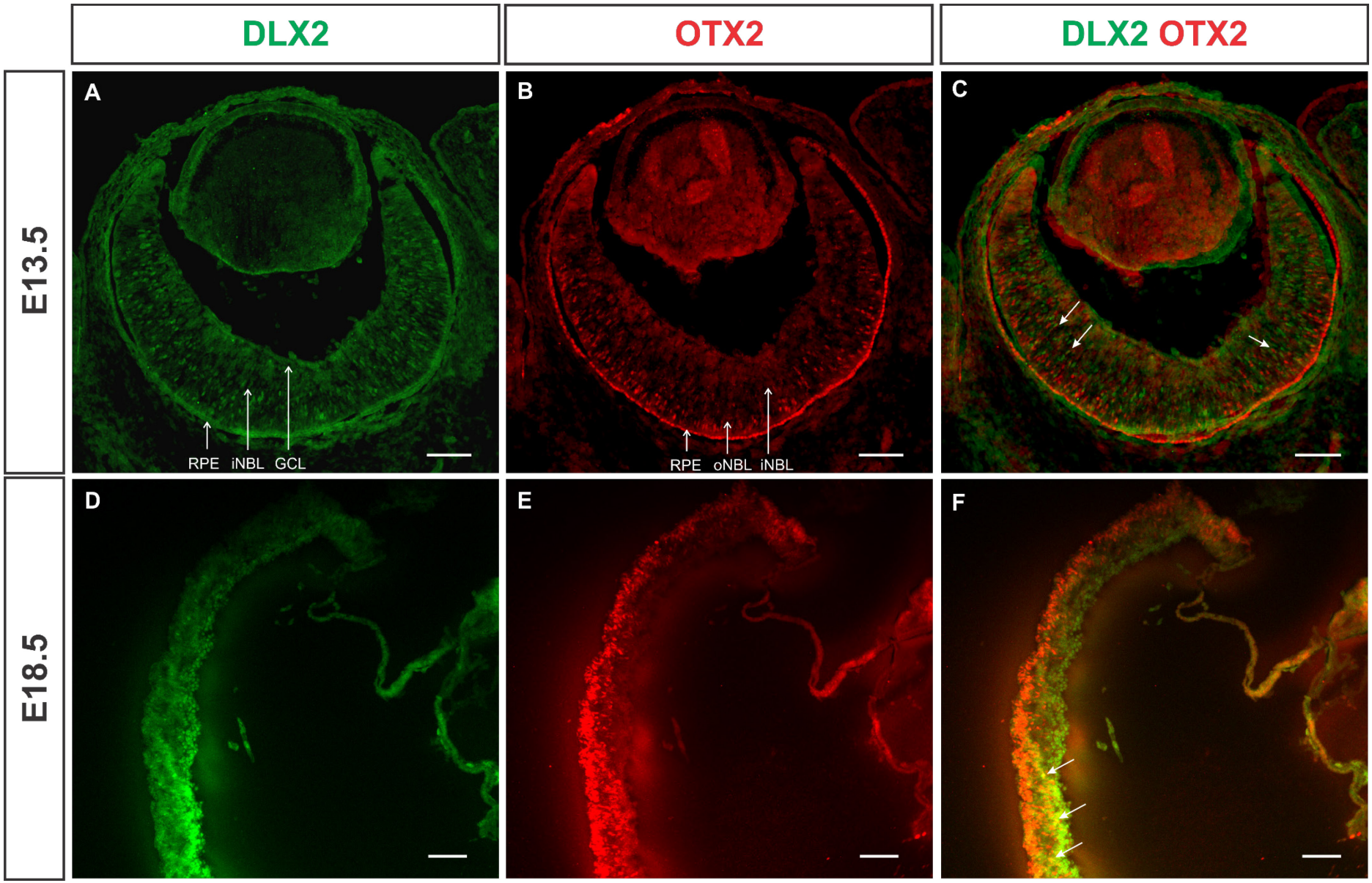
DLX2
OTX2
DLX2 OTX2
E13.5
E18.5
A
B
C
D
E
F
RPE
iNBL
GCL
RPE
oNBL
iNBL

Figure 4.1

DLX2 and OTX2 protein expression in the embryonic neural retina at embryonic day 13.5 (E13.5) and embryonic day 18 (E18.5)

A. Single immunofluorescence expression of DLX2 on a representative wildtype E13.5 mouse retina section.
B. Single immunofluorescence expression of OTX2 on a representative wildtype E13.5 mouse retina section.
C. Overlaid images of single immunofluorescence experiments using DLX2 and OTX2 antibodies on a representative wildtype E13.5 mouse retina section.
D. Single immunofluorescence expression of DLX2 on a representative wildtype E18.5 mouse retina section.
E. Single immunofluorescence expression of OTX2 on a representative wildtype E18.5 mouse retina section.
F. Double immunofluorescence expression of DLX2 and OTX2 on a representative wildtype E18.5 mouse retina section.

RPE, retinal pigmented epithelium; iNBL, inner neuroblastic layer; oNBL, outer neuroblastic layer; GCL, ganglion cell layer.

Scale bars are equivalent to 100μm.

4.2.1 The *Dlx1/Dlx2* regulatory regions contain multiple candidate OTX2 homeodomain protein binding sites

In order to determine whether OTX2 directly and specifically binds to regulatory regions of *Dlx1/Dlx2*, the DNA sequences of upstream the *Dlx1/Dlx2* promoters and intergenic regulatory regions were analyzed to identify candidate OTX2 binding motifs. It is important to distinguish the *Dlx1/Dlx* proximal/basal "promoter" from the regulatory regions that were

examined in the present study. The *Dlx1/Dlx2* proximal "promoter" refers to the basal/core promoter of *Dlx1* and *Dlx2* which contains the transcription start site, a binding site for RNA polymerases and binding sites for general transcription factors such as the TATA element and a B recognition element (within 30 to 40 base pairs). Whereas the regulatory regions that we were investigating are the distal promoter that is upstream (10 kilo-base pairs) of the basal promoter and contains various regulatory elements to facility other transcription factor binding. There are several candidate homeodomain motifs that OTX2 can recognize and bind to in target regulatory regions. The canonical or most enriched OTX2 binding site is TAATCC (Sakai et al., 2017). OTX2 also binds similar motifs with a certain level of flexibility at positions 4 and 5, and sometimes at position 6 (Samuel, Housset, Fant, & Lamonerie, 2014). Therefore, TAACCC, TAAGCC and TAATCT are also potential OTX2 binding motifs (Sakai et al., 2017). Therefore, a 10kb region upstream of the *Dlx1* and *Dlx2* transcriptional start site was analyzed using the UCSC Genome Browser. The entire sequence range was searched manually for candidate homeodomain binding motifs: TAATCC, TAACCC. TAAGCC and TAATCT. This *in silico* analysis revealed multiple putative OTX2 homeodomain binding sites (**Figure 4.2A**; **Table 4.1**).

The analysis revealed that the region upstream the *Dlx2* promoter contains 5 candidate binding sites (**Figure 4.2A**). Some candidate binding sites are fairly close to each other, thus they were grouped into one subregion. Thus, the *Dlx2* upstream region was subdivided into smaller subregions containing 1 to 2 binding sites each (Subregion 1, Subregion 2, Subregion 3, Subregion 4.12). The *Dlx1/2* intergenic region contains 5 candidate binding sites and was also subdivided into three smaller subregions containing 1 to 2 binding sites each (Subregion 5, Subregion 6.12, Subregion 9.12). The *Dlx1* gene locus contains one candidate binding site (Subregion 7). The region upstream the *Dlx1* promoter contains 2 candidate binding sites which

are fairly close together and were grouped into one Subregion 8.12. These subregions were used to conduct subsequent *in vitro* and *in vivo* experiments characterizing transcription factor-DNA interactions

The ChIP-seq datasets for several histone posttranslational modifications in the mouse forebrain at P0 (UCSC Genome Browser) showing locations of H3K27Me3, H3K27ac, H3K4Me2 and H3K4Me1 enrichment were also analyzed. ChIP-Seq data in the forebrain was searched because the neural retina is an extension of the developing forebrain and also ChIP-Seq data in the retina is not publicly available in the Genome Browser. H3K27Me3 is associated with chromatin that is repressively marked, whereas H3K27ac, H3K4Me2 and H3K4Me1 mark chromatin that is actively primed for transcription. Upstream the *Dlx2* promoter, there were many small repressive H3K27Me3 peaks which are statistically significant, as indicated by red rectangular boxes according to the UCSC genome browser (**Figure 4.2B**). The locations of the peaks correspond to subregions containing putative OTX2 binding motifs (**Figure 4.2A-B**). This *in silico* analysis supports that OTX2 may repress *Dlx2* expression. Furthermore, in the *Dlx1/Dlx2* intergenic region, there were a few identified H3K27Me3 peaks, as well as several prominent H3K4Me2 and H3K27ac peaks. H3K4Me2 and H3K27ac are generally considered as activating chromatin marks. Of note, H3K27ac is often viewed as an “active enhancer” mark. This explains why some H3K27ac peaks in the intergenic region correspond to locations of the intergenic enhancers *I12a* and *I12b*. In addition, upstream the *Dlx1* promoter, there was one H3K27Me3 peak and one small H3K27ac peak which corresponds to where the putative Subregion 8.12 was identified.

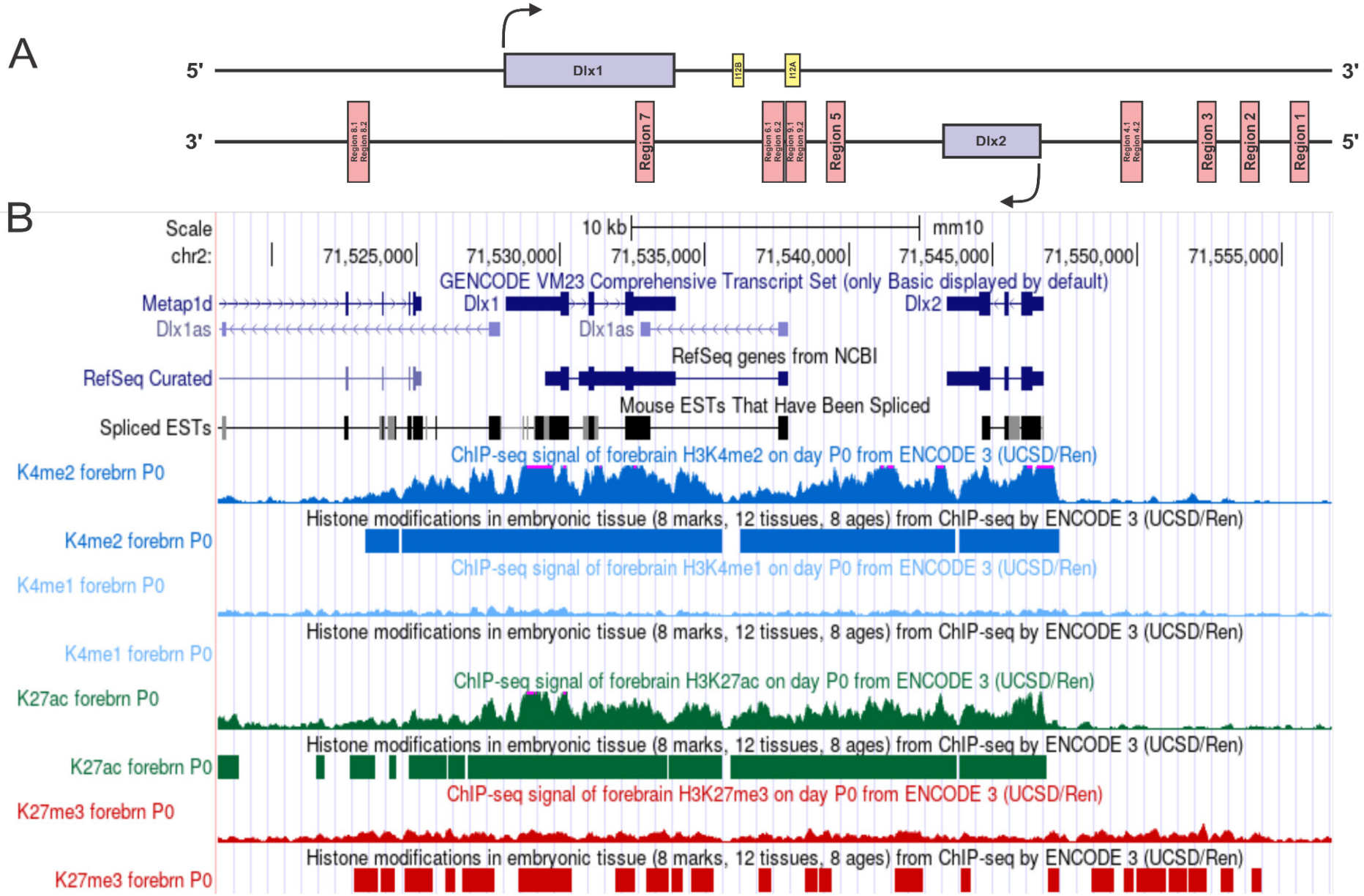
A
5'
3'
Dlx1
I12B
I12A
Dlx2
Region 8.1
Region 8.2
Region 7
Region 6.1
Region 6.2
Region 9.1
Region 9.2
Region 5
Region 4.1
Region 4.2
Region 3
Region 2
Region 1
B
Scale
chr2:
10 kb
mm10
71,525,000
71,530,000
71,535,000
71,540,000
71,545,000
71,550,000
71,555,000
GENCODE VM23 Comprehensive Transcript Set (only Basic displayed by default)
Metap1d
Dlx1
Dlx2
Dlx1as
Dlx1as
RefSeq genes from NCBI
RefSeq Curated
Mouse ESTs That Have Been Spliced
Spliced ESTs
ChIP-seq signal of forebrain H3K4me2 on day P0 from ENCODE 3 (UCSD/Ren)
K4me2 forebrn P0
Histone modifications in embryonic tissue (8 marks, 12 tissues, 8 ages) from ChIP-seq by ENCODE 3 (UCSD/Ren)
K4me2 forebrn P0
ChIP-seq signal of forebrain H3K4me1 on day P0 from ENCODE 3 (UCSD/Ren)
K4me1 forebrn P0
Histone modifications in embryonic tissue (8 marks, 12 tissues, 8 ages) from ChIP-seq by ENCODE 3 (UCSD/Ren)
K4me1 forebrn P0
ChIP-seq signal of forebrain H3K27ac on day P0 from ENCODE 3 (UCSD/Ren)
K27ac forebrn P0
Histone modifications in embryonic tissue (8 marks, 12 tissues, 8 ages) from ChIP-seq by ENCODE 3 (UCSD/Ren)
K27ac forebrn P0
ChIP-seq signal of forebrain H3K27me3 on day P0 from ENCODE 3 (UCSD/Ren)
K27me3 forebrn P0
Histone modifications in embryonic tissue (8 marks, 12 tissues, 8 ages) from ChIP-seq by ENCODE 3 (UCSD/Ren)
K27me3 forebrn P0

Figure 4.2

The Dlx1/Dlx2 regulatory regions, including the distal promoter regions upstream Dlx1, Dlx2 and the Dlx1/Dlx2 intergenic region, contain multiple candidate OTX2 homeodomain binding sites that correspond to histone modification peaks

A. Scaled schematic of the range spanning from 10kb upstream the *Dlx2* promoter to 10kb upstream the *Dlx1* promoter, where 83.6mm is equivalent to 10kb. Arbitrary numbers (i.e. Region 1, Region 2 etc.) were designated to these regulatory subregions each containing one to two putative OTX2 binding sites. The 10kb region upstream the *Dlx2* transcriptional start site contains 5 putative homeodomain binding motifs. Subregion 4.12 contains two binding motifs close together (Region 4.1/Region 4.2). The *Dlx1/Dlx2* intergenic region contains 5 putative homeodomain binding motifs. Subregion 6.12 and Subregion 9.12 each contain two binding motifs close together (Subregion 6.1/Subregion 6.2; Subregion 9.1/Subregion 9.2, respectively). Subregion 7 is located in the *Dlx1* locus. The 10kb region upstream the *Dlx1* transcriptional start site contains 2 putative homeodomain binding motifs close together, and thus were grouped into one Subregion 8.12.
B. The top 2 tracks are UCSC tracks displaying the genomic locations of *Dlx1* and *Dlx2* genes and 10kb upstream and downstream of the *Dlx1/Dlx2* bigenic cluster. The top track represents the *Dlx1/Dlx2* gene predicted by GENCODE. The track underneath is another gene prediction track curated from NCBI RefSeq reference collection. The Spliced EST track indicates possible splice variants of *Dlx1/Dlx2* genes when the gene sequences are aligned to mouse expressed sequence tags (EST). The next 8 colorful tracks are UCSC Genome Browser tracks that display ChIP-Seq enrichment for several histone

posttranslational modifications including H3K4Me2, H3K4Me1, H3K27ac and H3K27Me3 in this range in P0 mouse forebrain. ChIP-Seq signals, enriched for H3K4Me2 (dark blue), H3K4Me1 (light blue), H3K27ac (dark green), and H3K27Me3 (red), are displayed as two separate tracks corresponding to their respective colors. For each type of histone posttranslational modification, the top spiked track represents all enrichment signals; and the bottom rectangular-box track contains only statistically significant rectangular box-shaped peaks.

Table 4.1: Nucleotide positions of OTX2 binding motifs in the Dlx1/Dlx2 regulatory regions with Dlx2 TSS as position 0

Subregion	**Nucleotide position**
Dlx2 promoter Subregion 1	-8793 to -8616
Dlx2 promoter Subregion 2	-7129 to -6879
Dlx2 promoter Subregion 3	-5664 to -5422
Dlx2 promoter Subregion 4.1	-3162 to -2995
Dlx2 promoter Subregion 4.2	-2793 to -2638
Dlx2 promoter Subregion 4.12	-3162 to -2678
Dlx1/2 Intergenic Subregion 5	6776 to 6948
Dlx1/2 Intergenic Subregion 9.1	9721 to 9877
Dlx1/2 Intergenic Subregion 9.2	9845 to 10069
Dlx1/2 Intergenic Subregion 9.12	9721 to 9942
Dlx1/2 Intergenic Subregion 6.1	10420 to 10570
Dlx1/2 Intergenic Subregion 6.2	10694 to 10870
Dlx1/2 Intergenic Subregion 6.12	10420 to 10789
Dlx1 promoter Subregion 7	13398 to 13637
Dlx1 promoter Subregion 8.1	23284 to 23037

Dlx1 promoter Subregion 8.2	23357 to 23602
Dlx1 promoter Subregion 8.12	23037 to 23602

4.2.2 Multiple candidate OTX2 homeodomain protein binding sites upstream the *Dlx2* promoter are conserved among vertebrate species

Multiple alignment data of various vertebrate data from the UCSC Genome Browser were obtained. If some of these subregions are actual regulatory regions where OTX2 can bind, we would expect that they are conserved between various species. Subregions 1, 2, 4.1 and 4.2 upstream the *Dlx2* promoter contain putative OTX2 homeodomain binding motifs, such as TAATCC/GGATTA or TAACCC/GGGTTA that were conserved between various vertebrate species (**Figure 4.3**). The *Dlx1/Dlx2* intergenic subregion 9.12 (*I12a Dlx1/Dlx2* intergenic enhancer) contains one putative OTX2 homeodomain binding motif, TAATCT/AGATTA that was conserved among many vertebrate species (**Figure 4.3**). These data add confidence that these subregions to be examined are more likely to be "true" regulatory regions because the DNA motifs that transcription factors recognize are fairly well conserved between species (Nitta et al., 2015).

Subregion 1

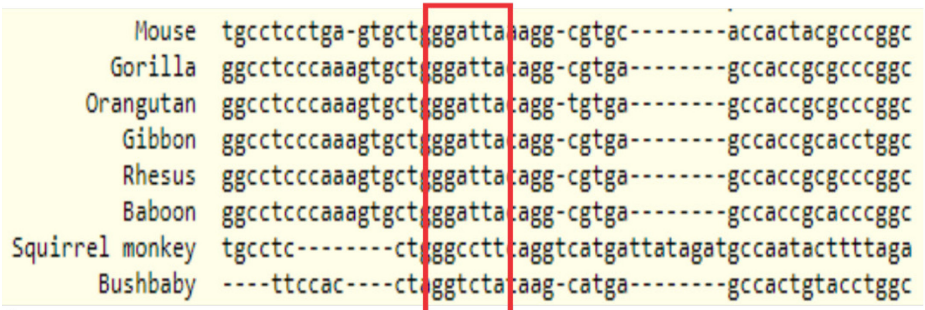

Subregion 2

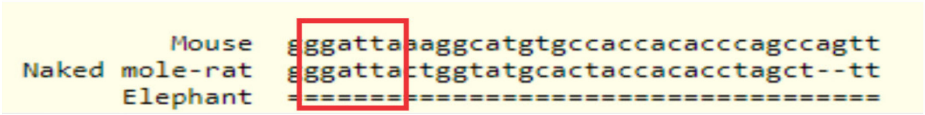

Subregion 4.1

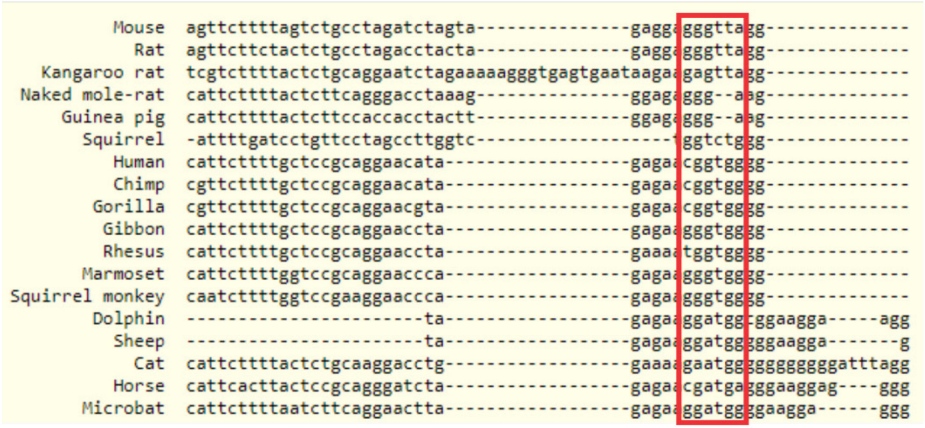

Subregion 4.2

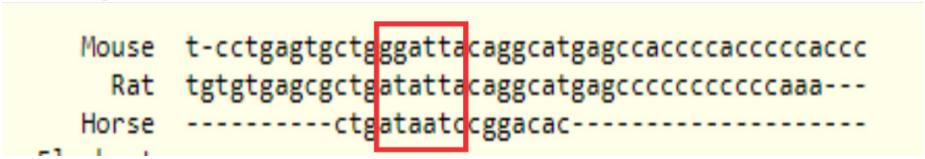

Subregion 9.12 (I12A)

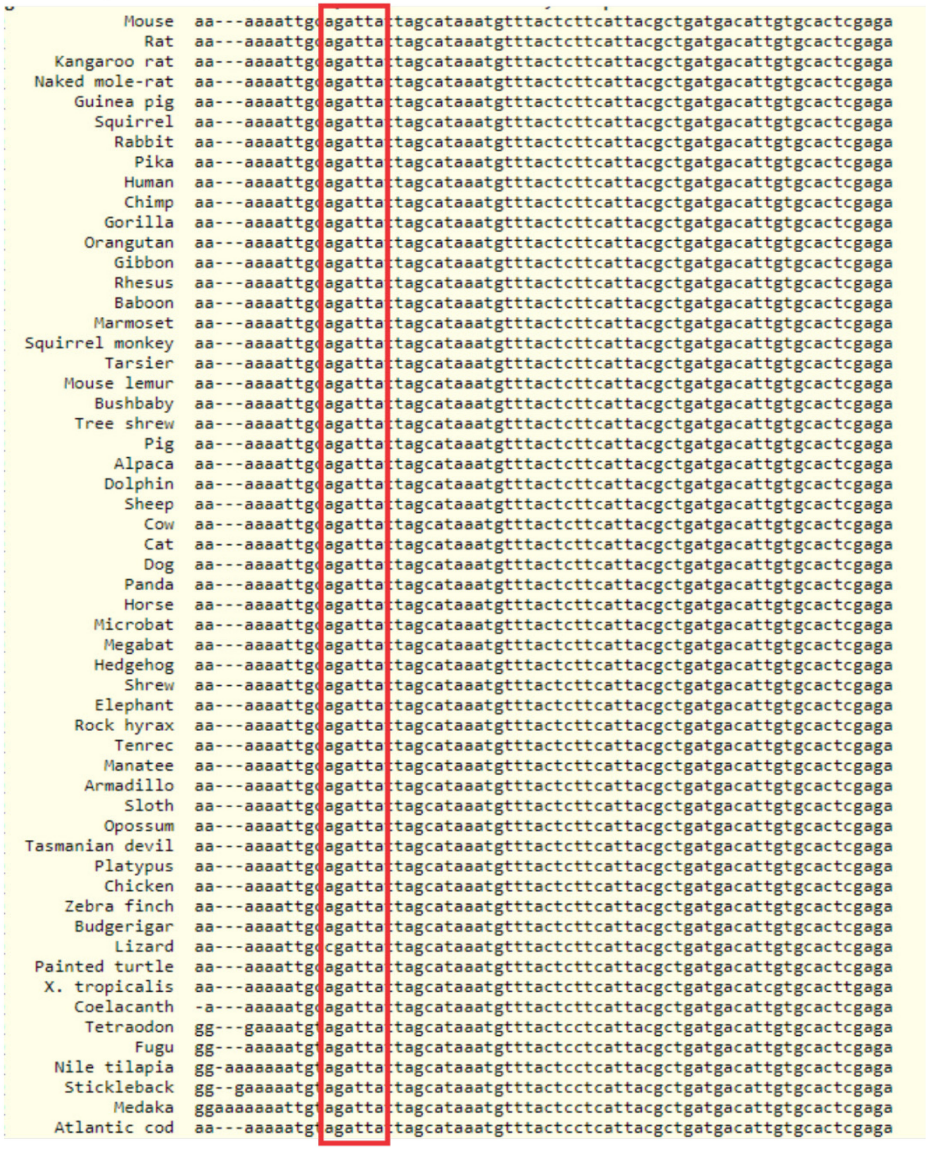

Figure 4.3

Multiple sequence alignments of candidate OTX2 homeodomain protein binding sites upstream the Dlx2 promoter between vertebrates

Multiple alignment data of Subregions 1, 2, 4.1 and 4.2 upstream the *Dlx2* promoter and the *Dlx1/Dlx2* intergenic enhancer, were obtained from the UCSC Genome Browser. The red box outlines the conserved motif. Subregions 1, 2, 4.1 and 4.2 contain putative OTX2 homeodomain protein binding motifs, such as TAATCC/GGATTA or TAACCC/GGGTTA, that were conserved between various vertebrate species. The *Dlx1/Dlx2* intergenic subregion 9.12 (*I12a Dlx1/Dlx2* intergenic enhancer) contains one putative OTX2 binding motif, TAATCT/AGATTA, that was conserved among multiple vertebrate species.

4.3 OTX2 directly binds upstream the *Dlx2* promoter, the *Dlx1/Dlx2* intergenic region, and upstream the *Dlx1* promoter *in vitro*

Electrophoretic mobility shift assays (EMSA) were conducted to determine if OTX2 directly binds a candidate regulatory subregion upstream the *Dlx1/Dlx2* promoter and in the intergenic region *in vitro*. Short (20-25bp) complementary oligonucleotides containing the TAATCC, TAAGCC, TAACCC motifs and short sequences flanking each motif were ordered and 5' labelled with [γ-32P]-dATP. Radiolabeled probes that correspond to each putative OTX2 binding motifs upstream the *Dlx2* promoter (Subregion1, Subregion 2, Subregion 3, Subregion 4.1, Subregion 4.2), in the *Dlx1/Dlx2* intergenic region (Subregion 5, Subregion 6.1, Subregion 6.2, Subregion 9.1, Subregion 9.2) and upstream the *Dlx1* promoter (Subregion 7, Subregion 8.1, Subregion 8.2) were then incubated with recombinant OTX2 protein and separated by polyacrylamide gel electrophoresis on a 4% acrylamide gel.

If OTX2 directly binds a candidate binding motif, we would expect an upwards mobility shift on the gel when probes are incubated with the recombinant OTX2 compared to the free probe, reflecting the formation of higher molecular weight DNA-protein complexes. When the specific OTX2 antibody was added to the binding reaction, we would expect a greater extent of upward mobility shift (or a "supershift"), which represents a DNA-protein-antibody complex with a higher molecular weight has formed. The supershift supports that OTX2 specifically and directly binds these subregions *in vitro*. In the cold competition lane, the specific unlabelled probe competes away the labelled target probe for binding the recombinant OTX2; thus, if binding is specific, we expect to see the shifted band representing the OTX2-probe complex to disappear. This control further supports that binding of the DNA motif by the transcription factor is specific.

There are several controls incorporated into this experiment for specificity of binding: (1) labelled probes alone where no recombinant OTX2 protein was added. (2) A "supershift" treatment to control for specificity of protein-DNA interaction where a specific OTX2 antibody was added to the binding reaction. (3) Lastly, there was a "cold competition" control, where an excess of unlabeled probe was added to the binding reaction to compete away binding of the labelled target. This controls for OTX2 protein specifically binding the target motif.

All subregions except Subregion 3 and Subregion 4.1 demonstrated protein-probe binding resultant shift and antibody-protein-probe binding resultant supershift (**Figures 4.4-4.6**). Hence, these results demonstrate OTX2 directly binds Subregions 1, 2 and 4.2 upstream the *Dlx2* promoter (**Figure 4.4**), Subregions 5, 6.1, 6.2, 9.1 and 9.2 of the *Dlx1/Dlx2* intergenic region (**Figure 4.5**), Subregions 7 in *Dlx1* locus and Subregion 8.1 and 8.2 upstream the *Dlx1* promoter (**Figure 4.6**) *in vitro*.

Subregion 3 and Subregion 4.1 upstream of the *Dlx2* promoter failed to bind OTX2 directly in EMSA *in vitro* (**Figure 4.4**) thus these individual subregions were not carried forward further for luciferase experiments. The entire Subregion 4.12 was still carried forward because Subregion 4.2 bound OTX2. Subregions 3 and 4.1 contained the TAACCC motif. This motif was also present in Subregions 6.2, 7 and 8.2, for which the EMSA experiments successfully showed OTX2 binding. This indicates OTX2 is capable of binding the TAACCC motif, and that OTX2 would not bind Subregion 3 and Subregion 4.1 specifically.

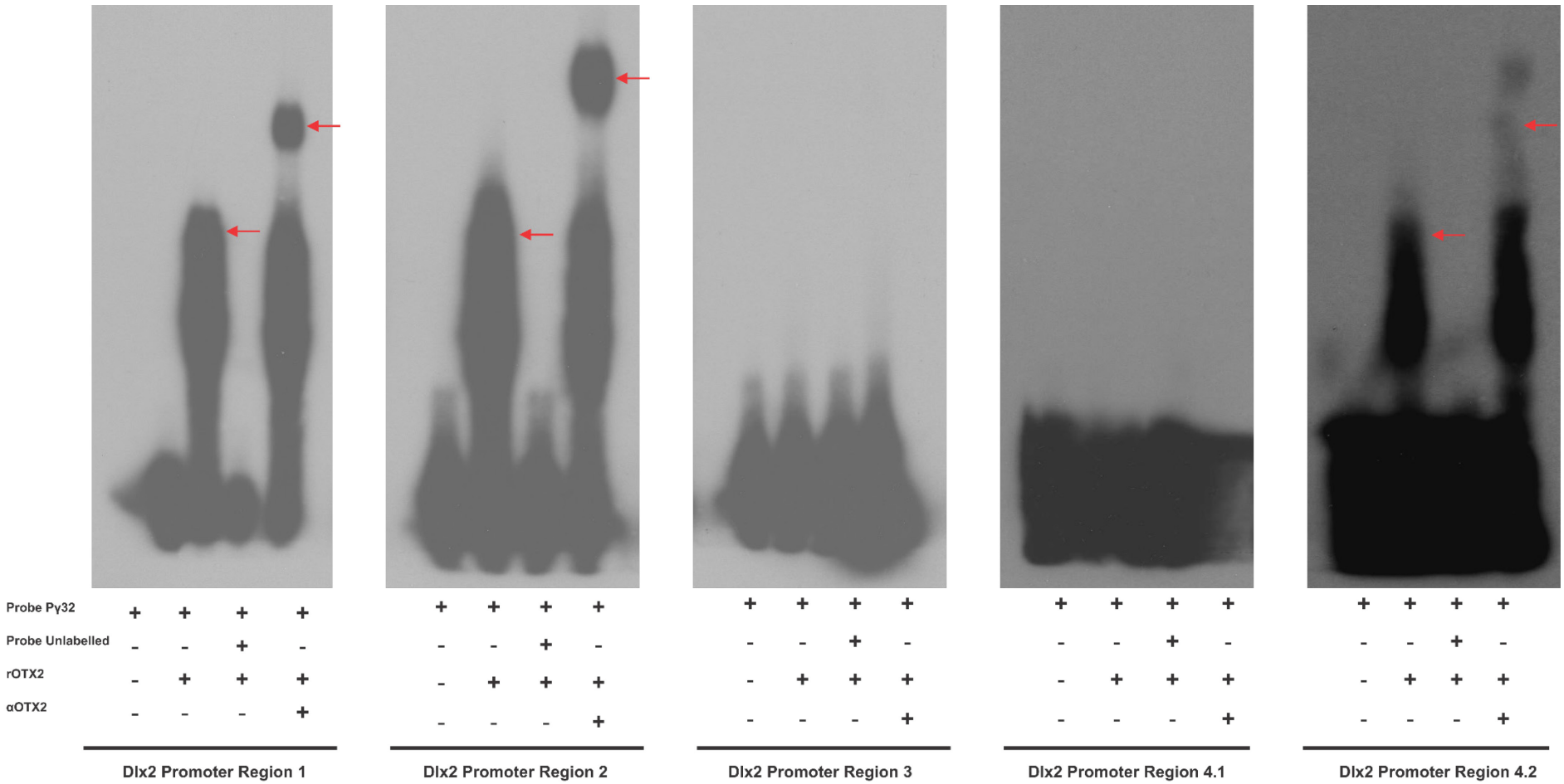
Probe Pγ32
Probe Unlabelled
rOTX2
αOTX2
+ + + +
- - + -
- + + +
- - - +
Dlx2 Promoter Region 1
Dlx2 Promoter Region 2
Dlx2 Promoter Region 3
Dlx2 Promoter Region 4.1
Dlx2 Promoter Region 4.2

Figure 4.4

EMSA with short oligonucleotide probes demonstrates that OTX2 directly binds subregions upstream the Dlx2 promoter in vitro

Short (20-25bp) complementary oligonucleotides containing the TAATCC and TAACCC motifs and short sequences flanking each motif were ordered and subsequently 5' labelled with [γ-32P]-dATP. EMSA was carried out as described in Chapter 3. From left to right are the EMSAs with short oligonucleotides of Subregion 1, 2, 3, 4.1 and 4.2.

For each subregion, lanes (left to right, respectively) represent binding reactions of: radiolabeled probes only; a "shift" lane where radiolabeled probes were incubated with an OTX2 recombinant protein; a "cold competition" lane where radiolabeled probes were incubated with an OTX2 recombinant protein and a 30-fold excess of unlabelled probe; and a "supershift" lane where radiolabeled probes were incubated with an OTX2 recombinant protein and a goat polyclonal OTX2 antibody. The "shift" and "supershift" on the gel is indicated by red arrows for each subregion.

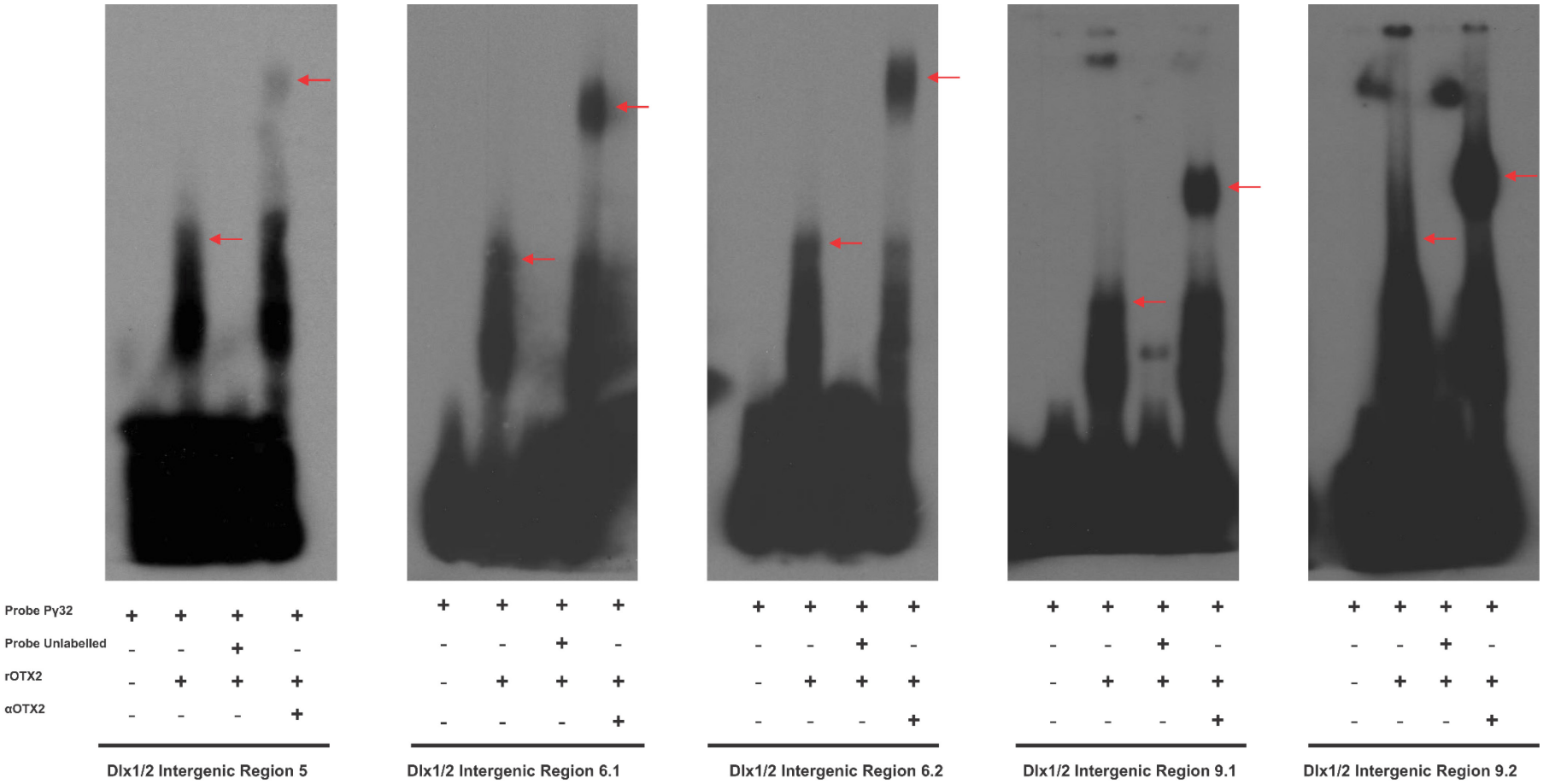
Probe Pγ32
Probe Unlabelled
rOTX2
αOTX2
Dlx1/2 Intergenic Region 5
Dlx1/2 Intergenic Region 6.1
Dlx1/2 Intergenic Region 6.2
Dlx1/2 Intergenic Region 9.1
Dlx1/2 Intergenic Region 9.2

Figure 4.5

EMSA with short oligonucleotide probes demonstrates that OTX2 directly binds subregions in the Dlx1/Dlx2 intergenic region in vitro

Short (20-25 bp) complementary oligonucleotides containing the TAATCC, TAACCC and TAATCT motifs and short sequences flanking each motif were ordered and subsequently 5' labelled with [γ-32P]-dATP. EMSA was carried out as described in Chapter 3. From left to right are the EMSAs with short oligonucleotides of Subregion 5, 6.1, 6.2, 9.1 and 9.2.

For each subregion, lanes (left to right, respectively) represent binding reactions of radiolabeled probes only; a "shift" lane where radiolabeled probes were incubated with an OTX2 recombinant protein; a "cold competition" lane where radiolabeled probes were incubated with an OTX2 recombinant protein and a 30-fold excess of unlabelled probe; and a "supershift" lane where radiolabeled probes were incubated with an OTX2 recombinant protein and a goat polyclonal OTX2 antibody. The "shift" and "supershift" on the gel is indicated by red arrows for each subregion.

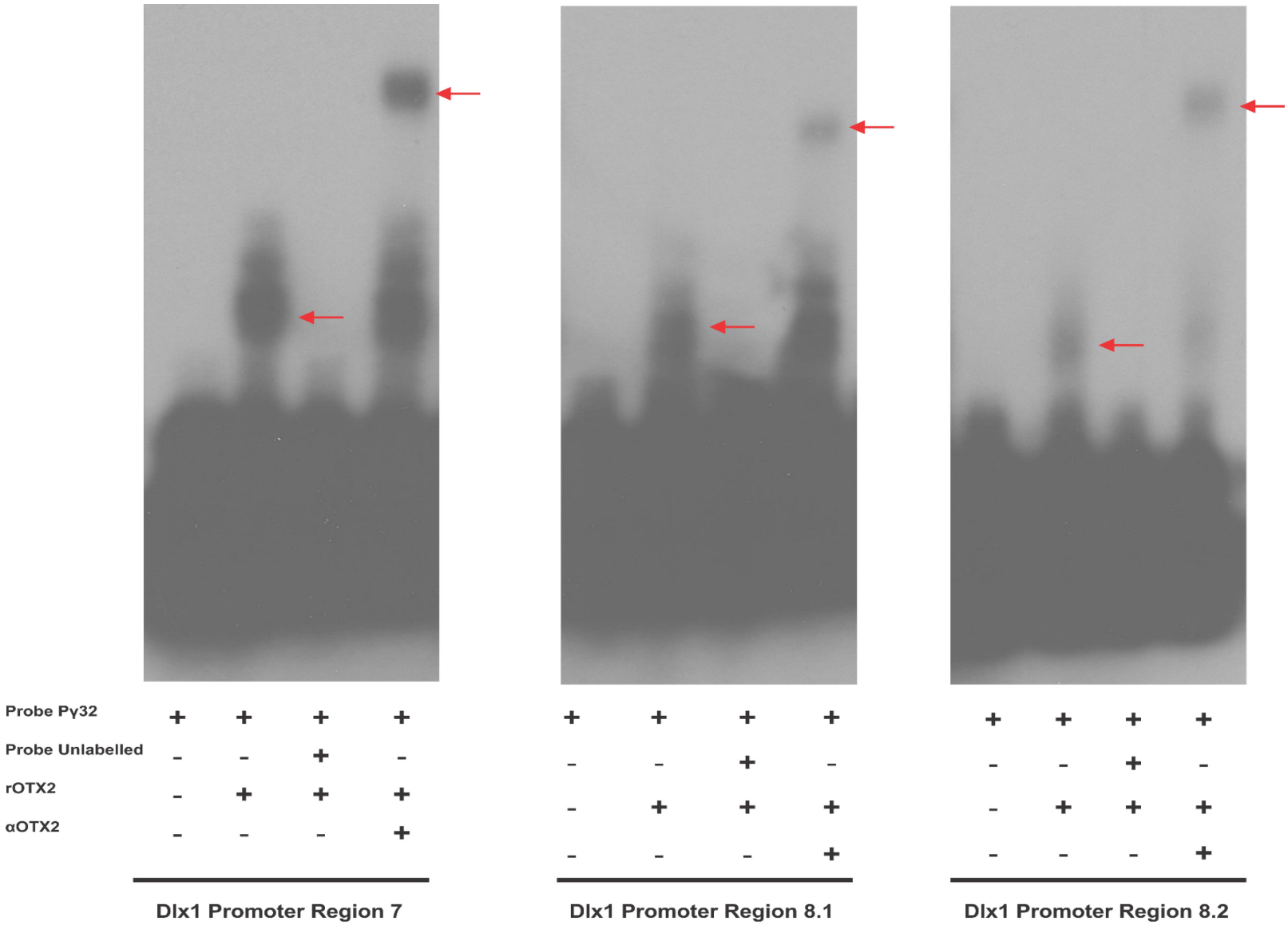
Probe Pγ32
Probe Unlabelled
rOTX2
αOTX2
+ + + +
- - + -
- + + +
- - - +
Dlx1 Promoter Region 7
+ + + +
- - + -
- + + +
- - - +
Dlx1 Promoter Region 8.1
+ + + +
- - + -
- + + +
- - - +
Dlx1 Promoter Region 8.2

Figure 4.6

EMSA with short oligonucleotide probes demonstrates that OTX2 directly binds a subregion in Dlx1 and subregions upstream the Dlx1 promoter in vitro

Short (20-25 bp) complementary oligonucleotides containing the TAATCC, TAAGCC and TAACCC motifs and short sequences flanking each motif were ordered and subsequently 5' labelled with [γ-32P]-dATP. EMSA was carried out as described in Chapter 3. From left to right are the EMSAs with short oligonucleotides of Subregion 7, 8.1 and 8.2.

For each subregion, lanes (left to right, respectively) represent binding reactions of radiolabeled probes only; a "shift" lane where radiolabeled probes were incubated with an OTX2 recombinant protein; a "cold competition" lane where radiolabeled probes were incubated with an OTX2 recombinant protein and a 30-fold excess of unlabelled probe; and a "supershift" lane where radiolabeled probes were incubated with an OTX2 recombinant protein and a goat polyclonal OTX2 antibody. The "shift" and "supershift" on the gel is indicated by red arrows for each subregion.

4.4 OTX2 occupies the *Dlx2* promoter and the *Dlx1/Dlx2* intergenic enhancer *I12a in vivo* at E18.5

After establishing that OTX2 can directly and specifically bind *Dlx1/Dlx2* regulatory regions *in vitro* by EMSA, I next performed chromatin immunoprecipitation (ChIP) to determine whether OTX2 specifically occupies these putative binding sites *in vivo*. This assay is conducted because it detects protein-DNA interactions that take place within the context of living cells by capturing regulatory protein factors at their binding/occupying DNA sites *in vivo* (Das, Ramachandran, vanWert, & Singal, 2004). Thus, the ChIP assay results should complement the

in vitro EMSA results to help us determine the *in vivo* locations of OTX2 binding sites more precisely.

Dissected E18.5 retinal tissues were first crosslinked with formaldehyde to preserve protein-DNA interactions. Embryonic day 18.5 was chosen to carry out the ChIP experiments because rod photoreceptor genesis peaks right after birth. I reckon that regulation to suppress alternative cell fates such as RGC fate may occur right before the peak of photoreceptor genesis. Furthermore, *Otx2* is expressed in the outer retina which is the presumptive photoreceptor layer whereas *Dlx2* is primarily expressed in the inner retina at this time point (**Figure 4.1**) (Martinez-Morales et al., 2001). The distinct and almost separate expression domains of OTX2 and DLX2 may indicate cross-regulation at this stage. Next, chromatin was sonicated to individualize the complexes, and the sheared protein-chromatin complexes were immunoprecipitated with an OTX2 antibody. Negative control samples for each tissue type were also immunoprecipitated with a non-specific IgG antibody and without antibody. Following the chromatin immunoprecipitation, immunoprecipitated complexes were reverse cross-linked and chromatin was analyzed using PCR with primer sets designed to flank candidate binding motifs-containing subregions upstream the *Dlx2* promoter region and in *Dlx1/Dlx2* intergenic region. Since *Dlx1* gene function is largely redundant to *Dlx2* (D. D. Eisenstat et al., 1999), Subregions 7, 8.1 and 8.2 were not analyzed by ChIP and not carried forward for luciferase reporter assays.

I hypothesized that OTX2 occupies the regulatory region upstream *Dlx2* and the *Dlx1/Dlx2* intergenic region *in vivo* at E18.5 to regulate *Dlx2* expression. If OTX2 regulates *Dlx2* expression by occupying these regulatory regions, we would expect those EMSA-positive subregions to be bound by OTX2 protein which is then bound by the OTX2 antibody in the retina. Therefore, these subregions would be retrieved by beads conjugated to the OTX2

antibody and subsequently detected as an enriched PCR band corresponding to that subregion. When beads only (no OTX2 antibody), non-specific IgG antibody is applied, we would expect OTX2 protein-chromatin subregion complexes to not be bound by any antibody, thus would not be retrieved by the beads, thus would not be detected by PCR. We would also expect the putative subregions from the spinal cord ChIP to not be detected by PCR because *Otx2* is not expressed in the spinal cord.

There are several controls incorporated into this experiment for both PCR amplification and specificity of binding. E18.5 spinal cord was also dissected along with the retinal tissues as a negative tissue control for the expression of *Otx2*. Chromatin immunoprecipitation of the spinal cord samples controls for cross-reactivity of the OTX2 antibody to other protein factors, and to confirm that the observed target DNA occupancy is specific for the OTX2 protein examined. Nonspecific goat IgG and beads only (no antibody) immunoprecipitations were negative controls to control for background of the assay and specificity of antibody-protein-DNA complex being immunoprecipitated. PCR analysis with a published positive OTX2 ChIP target locus *Irbp*/*Rbp3* (interphotoreceptor retinoid-binding protein) was also carried out as a positive control to aid in interpreting the results which would tell me if the observed enrichment is specific (Peng & Chen, 2005). Genomic DNA (gDNA) was used as positive control for PCR amplification. Non-template (H_2O) was used as a negative control for PCR amplification and contamination.

PCR products of Subregions 1 (R1), 2 (R2), 4.1 (R4.1), 4.2 (R4.2) and 4.12 (R4.12) upstream the *Dlx2* promoter were enriched (most intense amplification) in the E18.5 retina chromatin immunoprecipitated with an OTX2 antibody **(Figure 4.7**, E18.5 Retina AB+ chromatin lane). Enriched bands in OTX2 AB+ lanes supports that OTX2 occupies *Dlx2* promoter subregions 1, 2, 4.1, 4.2 and 4.12 in the mouse retina at E18.5. Subregion 2, Subregion

4.1 and subregion 4.2 were present also in the IgG and/or no antibody immunoprecipitated chromatins. Since amplification in the antibody immunoprecipitated chromatin is more intense for these subregions, they were still considered specific for OTX2 occupancy. These results suggest that Subregion 1, Subregion 2 and the entire Subregion 4.12 are occupied by OTX2 *in vivo*, and thus these subregions, which were also EMSA-positive, were carried forward for the luciferase reporter assay.

The PCR product of *Dlx1/2* intergenic Subregion 9.2 (R9.2), which is positioned at the *Dlx1/Dlx2* intergenic enhancer *I12a*, was enriched (more intense amplification) in E18.5 retina chromatin immunoprecipitated with an OTX2 antibody (**Figure 4.7**, E18.5 Retina AB+ chromatin lane). The PCR product of Subregion 9.1 (R9.1) in the *Dlx1/Dlx2* intergenic region was present in the retina antibody immunoprecipitated chromatin, the retina IgG immunoprecipitated chromatin as well as chromatin immunoprecipitated without antibody. However, this subregion was still considered specific for binding by OTX2 because amplification in the antibody (AB+) immunoprecipitated chromatin was more intense, thus likely to be more immunoenriched. Chromatin being pulled down in the IgG and AB- negative control samples was most likely due to beads sticking to the chromatin of these subregions. There was also amplification of Subregion 9.1 in the spinal cord pull downs. However, this could be due to non-specific binding of the beads to other factors that occupy this subregion and/or chromatin. Furthermore, the dissection of the spinal cord may have extended more rostrally closer to the hindbrain where *Otx2* is expressed at the midbrain/hindbrain boundary. The entire Subregion 9.12 demonstrated similar PCR amplification intensity between IgG and antibody immunoprecipitated chromatin; thus, I considered this enrichment to be nonspecific binding. However, Subregion 9.12 was still carried forward for luciferase experiments, because ChIP of

each individual subregion (R9.2 and R9.1) supported OTX2 occupancy despite the entire region not being enriched by PCR.

The positive control *Irbp* was found to be enriched for OTX2 binding as well, which was confirmatory. ChIP positive control *Irbp* generated confidence that Subregions 1, 2, and 4.12 upstream the *Dlx2* promoter, as well as Subregion 9.2 and 9.1 in the *Dlx1/Dlx2* intergenic region, contain binding motifs which OTX2 may occupy in the retina at this developmental stage.

In view of the positive EMSA and ChIP results for these subregions, I concluded that OTX2 occupies upstream the *Dlx2* promoter at Subregion 1, Subregion 2 and Subregion 4.12, and the *Dlx1/Dlx2* intergenic region at the *I12a* intergenic enhancer (Subregion 9.2 and 9.1) *in vivo* in the mouse retina just prior to birth. Based on these results, Subregions 1, 2, 4.12 and 9.12 were carried forward for assessment of functional consequences of OTX2 binding using luciferase reporter assays.

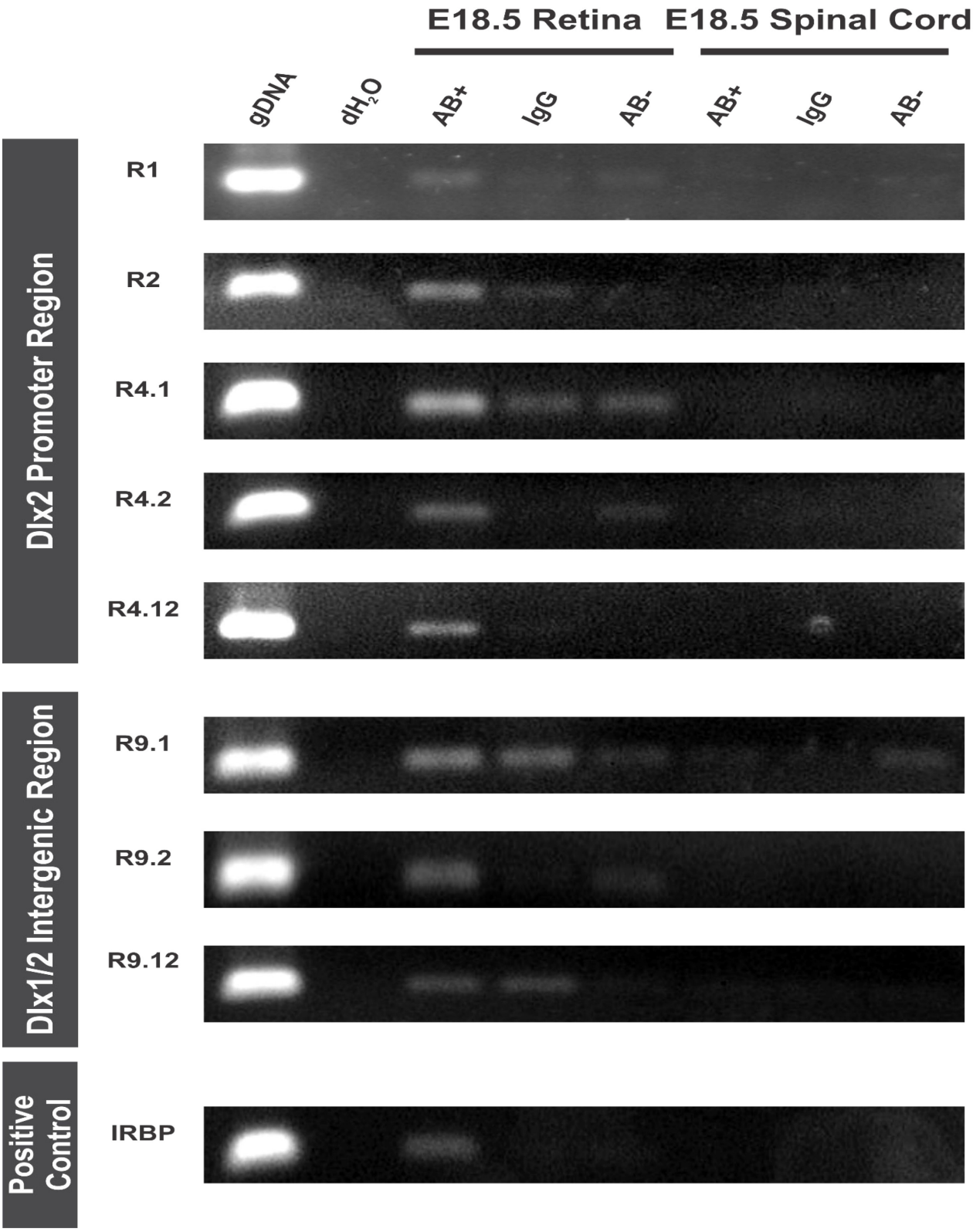
E18.5 Retina
E18.5 Spinal Cord
gDNA
dH2O
AB+
IgG
AB-
AB+
IgG
AB-
Dlx2 Promoter Region
R1
R2
R4.1
R4.2
R4.12
Dlx1/2 Intergenic Region
R9.1
R9.2
R9.12
Positive Control
IRBP

Figure 4.7

OTX2 occupies regions upstream the Dlx2 promoter and the Dlx1/2 intergenic enhancer I12a in vivo in the wildtype mouse retina at E18.5

Chromatin immunoprecipitation of E18.5 wildtype mouse retinal and spinal cord tissues with goat polyclonal OTX2 antibody (AB+), nonspecific goat IgG and beads only (no antibody, AB-). The immunoprecipitated chromatins were analyzed using qualitative end-point PCR with specific primers flanking subregions upstream the *Dlx2* promoter (R1, R2, R4.1, R4.2 and R4.12) and subregions in the *Dlx1/Dlx2* intergenic region (R9.1, R9.2 and R9.12). *Irbp*, which is a validated OTX2 target gene, was also analyzed as a positive control locus. Genomic DNA (gDNA) and non-template (molecular biology-grade H_2O) were positive and negative PCR controls, respectively.

Lanes (left to right):

gDNA: gDNA amplified by using primers of the specific regulatory subregions by PCR

dH_2O: negative PCR control

E18.5 Retina AB+: retina chromatin immunoprecipitated with goat OTX2 antibody

E18.5 Retina IgG: retina chromatin immunoprecipitated with goat IgG

E18.5 Retina AB-: retina chromatin immunoprecipitated with beads only (no antibody)

E18.5 Spinal Cord AB+: spinal cord chromatin immunoprecipitated with goat OTX2 antibody

E18.5 Spinal Cord IgG: spinal cord chromatin immunoprecipitated with goat IgG

E18.5 Spinal Cord AB-: spinal cord chromatin immunoprecipitated with beads only (no antibody)

Rows (top to bottom):

Subregion 1 (R1); Subregion 2 (R2); Subregion 4.1 (R4.1); Subregion 4.2 (R4.2), Subregion 4.12 (R4.12) which is a combined Subregion of R4.1 and R4.2 containing two OTX2 binding motifs;

Subregion 9.1 (R9.1); Subregion 9.2 (R9.2); Subregion 9.12 (R9.12) which is a combined Subregion of R9.1 and R9.2 containing two OTX2 binding motifs; positive OTX2 ChIP target *Irbp* as a positive control. The experiment was performed in one biological replicate.

4.5 OTX2 binding regulatory subregions upstream the *Dlx2* promoter and the *Dlx1/Dlx2* intergenic enhancer *I12a* affects reporter gene transcription *in vitro*

We established that OTX2 binds regions upstream the *Dlx2* promoter as well as in the *Dlx1/Dlx2* intergenic region *in vitro* and *in vivo*. However physical binding or occupancy does not necessarily entail functional consequences on *Dlx2* gene transcription. We next investigated whether the binding of EMSA-identified and ChIP-validated subregions by OTX2 has any functional effect on transcriptional activity by performing Dual-Luciferase reporter assays in HEK293 cells. HEK293 cells were chosen because they do not express endogenous OTX2 (Courtois et al., 2003). This assay allows us to characterize and monitor the effects on transcription driven by regulatory regions of the gene of interest, *Dlx2*, and investigate the contribution of OTX2 *in vitro.* The expression of the reporter gene, luciferase, correlates with the expression level of the gene of interest. The advantage of this assay is that, in contrast with directly measuring gene transcription, the reporter gene transcription level can be quantified more easily (Bauer, 2011).

Since we hypothesized that OTX2 negatively regulates *Dlx2* to repress RGC fate, we would expect OTX2 represses *Dlx2* gene transcription by binding these EMSA-positive-and-ChIP-validated subregions. We would expect a decrease in reporter gene expression with OTX2 co-expression. On the contrary, if OTX2 activates *Dlx2* gene expression by binding these

EMSA-positive-and-ChIP-positive subregions, an increase in reporter gene expression would be observed when OTX2 is co-expressed *in vitro*.

In order to conduct the luciferase assay, first the EMSA-positive-and-ChIP-positive *Dlx2* regulatory subregions (Subregions 1, 2, 4.12 and 9.12) were each inserted, upstream of the luciferase gene, into the pGL4.23 Minimum Promoter Firefly luciferase reporter vector. [pGL4.23-Dlx2-regulatory-subregion-containing reporter constructs] and an OTX2-FLAG expression vector [pcDNA3.1+/C-(K)-DYK-OTX2] were co-transfected in HEK293 cells. In this assay, the luciferase gene expression is under the control of the regulatory subregion of *Dlx2* and will serve as a "reporter" of its transcriptional activity. Luciferase gene product will bioluminesce in the presence of its substrate which can be easily measured. The experimental luciferase reporter gene (Firefly luciferase) expression is normalized to background Renilla luciferase activity.

There are several controls incorporated into the experiment to control for the effect of expressing each plasmid. For instance, pCDNA was co-transfected with an empty pGL4.23 construct to control for the effect of transfecting each plasmid type. The OTX2 expression vector was co-transfected with empty pGL4.23 to control for the effect of expressing *Otx2* alone on transcription in HEK293 cells. Luciferase reporter construct containing the subregion of interest was co-transfected with an empty expression vector pCDNA to control for the effect of expressing this regulatory region alone on transcription in HEK293 cells. Cells were also transfected with a vector providing neutral weak constitutive expression of Renilla luciferase (pRL-TK) as an internal control. Western Blotting was conducted to demonstrate successful expression of OTX2 following transfection of the OTX2 expression vector (**Figure 4.8**). Cells that were not treated with doxycycline express FOXC1-FLAG (Dox- lane, **Figure 4.8**) and were

used as positive control for the FLAG antibody. FOXC1-FLAG is ablated in cells treated with doxycycline (Dox+ lane, **Figure 4.8**), thus used as a negative control. Previous samples transfected and using untagged OTX2 expression vectors (obtained from Dr. Thomas Lamonerie) were used as a negative control. Untransfected samples were used as an additional negative control for specificity of the anti-FLAG antibody. There were many background signals which can be optimized in the future by further diluting the anti-FLAG secondary antibody 1: 10,000 to reduce the background bands.

Figure 4.9 demonstrates that for Subregion 1 (R1), there is a statistically significant decrease when the R1 reporter construct was co-transfected with empty expression vector backbone pCDNA in HEK293 cells. There is a significant decrease in transcription when the OTX2 expression vector was co-transfected with the R1 reporter construct compared to the OTX2 expression plasmid co-transfected with empty pGL4.23 plasmid. However, this decrease is likely due to the presence of R1 reporter plasmid and independent of OTX2 expression. Therefore, the change in luciferase gene expression was not statistically significant when the R1 reporter construct was co-transfected with the OTX2 expression vector compared to the R1 reporter construct alone.

For Subregion 2 (R2), changes in reporter gene expression were not statistically significant between any co-transfection treatment groups. Thus, OTX2 binding Subregion 2 did not influence reporter gene transcription.

For Subregion 4.12 (R4.12), there was a statistically significant increase in reporter gene expression when OTX2 expression plasmid was co-transfected with the R4.12 reporter construct compared to the R4.12 reporter construct co-transfected with the empty expression vector backbone pCDNA. Co-expression of OTX2 and the Subregion 4.12 reporter gene construct

increased transcription by 2-fold. This increase in transcription was unexpected from the original hypothesis.

For Subregion 9.12 (R9.12) which is the intergenic enhancer *I12a*, there was a statistically significant increase when the R9.12 reporter construct was co-transfected with the empty expression vector backbone pCDNA in HEK293 cells. There was dramatic upregulation of reporter gene expression when OTX2 was co-transfected with the R9.12 reporter construct, which is additional to the effect of adding the R9.12 reporter construct. This suggests that the upregulation of transcription was dependent on *Otx2* expression and the binding of Subregion 9.12 by OTX2. Co-transfection of OTX2 with Subregion 9.12 reporter construct increased reporter gene expression by about 2-fold. This increase in transcription was also unexpected from the original hypothesis. However, this could be explained in part by the fact that R9.12 is an evolutionarily conserved enhancer element.

Taken together, these results suggest that OTX2 could repress or activate gene repression by specifically interacting with regions upstream the *Dlx2* promoter *in vitro*. OTX2 could activate gene transcription by interacting with the *Dlx1/Dlx2* intergenic enhancer *I12a in vitro*. OTX2 eliciting a transcriptional response is consistent with the hypothesis that OTX2 regulates *Dlx2* gene expression by interacting with these regulatory regions.

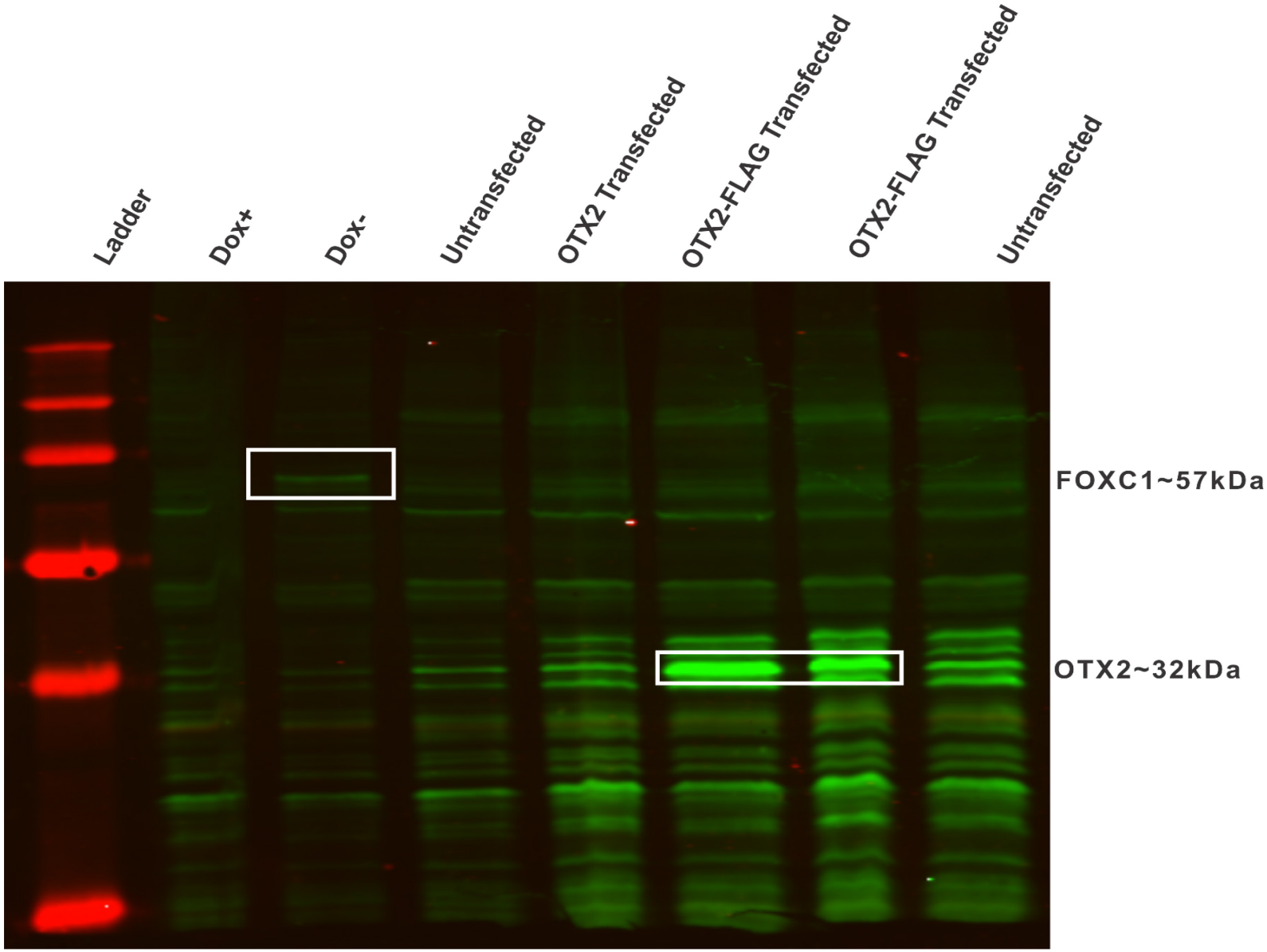
Ladder
Dox+
Dox-
Untransfected
OTX2 Transfected
OTX2-FLAG Transfected
OTX2-FLAG Transfected
Untransfected
FOXC1~57kDa
OTX2~32kDa

Figure 4.8

OTX2 is expressed when OTX2-FLAG expression plasmid is transfected in HEK293 cells as determined by Western Blot

Western blot image of HEK293 samples transfected with OTX2-FLAG expression vector (OTX2-FLAG Transfected lanes), probed with anti-FLAG antibody. Cells (Dox- lane, without Doxycycline treatment) expressing FLAG-tagged-FOXC1 is a positive control sample for FLAG expression. Previous samples transfected (OTX2 transfected lane) using another untagged OTX2 expression vector were also analyzed as a negative control for FLAG expression. Untransfected samples are an additional negative control for specificity of the anti-FLAG antibody. The white box at 32kDa encircles expressed OTX2-FLAG protein. The white box at 57kDa encircles expressed FOXC1-FLAG protein.

Lanes (left to right)

1. Ladder: molecular size marker
2. Dox+: Cells treated with Doxycycline to ablate FOXC1-FLAG expression
3. Dox-: Cells expressing FOXC1-FLAG
4. Untransfected: untransfected HEK293 cells from previous transfection attempts using another OTX2 expression vector without FLAG tag
5. OTX2 transfected: HEK293 cells transfected with another OTX2 expression vector without FLAG tag from previous transfection attempts
6. Sample I OTX2-FLAG Transfected: one plate of HEK293 cells transfected with OTX2-FLAG expression vector
7. Sample II OTX2-FLAG Transfected: another plate of HEK293 cells transfected with OTX2-FLAG expression vector
8. Untransfected: untransfected HEK293 cells sample

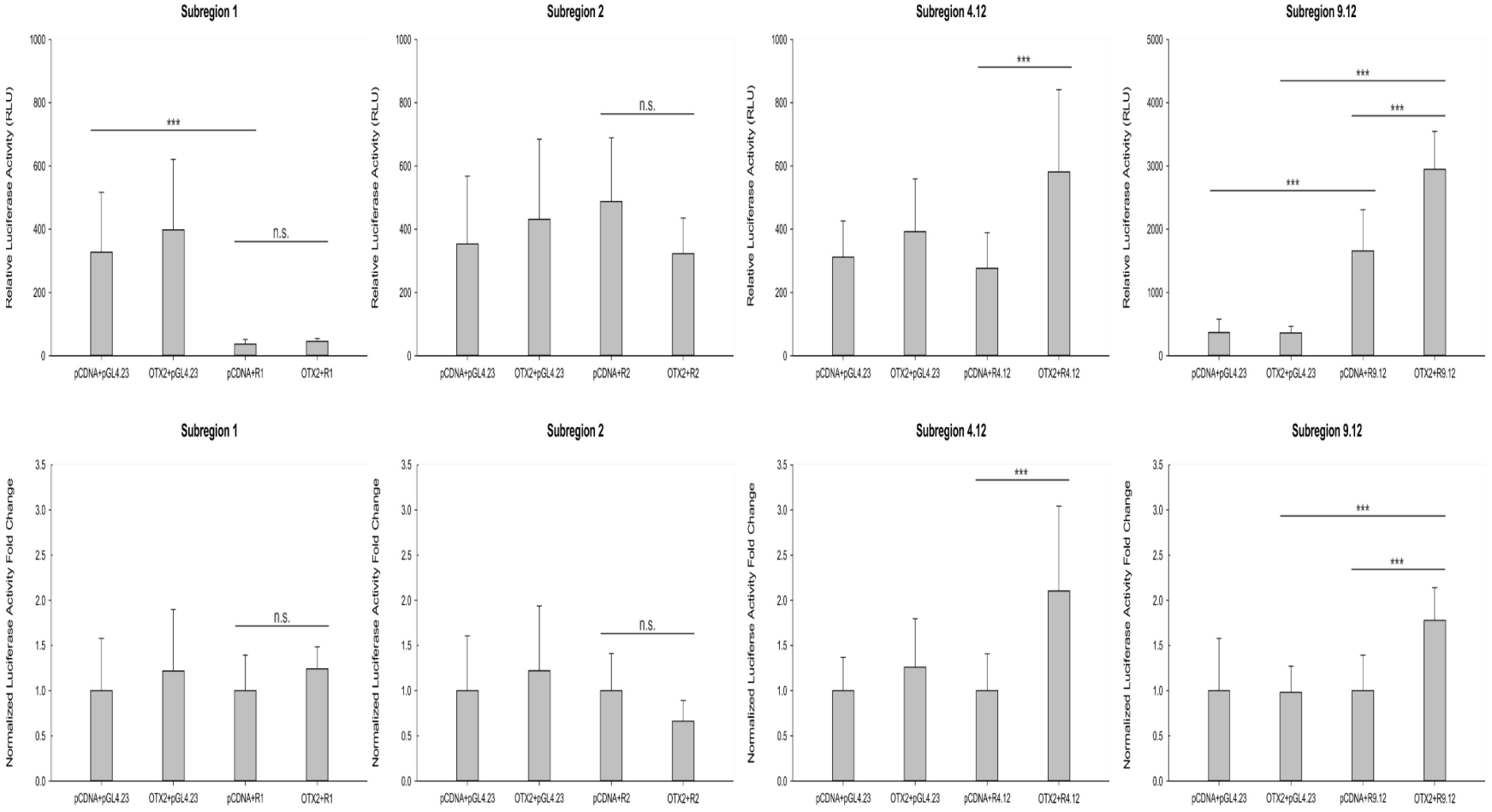
Subregion 1
Relative Luciferase Activity (RLU)
1000
800
600
400
200
0
***
n.s.
pCDNA+pGL4.23
OTX2+pGL4.23
pCDNA+R1
OTX2+R1
Subregion 2
Relative Luciferase Activity (RLU)
1000
800
600
400
200
0
n.s.
pCDNA+pGL4.23
OTX2+pGL4.23
pCDNA+R2
OTX2+R2
Subregion 4.12
Relative Luciferase Activity (RLU)
1000
800
600
400
200
0
***
pCDNA+pGL4.23
OTX2+pGL4.23
pCDNA+R4.12
OTX2+R4.12
Subregion 9.12
Relative Luciferase Activity (RLU)
5000
4000
3000
2000
1000
0
***
***
***
pCDNA+pGL4.23
OTX2+pGL4.23
pCDNA+R9.12
OTX2+R9.12
Subregion 1
Normalized Luciferase Activity Fold Change
3.5
3.0
2.5
2.0
1.5
1.0
0.5
0.0
n.s.
pCDNA+pGL4.23
OTX2+pGL4.23
pCDNA+R1
OTX2+R1
Subregion 2
Normalized Luciferase Activity Fold Change
3.5
3.0
2.5
2.0
1.5
1.0
0.5
0.0
n.s.
pCDNA+pGL4.23
OTX2+pGL4.23
pCDNA+R2
OTX2+R2
Subregion 4.12
Normalized Luciferase Activity Fold Change
3.5
3.0
2.5
2.0
1.5
1.0
0.5
0.0
***
pCDNA+pGL4.23
OTX2+pGL4.23
pCDNA+R4.12
OTX2+R4.12
Subregion 9.12
Normalized Luciferase Activity Fold Change
3.5
3.0
2.5
2.0
1.5
1.0
0.5
0.0
***
***
pCDNA+pGL4.23
OTX2+pGL4.23
pCDNA+R9.12
OTX2+R9.12

Figure 4.9

OTX2 binding to Dlx2 regulatory regions including subregions upstream the Dlx2 promoter and the Dlx1/Dlx2 intergenic enhancer I12a significantly affects reporter gene transcription in vitro

ChIP-EMSA-positive *Dlx2* promoter subregions and the *I12a* intergenic enhancer were subcloned, upstream of the luciferase gene, into the pGL4.23 Minimum Promoter Firefly luciferase reporter vector. The reporter construct containing the *Dlx2* promoter subregions (pGL4.23-*Dlx2* regulatory subregion reporter constructs) was co-transfected with OTX2 expression vector (pcDNA3.1+/C-(K)-DYK-OTX2) into HEK293 using Lipofectamine 2000. As an internal control for the amount of DNA transfected into the cells and the general ability of the cells to express protein, cells were also co-transfected with a vector providing neutral weak constitutive expression of another reporter protein Renilla luciferase (pRL-TK). Firefly and Renilla luciferase activities were measured using the Dual-Luciferase Reporter Assay system. Firefly luciferase data were normalized to Renilla luciferase activity for each well.

Top Row: Relative luciferase activity of co-transfecting OTX2 and Subregion 1, 2, 4.12 and 9.12 reporter constructs in HEK293 cells.

Bottom Row: Normalized fold-change for Subregions 1, 2, 4.12 and 9.12 was calculated by normalizing to the average Firefly to Renilla ratio in control cells that were co-transfected with empty pcDNA3 and pGL4.23, respectively.

Three technical replicates (i.e. three wells transfected for each condition) and three biological replicates (N=3) were performed for all subregion-containing reporter constructs. One set of co-transfections including control co-transfection followed by Dual-Reporter Luciferase assay reading was considered a biological replicate. Statistical significance was calculated using an ANOVA test. Error bars for the relative luciferase expression graphs (top row) represent

standard deviation of RLUs. Error bars for normalized fold change graphs (bottom row) represent the standard deviation of the fold-change in expression.

4.6 Retina morphology may be altered, including expansion of the GCL, and thinning of the INL, in the *Otx2* heterozygous knockout (*Otx2*$^{+/GFP}$) mutant eye at P100

We have established that OTX2 binds *Dlx2* regulatory regions *in vitro* and *in vivo*. We have also established binding of the *Dlx2* regulatory regions by OTX2 *in vitro* elicits both repression and activation of reporter gene transcription. However, these assays do not explain the function of this interaction in the relevant biological context. Mutating *Otx2 in vivo* would be ideal to study its function in retinogenesis and gene regulation. Unfortunately, homozygous *Otx2* null mice are headless and cannot survive. However, heterozygous *Otx2* mice with GFP insertion in one *Otx2* allele (*Otx2*$^{+/GFP}$) survive and are in general "normal" and can reproduce (Bernard et al., 2014). Thus, next we used this animal model to examine the functional effect of ablating one allele of *Otx2* on retina morphology.

Histological analysis of wildtype and *Otx2*$^{+/GFP}$ eye sections was conducted by hematoxylin and eosin staining. P100 wildtype (*Otx2*$^{+/+}$) and *Otx2*$^{+/GFP}$ eye tissues were received from our collaborator in France. The eyes were fixed, paraffin embedded and sectioned. H&E staining was performed. If *Otx2* represses retinal ganglion cell fate, we would expect the ganglion cell layer thickness to be increased in the *Otx2*$^{+/GFP}$ mutant.

Despite the disrupted morphology, I observed that retina morphology may be affected in the *Otx2*$^{+/GFP}$ mouse retina when compared to wildtype littermate controls. The INL thickness was reduced at P100 in the *Otx2*$^{+/GFP}$ mutant compared to the control at both 20X and 40X magnification (**Figure 4.10**). This is also observed according to our collaborator's published

work (Bernard et al., 2014). Furthermore, haematoxylin staining of the retinal ganglion cell nuclei was more intense and the ganglion cell layer appears to be expanded in the P100 *Otx2*$^{+/GFP}$ mutant mouse retina compared to the control. This result is consistent with our hypothesis that when *Otx2* expression is reduced, *Dlx2* expression is de-repressed, which would possibly result in the upregulation of ganglion cell production leading to an expansion of the ganglion cell layer. Unfortunately, these results were only observed in two mutant eyes and could not be repeated in more biological replicates until we ask our collaborator to collect and send more tissues.

Studies in homozygous knock-in mice expressing a mutated form of OTX2 protein have shown that after 10 months, the number of cells in the ganglion cell layer is significantly reduced possibly due to an insufficient amount of OTX2 protein being transferred to the RGC, which consequently promotes RGC degeneration (Bernard et al., 2014; Torero Ibad et al., 2011). This is not what was observed in our results for the P100 *Otx2*$^{+/GFP}$ mutant mouse retina. This could be due to the age difference. *Otx2* regulation in the retina is complex and multifaceted and it would definitely be interesting in the future to examine in more detail the histological changes at various embryonic and postnatal ages.

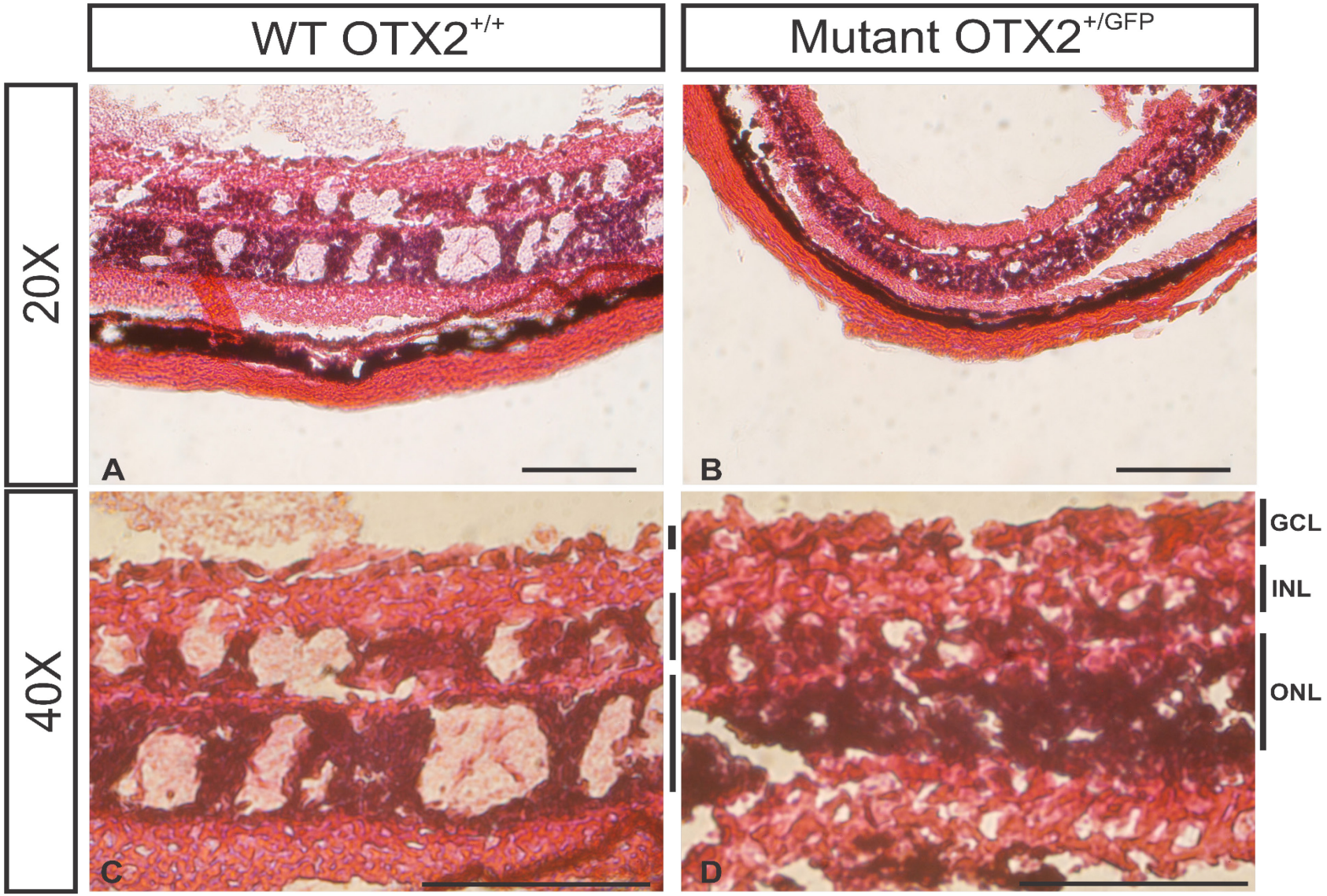
WT OTX2+/+
Mutant OTX2+/GFP
20X
40X
A
B
C
D
GCL
INL
ONL

Figure 4.10

The inner nuclear layer (INL) thickness may be reduced, and the ganglion cell layer (GCL) may be expanded in P100 Otx2 heterozygous knockout (Otx2$^{+/GFP}$) mutant mouse retina

Retina morphology of P100 wildtype control mouse retina (A, C) and OTX2$^{+/GFP}$ mutant mouse retina (B, D) at 20X (A-B) and 40X (C-D) magnification demonstrated by haematoxylin-and-eosin-stained paraffin sections. The retina section is oriented with the inner retina (retinal ganglion cell layer, GCL) at the top and outer retina (outer nuclear layer, ONL) and the RPE at the bottom, as indicated by lines and labels in C and D. Inner nuclear layer (INL) thickness appears to be decreased in the OTX2$^{+/GFP}$ mutant retina compared to the wildtype at 20X and 40X magnification. Haematoxylin staining of the retinal ganglion cell nuclei is stronger and the ganglion cell layer (GCL) appears to be expanded in thickness in the *Otx2*$^{+/GFP}$ mutant mouse retina compared to the wildtype at 40X magnification.

GCL, ganglion cell layer

INL, inner nuclear layer

ONL, outer nuclear layer

Two biological replicates (two wild-type eyes and two mutant eyes) were assessed.

Scale bar is equivalent to 100 μm

4.7 Retinal layer(s) where *Dlx2*-expressing cells are localized may be expanded in the *Otx2* heterozygous knockout (*Otx2*$^{+/GFP}$) mutant retina at P100

After we had characterized the effect of ablating one allele of *Otx2* on retina morphology, next we determined whether DLX2 expression level was specifically altered *in situ* in the heterozygous *Otx2* mutant mouse retina. P100 wildtype (*Otx2*$^{+/+}$) and mutant (*Otx2*$^{+/GFP}$) eye

tissues were received from our collaborator in France. The eyes were fixed, paraffin embedded and sectioned. Single immunofluorescence using DLX2 antibody was performed on P100 wildtype (*Otx2*$^{+/+}$) and heterozygous *Otx2* (*Otx2*$^{+/GFP}$) mutant eye paraffin embedded sections. If *Otx2* represses ganglion cell fate by repressing *Dlx2*, we would expect an increase in DLX2 expression in the *Otx2*$^{+/GFP}$ mutant retina. Negative controls where sections were incubated with blocking buffer only (no primary antibody) followed by secondary antibody and DAPI were also conducted.

Due to morphology of the retina frequently disrupted during the immunofluorescence procedures, it was difficult to decipher retina anatomy. DAPI is used to visualize the nuclei; thus, DAPI stained the nuclei of the inner nuclear layer (INL) and the outer nuclear layer (ONL). With those layers visualized by DAPI as a reference, we were able to identify the ganglion cell layer (GCL) to be the uppermost layer most distal to where the thicker DAPI stained layer at the bottom (**Figure 4.11**).

In both wildtype and *Otx2*$^{+/GFP}$ mutant mouse retina, DLX2 was clearly detected at high levels in both the ganglion cell layer (GCL) and the inner nuclear layer (INL). This result is consistent with the literature as *Dlx2* is expressed in the GCL (RGC and displaced amacrine cells) and INL (amacrine and horizontal cells) throughout adulthood (de Melo et al., 2003). There was also fluorescence signal detected in the photoreceptor layer; however, this could be background signals as immunofluorescence images of published work of the lab also display these background signals in the photoreceptor layer (de Melo et al., 2003). Interestingly, in the P100 heterozygous *Otx2*$^{+/GFP}$ mutant mouse retina, the layer(s) where *Dlx2*-expressing cells localize (ganglion cell layer and/or inner nuclear layer) appear to be expanded (**Figure 4.11D**). However, it is difficult to conclude that this apparent expansion of DLX2-expressing domain is

from the ganglion cell layer or from the inner nuclear layer, as the layers appear to be “merged” together. Furthermore, it cannot be concluded that there is any change in DLX2 expression until cell-counting is conducted to quantify the expression level in sections with more intact retina morphology. Since these tissues were received from another lab, unfortunately this experiment could not be repeated until our collaborator collects and sends more tissue.

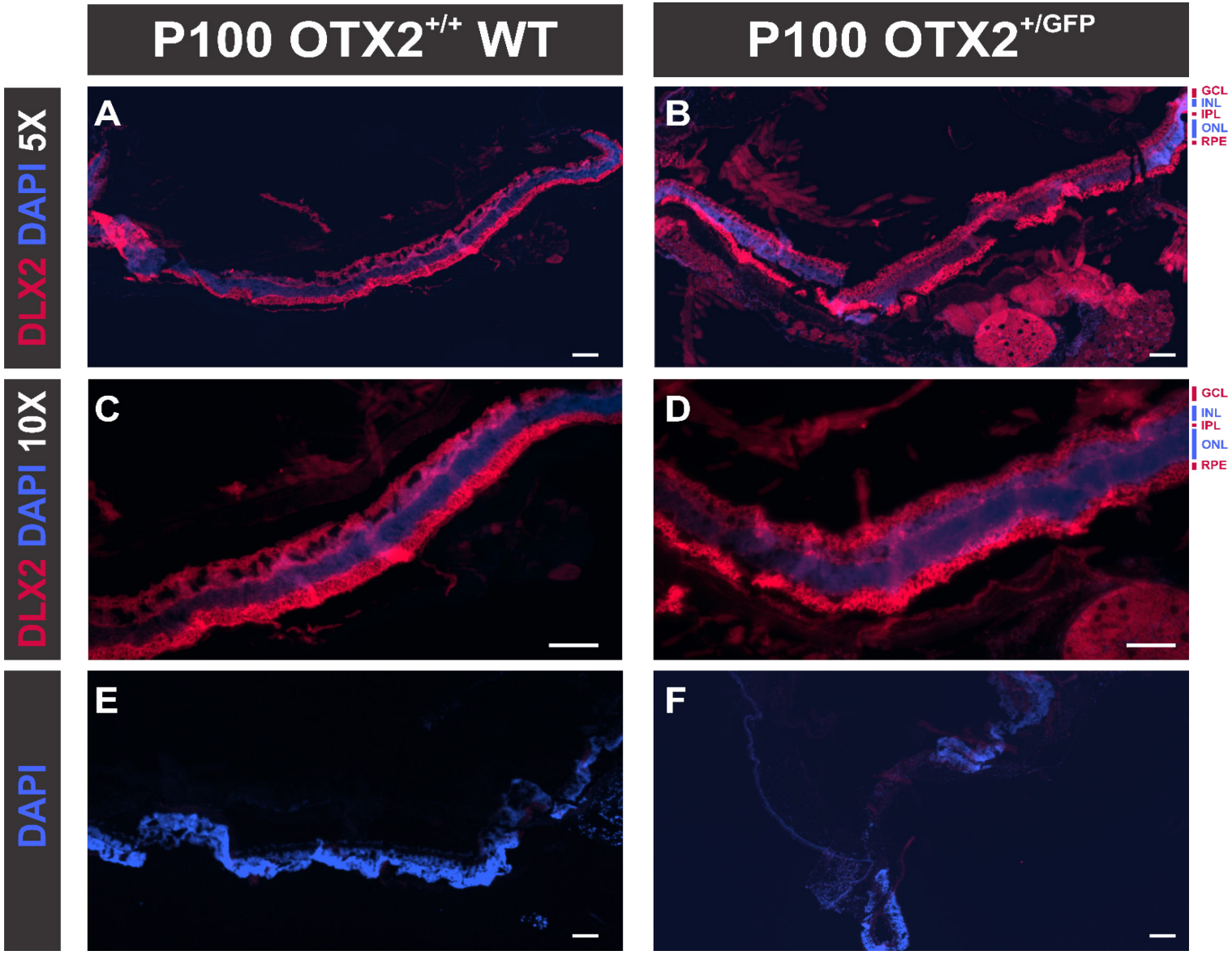
P100 OTX2+/+ WT
P100 OTX2+/GFP
DLX2 DAPI 5X
DLX2 DAPI 10X
DAPI
A
B
C
D
E
F
GCL
INL
IPL
ONL
RPE
GCL
INL
IPL
ONL
RPE

Figure 4.11

Retinal layer(s) where DLX2-expressing cells are localized may be expanded in P100 Otx2 heterozygous knockout (Otx2$^{+/GFP}$) mutant mouse retina

Single immunofluorescence is performed with DLX2 antibody on paraffin-embedded mouse retina sections of P100 wildtype (*Otx2*$^{+/+}$) and P100 *Otx2* heterozygous (*Otx2*$^{+/GFP}$) knockout mutant mice imaged at 5X (A-B) and 10X (C-D). Sections were also incubated with the secondary antibody and DAPI only to serve as a negative control for background autofluorescence (E-F). The retina section is oriented with the inner retina (retinal ganglion cell layer, GCL) being the uppermost layer. The inner nuclear layer (INL) is indicated by the thinner DAPI stained layer between the GCL and ONL. The outer nuclear layer (ONL) is the layer at the bottom indicated by the thicker DAPI stained layer. The RPE is the bottom most layer, which is autofluorescent with red signals.

GCL, ganglion cell layer

INL, inner nuclear layer

IPL, inner plexiform layer

ONL, outer nuclear layer

RPE, retinal pigmented epithelium

Two biological replicates (two wildtype eyes and two mutant eyes) were assessed.

Scale bar is equivalent to 100 μm.

Chapter 5: Discussion

Little is known about the upstream transcriptional regulation of *Dlx1/Dlx2* during retina development. In this project, I assessed the regulation of *Dlx2* by OTX2. Specifically, I investigated whether OTX2 directly binds and occupies *Dlx1/Dlx2* regulatory regions to repress *Dlx1/Dlx2* expression during retina development. This is the first report, to our knowledge, assessing the transcriptional regulation of *Dlx2* by OTX2 in the developing retina. We provided evidence that OTX2 can directly bind and occupy *Dlx2* regulatory regions, possibly to regulate *Dlx2* transcription. Regulation of *Dlx2* by OTX2 is further supported by preliminary evidence demonstrating an expansion of the ganglion cell layer and DLX2-expressing domain in the retina of loss-of-function *Otx2* heterozygous mutant mice. This section will discuss the results, the limitations, and extend to possible mechanisms through which OTX2 regulates *Dlx2* expression in regulating retinal cell fate decisions in the developing retina.

OTX2 and DLX2 have some overlapping, as well as distinct expression patterns

At E13.5, *Dlx2* is expressed throughout the retina; its expression is concentrated in the central and inner portions of the retina (**Figure 4.1A**). At this embryonic stage, *Otx2* is expressed primarily in the outer retina (**Figure 4.1B**) although there are some co-expressing DLX2+/OTX2+ cells (**Figure 4.1C**). By E18.5, DLX2 is localized to the innermost retinal layers, such as the ganglion cell layer (GCL) and the inner neuroblastic layer (iNBL) (**Figure 4.1D**). This contrasts with OTX2, which localizes primarily to the outer neuroblastic layer (oNBL) (**Figure 4.1E**). Hence, I observed that OTX2 and DLX2 expression domains are primarily distinct at E18.5 (**Figure 4.1F**). This is consistent with our hypothesis. The lack of DLX2 expression in the outer retina (i.e. the prospective photoreceptor layer) supports that OTX2 may restrict *Dlx2* expression in the outer neural retina potentially to suppress RGC fate in the photoreceptor precursors. I have also observed that some cells co-express OTX2 and DLX2

at both E13.5 and E18.5 in the neuroblastic layer, although less co-expression is observed at E18.5. The presence of DLX2+/OTX2+ RPCs at E13.5 may reflect a role of OTX2 and DLX2 working together to establish the "genetic programming" critical for the differentiation of specific retinal cell types. Later at E18.5, a subset of late-born cells still requires co-expression of OTX2 and DLX2 to commit to the appropriate retinal cell types, while the majority of OTX2+ or DLX2+ precursors become localized to their respective layers to repress alternative cell fates, such as to repress RGC fate in the photoreceptor precursors in the outer layers, or to promote RGC fate in the GCL, respectively. Furthermore, co-expression of OTX2 and DLX2 during late embryonic development at E18.5 can also be explained by the fact that *Otx2* is also important for the formation of bipolar cells and since DLX2 co-localizes with bipolar cell marker protein kinase C (PKC) (de Melo et al., 2003), we postulate that perhaps OTX2 and DLX2 function synergistically and in a combinatorial fashion to promote and maintain bipolar cells in this subset of OTX2+/DLX2+ progenitor cells. One limitation of these results is that the E13.5 data were overlaid images of single immunofluorescence experiments, thus they do not offer conclusive co-localization information of OTX2 and DLX2. For the future, double immunofluorescence experiments should be conducted at E13.5 which will target both OTX2 and DLX2 in the same retina section to determine whether OTX2 and DLX2 co-localize at this embryonic age.

OTX2 can directly bind and interact with Dlx2 regulatory subregions and the Dlx1/Dlx2 intergenic enhancer I12a in vitro and in vivo

ChIP-Seq data of histone posttranslational modifications and multiple alignment data from the UCSC Genome Browser support that transcription factors could potentially bind to *Dlx* regulatory regions. There are several subregions upstream the *Dlx2* promoter that are enriched in H3K27me3 histone modifications which mark chromatin that is in a repressive state (**Figure**

4.2A-B). In the *Dlx1/Dlx2* intergenic region, there are prominent H3K4Me2 and H3K27ac histone modification peaks suggesting that this intergenic region presents an active chromatin landscape. Taken together, this supports that OTX2 may bind upstream the *Dlx2* promoter in a repressive chromatin context. In contrast, OTX2 may bind the *Dlx1/Dlx2* intergenic region in an activating chromatin context. Multiple alignments data revealed that subregions upstream the *Dlx2* promoter and in the *Dlx1/Dlx2* intergenic region contain binding motifs that are evolutionarily conserved across various vertebrate species which make them more likely to be important regulatory regions (**Figure 4.3**). There are certain subregions that were aligned to three species, such as Subregion 2 and Subregion 4.2. However, there is a distinct possibility that the alignment algorithms may not correctly align the motifs because those motifs are very short, sometimes degenerate, and may even be in the reverse orientation or changed their position (Gordân, Narlikar, & Hartemink, 2010). Kheradpour et al. have shown examples of *Drosophila melanogaster Mef*-2 binding sites that are not correctly aligned to the orthologous sites in 11 related Drosophila species (Gordân et al., 2010; Kheradpour, Stark, Roy, & Kellis, 2007). In summary, these *in silico* analyses provide support that OTX2 may bind these candidate regulatory subregions to regulate *Dlx2* expression.

In vitro and *in vivo* experiments were subsequently conducted to validate that OTX2 can bind these candidate binding sites. OTX2 regulates transcription of target genes by binding to sites containing TAATNC consensus motifs with certain flexibility in 5^{th} and 6^{th} position. I have identified several putative OTX2 binding sites (TAATCC/TAACCC/TAAGCC/TAATCT) within 10kb upstream the *Dlx1* and *Dlx2* transcriptional start sites and the *Dlx1/2* intergenic region. From those candidate motifs, I determined that 11 subregions (R1, R2, R4.2, R5, R6.1/R6.2, R9.1/R9.2, R7, R8.1/R8.2) were bound by recombinant OTX2 in EMSAs. I also

determined 4 subregions (R1, R2, R4.1/R4.2 and the entire R4.12, R9.1/R9.2) were occupied by OTX2 *in vivo* via ChIP assays. These findings support the hypothesis that OTX2 can regulate *Dlx1/Dlx2* possibly to regulate retinal cell fate decisions.

Electrophoretic mobility shift assays (EMSA) revealed that recombinant OTX2 protein can directly bind most of these potential regulatory subregions upstream *Dlx1* and *Dlx2* and in the intergenic region except for Subregion 3 and Subregion 4.1 *in vitro* (**Figure 4.4-4.6**). The ability to bind these regulatory regions directly is consistent with a regulatory role for OTX2 in regulating *Dlx1/Dlx2*. One limitation of the EMSA experiment is that the oligonucleotide probes that I used were short (~20bp) and did not contain sufficient sequence surrounding the homeodomain binding motif to recapitulate the chromatin environment of "complete" binding sites. In addition, the detection of a binding event *in vitro* via EMSA may not signify a functional *in vivo* interaction. Furthermore, the recombinant protein used does not have post-translational modifications which may be required for binding *in vivo*. Thus, one important future direction is to conduct these experiments using nuclear extracts obtained from E18.5 retina which contains endogenous OTX2 protein and labelled DNA fragments isolated from the subsequent ChIP experiments to confirm whether binding is direct and specific *in vivo*.

To assess whether OTX2 interacts with these potential regulatory subregions *in vivo*, chromatin immunoprecipitation (ChIP) followed by end-point PCR in E18.5 WT mouse retina was conducted. E18.5 was chosen as an appropriate developmental time point for this experiment because there is a wave of photoreceptor genesis immediately preceding birth, so I reasoned that the regulation of *Dlx2* by OTX2 to promote photoreceptor development would occur around that timepoint. Also, the distinct expression domains of OTX2 and DLX2 at E18.5 suggested cross-regulation at this developmental stage (**Figure 4.1D-F**) which further indicates

that E18.5 was an appropriate embryonic time point to conduct these ChIP experiments. OTX2 ChIP revealed that OTX2 occupied several potential regulatory subregions upstream *Dlx2* and the *Dlx1/Dlx2* intergenic enhancer *in vivo* (**Figure 4.7**). These results provide support that OTX2 could potentially regulate *Dlx2* expression by occupying these binding sites upstream *Dlx2* and the *I12a* intergenic enhancer. In fact, the *Dlx2* promoter has been reported to be bound by OTX2 in interneurons of the embryonic and postnatal cortex (Sakai et al., 2017), which further supports regulation of *Dlx2* by OTX2. Together the EMSA and ChIP results support *in vitro* and *in vivo* protein-DNA interactions, which is consistent with OTX2 having a regulatory function on *Dlx2* gene expression.

One technical limitation of these ChIP experiments is that the entire eye nuclei were isolated for ChIPs. This would be valid because *Otx2* is expressed only in the neural retina and retinal pigmented epithelium. In hindsight, this can be a source of error because OTX2 is a low-abundance transcription factor so the many other proteins in the eye lysates could make the immunoprecipitation less efficient, thus "diluting" the enrichment signal. This transcription factor is not abundant among all the proteins of the eye, so the antibody might not efficiently immunoprecipitate the desired protein. Future directions include isolating only the retina and conducting chromatin immunoprecipitation using only the retina if possible, also excluding the RPE. Furthermore, other ChIP experiments at E18.5 were inconclusive because negative and positive controls were not conclusive (data not shown). It is possible that this phenomenon could be attributed to technical error. Other OTX2 ChIP experiments were conducted by applying the antibody first and then applying the beads so perhaps antibody binding to the protein-DNA complex is lost before the beads were applied to retrieve the complexes resulting in non-specific binding of the beads. However, setting this aside, inherent variabilities during the major steps of

ChIP experiments, such as fixation, fragment size during chromatin shearing, crosslinking, immunoprecipitation and protein-DNA washing efficiencies, are major limitations of ChIP experiments (Mukhopadhyay, Deplancke, Walhout, & Tissenbaum, 2008). For example, fixation may not be complete in some experiments, thus variability in target DNA sequences cross-linked to the protein factor is always present. So, the effects of variable fixation would be observed. Furthermore, sometimes the antibody does not efficiently immunoprecipitate the complexes. These variabilities interfere with interpretation of results. Therefore, for the future, optimizing and controlling the experimental conditions for each step is important to ensure consistent results. One important limitation of using standard qualitative PCR to analyze immunoprecipitated chromatin is that sometimes enrichment could simply be due to some immunoprecipitated samples containing more input chromatin. This drawback can be overcome by quantifying the input DNA from each sample prior to immunoprecipitation and utilizing an equal amount of chromatin in the immunoprecipitation. One future direction is to conduct ChIP followed by quantitative real-time PCR. It is also important to include a negative OTX2 target locus as a negative locus control to ensure that the observed enrichment is specific. Furthermore, ChIP experiments in general do not demonstrate direct binding. OTX2 could interact with a regulatory subregion through a protein complex but without directly binding to the DNA motif itself, which will still show as an enrichment. This may explain that OTX2 cannot bind Subregion 4.1 directly via EMSA but still appears to be more enriched in the AB+ sample via ChIP (**Figure 4.7**). Another future direction to optimize the ChIP experiment is to conduct ChIP with micrococcal nucleases instead of sonication, because immuno-precipitation is highly specific and efficient using this method (Das et al., 2004). In addition, although we have demonstrated that ChIP is associated with these specific subregions *in vivo*, it is difficult to

determine in what cells this association is present. Thus, one future direction would be to conduct ChIP-Seq and use a bioinformatics approach to examine these interactions in a more precise and cell-type specific manner.

OTX2 can potentially repress and activate reporter activity of subregions upstream the Dlx2 promoter, while activating the reporter activity of the Dlx1/Dlx2 intergenic enhancer I12a

Based on the positive EMSA and ChIP results, I performed functional assessments of OTX2 occupation of the *Dlx2* regulatory regions. Since protein-DNA interactions may not confer function, luciferase reporter assays were conducted to determine if OTX2 binding to any putative *Dlx2* regulatory subregions could regulate transcription *in vitro*. In line with our hypothesis, if OTX2 represses *Dlx2* by binding to any of these EMSA-positive ChIP-positive subregions, a decrease in reporter gene expression would be expected with OTX2 co-expression. However, luciferase reporter assays revealed that OTX2 could either activate or repress reporter activity driven by regulatory subregions upstream the *Dlx2* promoter in HEK293 cells (**Figure 4.9**).

Although OTX2 was able to directly bind and associate with many regulatory subregions, only two subregions elicited an activating transcriptional response to OTX2 in HEK293 cells. Luciferase reporter assays demonstrated that OTX2 significantly activated reporter gene transcription driven by Subregion 4.12 upstream *Dlx2* and Subregion 9.12 (*Dlx1/Dlx2* intergenic enhancer I12a). In particular, OTX2 activated the reporter activity of the *I12a* intergenic enhancer in HEK293 cells by a drastic amount (from 200 to 4000 RLU, **Figure 4.9**). Subregion 9.12 is evolutionarily conserved among many species (**Figure 4.3**) and contains two putative OTX2 binding motifs close together, which could explain the dramatic activation of transcription by OTX2. Subregion 9.12 (*I12a* intergenic enhancer) is enriched with H3K27ac which is a chromatin signature of "primed enhancers" (**Figure 4.2B**). This is consistent with the fact that

co-transfecting this element with OTX2 activated reporter gene transcription *in vitro*. Interestingly, the transcriptional activating effect of Subregion 4.12 is not consistent with the presence of H3K27me3 marks upstream the *Dlx2* promoter (**Figure 4.2B**). In this case, I speculate that *in vivo*, these repressive chromatin marks may be cleared when certain transcription factors bind to enhancer regions to recruit demethylase (Saxena et al., 2017). At face value, this transcriptional activating effect does not support our original hypothesis that OTX2 represses *Dlx2*. However, this can be explained by the transactivating properties of the OTX2 protein, so perhaps it can activate certain factors that remodel chromatin to enable transcriptional repression. In addition, perhaps under certain environmental signals, OTX2 could activate *Dlx2* during development to activate RGC genes necessary for RGC development.

I observed that Subregion 1 may drive transcription repression by OTX2 in HEK293 cells. Although this repressive activity is independent of OTX2, we did detect a statistically significant decrease in reporter gene transcription when the Subregion 1 construct was transfected compared to the control empty reporter. This result suggests that Subregion 1 can drive repression of the reporter gene. This suggests that this element may confer regulatory activity for *Dlx2* expression independent of the presence of OTX2. Another possibility is that this result does not necessarily mean that OTX2 is unable to repress reporter activity via Subregion 1. HEK293 cells were chosen because they have no endogenous OTX2 expression and also for ease of transfection. HEK293 cells and retinal progenitor cells are very different in terms of what extrinsic or intrinsic factors may be present. It is possible that other transcription factors present in HEK293 cells bind Subregion 1 to repress transcription of the reporter gene and binding of these other factors in turn prevents OTX2 from accessing this regulatory subregion. These factors can also modulate the ability of OTX2 to exert transcriptional control. It

is still plausible that in the embryonic retina, OTX2 can repress transcription via Subregion 1. One future direction would be to recapitulate the biological condition and assess whether *Dlx2* gene expression can be repressed or activated by OTX2 *in vivo*. This can be achieved by conducting *in utero* electroporation in the developing mouse retina either to disrupt or overexpress OTX2 protein, and subsequently assess the expression of *Dlx2* in the electroporated cells which now express GFP using immunostaining (de Melo & Blackshaw, 2011). Prior work from the laboratory used *in utero* electroporation of *Dlx2* to activate *Brn3b* expression (Zhang et al., 2017).

Luciferase reporter assays also revealed that co-transfection of OTX2 and Subregion 2 does not affect reporter gene transcription. This result can be explained by the fact that in eukaryotes, gene expression is usually regulated by a combination of protein factors that work in a coordinated fashion. In the current biological context, which is the transformed human embryonic kidney, perhaps those factors necessary to facilitate or impeded RNA polymerase recruitment to the *Dlx2* basal promoter through upstream Subregion 2 were not present.

Whether OTX2 is regulating the reporter activity of these subregions individually is a very different question than whether OTX2 regulates the reporter activity of the entire *Dlx2* promoter-upstream region as a whole. For example, even though OTX2 does not affect reporter activity of Subregion 2 individually *in vitro*, this does not necessarily mean that OTX2 would not regulate this particular subregion *in vivo*. Thus, another limitation of this experiment is that adding in an isolated regulatory element into a reporter plasmid for *in vitro* expression experiment really does not recapitulate the chromatin context where the regulatory regions are intact and conformational changes required for *in vivo* regulation are preserved. In the retina, OTX2 may occupy the region upstream the basal promoter to regulate endogenous *Dlx2* gene

expression in a way that is likely very different from how OTX2 would regulate reporter gene activity via a short piece of regulatory subregion DNA in HEK293 cells. Therefore, one important future direction would be to repeat the experiment by constructing the full 10 kb upstream region reporter construct to assess the overall regulatory effect of the full 10kb regulatory region, which contains several binding motifs for OTX2 and for other transcription factors, on *Dlx2* transcription. Subsequently, it would be helpful to use site-directed mutagenesis or CRISPR/*Cas9* mediated gene editing to mutate or delete sub-sections of the entire regulatory region to determine which specific subregion has a critical effect on *Dlx2* transcription.

Taken together, the luciferase assays reveal that OTX2 can regulate *Dlx2* both positively and negatively. It is not uncommon that one transcription factor can have opposing functions (Boyle & Després, 2010). Whether a transcription factor activates or represses transcription depends on many things such as the regulatory element that the transcription factor is bound to, co-factors that it interacts, the structure of the surrounding chromatin/regulatory chromatin landscape, and the type of molecules available in the nuclear environment and the cell type. A transcription factor can function as an activator and a repressor as determined by the co-factors that may also bind to the transcription factor under certain contexts. For example, E2F transcription factors can function as both an activator and repressor of transcription depending on whether it interacts with retinoblastoma protein (pRB), other pocket proteins (p107 and p130) or Polycomb group proteins (PcG) (Dimova & Dyson, 2005). Activator E2Fs interact with histone acetyltransferases (HAT), whereas when pRB is recruited to promoters by these activator E2Fs, they can interact with different chromatin-modifying repressive complexes such as histone deacetylase (HDAC) or histone methyltransferase, which may possibly explain why E2Fs can activate and repress transcription (Dimova & Dyson, 2005). Another example is NFATc1, which

is an important NFAT factor in activated lymphocytes, that has an opposite effect on interleukin 2 transcription depending on whether it is sumoylated. There are SUMO sites in their C-terminus. When NFATC1/βC protein is sumoylated, it becomes bound by HDAC and its activity changes from a transcription activator to a repressor (Nayak et al., 2009). Therefore, it would be important to investigate potential co-regulators of OTX2 in the future. Furthermore, slightly different transcription binding sites may result in opposite regulatory effect on the same gene. For example, the glucocorticoid receptor results in gene activation when recruited to the glucocorticoid response element (GRE), but when recruited to another *cis*-regulatory element termed the negative GRE (nGRE), it leads to transcriptional repression (Boyle & Després, 2010). This may be the case for the present study, when OTX2 is recruited more distally to the *Dlx2* promoter (Subregion 1), it may repress *Dlx2* transcription, whereas when recruited more proximally to the *Dlx2* promoter and/or to the intergenic enhancer region it may lead to *Dlx2* activation. The biological reason for why OTX2 activates *Dlx2* is unknown. As discussed previously, under certain developmental contexts, OTX2 could activate *Dlx2* to help induce downstream programming during the differentiation of certain retinal cell types. For example, some *Chx10*-expression and PKC-expressing bipolar cells also express *Dlx2* (de Melo et al., 2003) which indicate that DLX2 could play a role in bipolar cell development. I speculate that OTX2 may activate the transcription of *Dlx2* in combination with other transcription factors such as *Chx10* to promote bipolar cell development. Another mechanism that influences whether a transcription factor activates or represses transcription is the chromatin structure or state surrounding its target genes. Interestingly, in the childhood malignant brain tumour medulloblastoma, OTX2 is critical in maintaining OTX2-bound promoters in a bivalent state where OTX2 can affect H3K27 methylation levels to poise target genes for both transcriptional

activation and repression (Bunt et al., 2013). Perhaps OTX2 occupies *Dlx2* regulatory regions, and simultaneously recruits another factor that could remodel the chromatin landmarks surrounding *Dlx2* in order to activate or repress its expression depending on the development and cellular contexts.

Furthermore, these reporter assays are *in vitro* experiments, and the results may not fully reflect the role of OTX2 in regulating *Dlx2* in a biological tissue such as the embryonic retina where gene regulation is very dynamic which is regulated at many strategies (chromatin structure, signaling molecules and other factors etc) and by many molecular events and affected by the biological environment and cell type. The entire regulatory region upstream *Dlx2* may contain binding sites for regulatory factors other than OTX2, which may not be present in HEK293 cells. One example is the NFκB transcription factor complex, which is regulated by many events that take place during the development of a particular cell type and this transcription factor is active in many cell types (Smale, 2011). Some of its target genes in mouse macrophages normally have repressive histone marks. However when a certain demethylase, *Aof1* is present, this repressive mark is removed, and this subset of target genes can then be activated in this case (Smale, 2011). Activators and repressor transcription factors may also interplay in a dynamic fashion to control the regulation of *Dlx2* gene expression. OTX2 may still repress *Dlx2* in combination with other factors or when other factors deposit certain chromatin repressive marks onto the chromatin in a specific developmental context. Therefore, it may also be the case that OTX2 will interact with different subregions upstream the *Dlx2* promoter to activate and repress *Dlx2* for different functions and/or fine-tune *Dlx2* expression but the purpose remains unknown. In addition, the binding sites for other transcription factors may overlap with OTX2 binding sites. For instance, in the forebrain, *Ascl1/Mash1* bind the *Dlx1/Dlx2* intergenic

enhancers (Parras et al., 2007; Petryniak, Potter, Rowitch, & Rubenstein, 2007). Likewise, there could be such transcription factors with overlapping binding sites as OTX2, such as OTX1, in the retina to regulate retinal development, that is not present in HEK293 cells. One future direction to circumvent this drawback is to conduct the reporter assay in living rodents using bioluminescence imaging to track gene expression in transfected tissues. It would be interesting to explore binding sites for other protein factors that overlap with and/or are intercalated between these subregions upstream *Dlx2* and around the intergenic enhancer. It would also be interesting to observe if there is a compensatory increase in these other factors when OTX2 is ablated in the developing retina.

Another limitation of these experiments is that we have only depicted the effect of OTX2 at one expression level. However, expression levels of OTX2 are important to influence binary cell fate decisions (C. Chan et al., 2019; Wang et al., 2014). For example, high levels of OTX2 drive bipolar cell formation, as opposed to rod photoreceptors (Wang et al., 2014). This could also be applied to the context of RGC versus photoreceptor cell fate decisions. Potentially, when OTX2 is expressed at a certain level, it represses *Dlx2* to promote photoreceptor differentiation while at other levels it activates *Dlx2* and other RGC genes to promote RGC and/or bipolar cell development. Therefore, one important future direction is to investigate the reporter activity of these *Dlx2* regulatory subregions using various expression levels of OTX2.

In addition, OTX2 uses various transcription start sites on different exons to produce different mRNAs and protein isoforms. The relative levels of the RNA variants change during retina development which means that perhaps variant OTX2 proteins with different functions are produced in tissue-and/or time-course-specific biological settings to regulate various aspects of retina and/or neuronal development (Courtois et al., 2003). Different variant proteins can form

different partnerships with other factors. The OTX2 expression vector used in this experiment produces the variant B protein isoform. Variant A is also expressed in the developing retina. One future direction would be to conduct luciferase experiments using OTX2 variant A.

Taken together, the luciferase reporter assay results reveal both activating and repressing sites upstream *Dlx2*, as well as an activating site in the *I12a* intergenic enhancer, with which OTX2 may interact to regulate transcription both negatively and positively. These luciferase reporter assay data suggest that these activating and repressive elements are intercalated in these regulatory regions to influence *Dlx2* transcription in a precise and multifaceted fashion.

Reduced Otx2 expression may lead to a decrease in inner nuclear layer thickness, an expanded retinal ganglion cell layer, as well as an expansion of DLX2 expression domain in Otx2 loss-of-function mutant mouse retina at P100

Lastly to assess the *in vivo* effect of loss of *Otx2* in the retina, H&E staining and immunofluorescence was performed to compare morphology and DLX2 expression between P100 wildtype and heterozygous $Otx2^{+/GFP}$ mutant mouse retinas. H&E histology (**Figure 4.10A-D**) revealed that the inner nuclear layer thickness may be decreased in the heterozygous $Otx2^{+/GFP}$ mouse retina. This was also observed in our collaborator's lab (Bernard et al., 2014). The inner nuclear layer is where bipolar cells, amacrine cells and horizontal cells are located. This result can be explained by the observation that *Otx2* is important for the development of cell types in the inner nuclear layer such as bipolar cells (Koike et al., 2007). Decreased OTX2 levels lead to bipolar cell death. In addition, we have discovered that the haematoxylin staining of the ganglion cell nuclei appear to be more intense and the ganglion cell layer may be expanded in the mutant mouse retina. This result suggests an increase in retinal ganglion cell-like cells when OTX2 is reduced which results in an expanded ganglion cell layer observed in the $Otx2^{+/GFP}$ mutant mouse retina. This supports our hypothesis that OTX2 represses *Dlx2 t*o promote

photoreceptor fate. However, studies in homozygous knock-in mice expressing a mutated form of OTX2 protein have shown that after 10 months, the number of cells in the ganglion cell layer is significantly reduced possibly due to an insufficient amount of OTX2 protein being transferred to the RGCs, which consequently promotes RGC degeneration (Bernard et al., 2014; Torero Ibad et al., 2011). This is not what we observed for the P100 retina. This could be due to the age difference. *Otx2* regulation in the retina is complex and it would definitely be interesting in the future to examine the histological changes at various embryonic and postnatal ages in more detail.

Subsequently, to determine the effect of ablating one allele of *Otx2* on *Dlx2* expression specifically in the mouse retina, single immunofluorescence using DLX2 antibody was performed to compare DLX2 expression between the wildtype and the heterozygous $Otx2^{+/GFP}$ mutant mouse retina. In both wildtype and mutant retinas, DLX2 is expressed in the ganglion cell layer and possibly the inner nuclear layer (upper red layers of **Figure 4.11A-D**). If DLX2 is expressed in the inner nuclear layer, we would expect DLX2 to co-localize with DAPI. However, in these tissues it is difficult to determine whether the red DLX2 colocalizes with the blue DAPI in the upper layers because they do appear to be in "separate layers". One technical challenge that greatly hindered me from interpreting the results is that the morphology of the retina was disrupted during the staining procedures. So, this result could be due to the disrupted morphology and so DLX2 is actually expressed in the inner nuclear layer in these samples. In this case, this is as expected because DLX2 is restricted to the GCL and the INL throughout adulthood (de Melo et al., 2003). Due to disrupted morphology, it is also difficult to definitively compare DLX2 expression levels between the wildtype and mutant retina sections. **Figure 4.11D** demonstrated that the domain where DLX2 is expressed (upper red layers) in the mutant may be

expanded. Unfortunately, these DLX2-expressing layers appear to be merged, and when compared with the wildtype sections, the expanded layers could be the ganglion cell layer and/or the inner nuclear layer (**Figure 4.11C-D**). If this result is real, this is consistent with our hypothesis that OTX2 represses *Dlx2*. So when OTX2 is reduced, we would expect DLX2 expression to be upregulated in the ganglion cell layer to promote RGC fate (Zhang et al., 2017). In addition, if the observed result is real, it would be consistent with what Omori et al. observed that *Dlx1* and *Dlx2* transcript levels are increased in *Otx2* conditional knockout retinas (Omori et al., 2011).

One limitation is that the knockout tissue morphology has variabilities, one future direction is to optimize the fixation time. Another important future direction is to conduct qRT-PCR gene expression analysis of *Dlx2* between the wildtype and $Otx2^{+/GFP}$ mouse retina tissue at various time points to confirm the aforementioned results. In addition, once more tissues are collected and sectioned, cell counting is to be conducted to quantitatively assess DLX2 expression level. Furthermore, one technical limitation is that the specific age at which these mice were harvested was pre-determined by our collaborator. Thus, one critical future direction is to assess the effect of ablating one *Otx2* allele at various embryonic stages by conducting histological analysis and immunostaining for DLX2 protein expression in the $Otx2^{+/GFP}$ mutant at other developmental time points.

Another important limitation of this experiment is that we only assessed the function of the one wild type allele *Otx2*. *Otx2* gene dosage can have a significant functional effect (Bernard et al., 2014; Wang et al., 2014). The loss of two *Otx2* alleles in the retina specifically may have completely different phenotypes. Therefore, one important future direction is to assess mice with various doses of mutated OTX2 protein generated by our collaborator. In the long run, it would

be worthwhile to generate a retina specific *Otx2* conditional knockout mouse model and assess *Dlx2* expression in the CKO mutant. It would be crucial to study the function of knocking out *Otx2* in the eye by determining visual acuity and conducting electroretinography and optical coherence tomography in the mutant mice. It would be also interesting to cross our *Dlx1/Dlx2* DKO mutant mouse to a *Otx2*-GFP reporter mouse to determine the effect of ablating *Dlx2* on *Otx2* expression, thereby further elucidating the gene regulatory networks shared by these two critical transcription factors during retinal development.

Chapter 6: Conclusions and Future Directions

In our *Dlx1/Dlx2* DKO, there is increased retinal ganglion cell death and an ectopic expression of photoreceptor genes such as *Crx*. In knockout animal models of *Otx2*, such as in mice and chicks, upregulation of *Dlx1/Dlx2* and other retinal ganglion cell markers including *Brn3b* is observed (Ghinia Tegla et al., 2020; Omori et al., 2011). Therefore, we hypothesize that OTX2 restricts retinal ganglion cell fate in retinal progenitor cells that are destined to become photoreceptor cells by suppressing *Dlx1/Dlx2* genes which are critical for retinal ganglion cell differentiation.

In this project, I investigated if OTX2 directly regulates *Distal-less* genes (*Dlx1/Dlx2*) during retina development to repress *Dlx1/Dlx2* repression. We have found that in the mouse retina *Otx2* and *Dlx2* have some overlapping and distinct expression patterns early during embryonic development, and more distinct expression domains later during embryonic development. OTX2 can directly bind regulatory regions upstream the *Dlx1* and *Dlx2* promoters, and in the *Dlx1/Dlx2* intergenic region *in vitro*. In E18.5 wildtype mouse retina, OTX2 occupies regulatory regions upstream the *Dlx2* promoter and the *Dlx1/Dlx2* intergenic enhancer region *in vivo*. We have also demonstrated that OTX2 may bind subregions upstream the *Dlx2* promoter and the *I12a* intergenic enhancer to repress and activate reporter gene transcription *in vitro*. Preliminary loss-of-function assessment reveals that reduced OTX2 may result in reduced inner nuclear layer thickness and an expanded ganglion cell layer. Loss of one allele of *Otx2* gene function will potentially also result in an expanded *Dlx2*-expressing domain.

Based on the data presented in this study, I can conclude that OTX2 has the ability to regulate *Dlx2* transcription by binding directly and occupying regulatory regions upstream *Dlx2* and in the intergenic region. I speculate that in the actual biological context of the developing retina, this process is dynamic and involves multiple factors that function with OTX2 to regulate

Dlx2 expression in deciding the fate of these retinal progenitor cells. In view of the evidence that OTX2 can activate and repress *Dlx2* transcription *in vitro*, I propose that OTX2 may have a dual role in regulating *Dlx2* depending on the presence of various extrinsic signals and the developmental and cellular contexts (**Figure 6.1**). The functional significance of OTX2 interacting with *Dlx2* in the retina requires further evaluation. One of the assessments that I conducted is examining *Otx2* loss of function in relation to *Dlx2* using a biologically relevant model organism, the $Otx2^{+/GFP}$ mouse. I assessed the morphology and DLX2 protein expression when one copy of *Otx2* was ablated. These results suggest that the inner nuclear layer and the ganglion cell layer may be affected and that *Dlx2*, which encode components associated with retinal ganglion cells, may be upregulated in the mutant. However due to technical challenges and the limited sample number, these results require further confirmation.

One future direction is to quantify DLX2 single positive, OTX2 single positive and DLX2/OTX2 double positive (i.e. co-expressing) cells at various developmental timepoints to precisely determine the changes in protein expression throughout development in wildtype mouse retina. Another important long-term future direction would be to generate a retina-specific conditional *Otx2* knockout mouse generated by breeding *Otx2*-flox mice with RPC-specific *Cre* mice. Then we can study OTX2 mediated regulation of *Dlx2* both embryonically and postnatally *in vivo* using quantitative RT-PCR to determine *Dlx2* mRNA expression level and immunofluorescence to determine DLX2 protein expression level changes at various developmental stages in the *Otx2* conditional knockout mutant retina. In fact Omori et al. observed that *Dlx1* and *Dlx2* transcript levels are increased in *Otx2* conditional knockout mouse retinas postnatally close to birth (Omori et al., 2011).

One important *in vivo* experiment to conduct for the future, in order to manipulate *Otx2* expression in the developing mouse retina in a spatially and temporally specific manner, is ablation or overexpression using *in vivo* electroporation of a silencing RNA expression vector for *Otx2* and/or introducing a mutated form of OTX2 protein (such as a DNA binding mutant), and by overexpressing *Otx2* into the developing mouse retina, followed by visualization of the electroporated cells using immunofluorescence (de Melo et al., 2011; Zhang et al., 2017). This experiment is an excellent method to assess the function of OTX2 in regulating *Dlx2* expression in the biologically relevant context. Another important future direction is to conduct the reporter assays in living rodents using bioluminescence imaging to track gene expression changes in transfected retina. Furthermore another important future direction is to conduct site-directed mutagenesis *in vivo* using CRISPR/*Cas9* to confirm if transcription factor binding is truly functionally relevant to regulating gene expression (Vinckevicius & Chakravarti, 2012). To understand the long-term effect of introducing or ablating *Otx2*, retrovirally mediated manipulation of *Otx2* can be conducted (Buch, Bainbridge, & Ali, 2008). As another long-term future direction, it would be also interesting to explore other factors that occupy and function in combination and an overlapping fashion with OTX2 in these regulatory regions to regulate *Dlx2* expression.

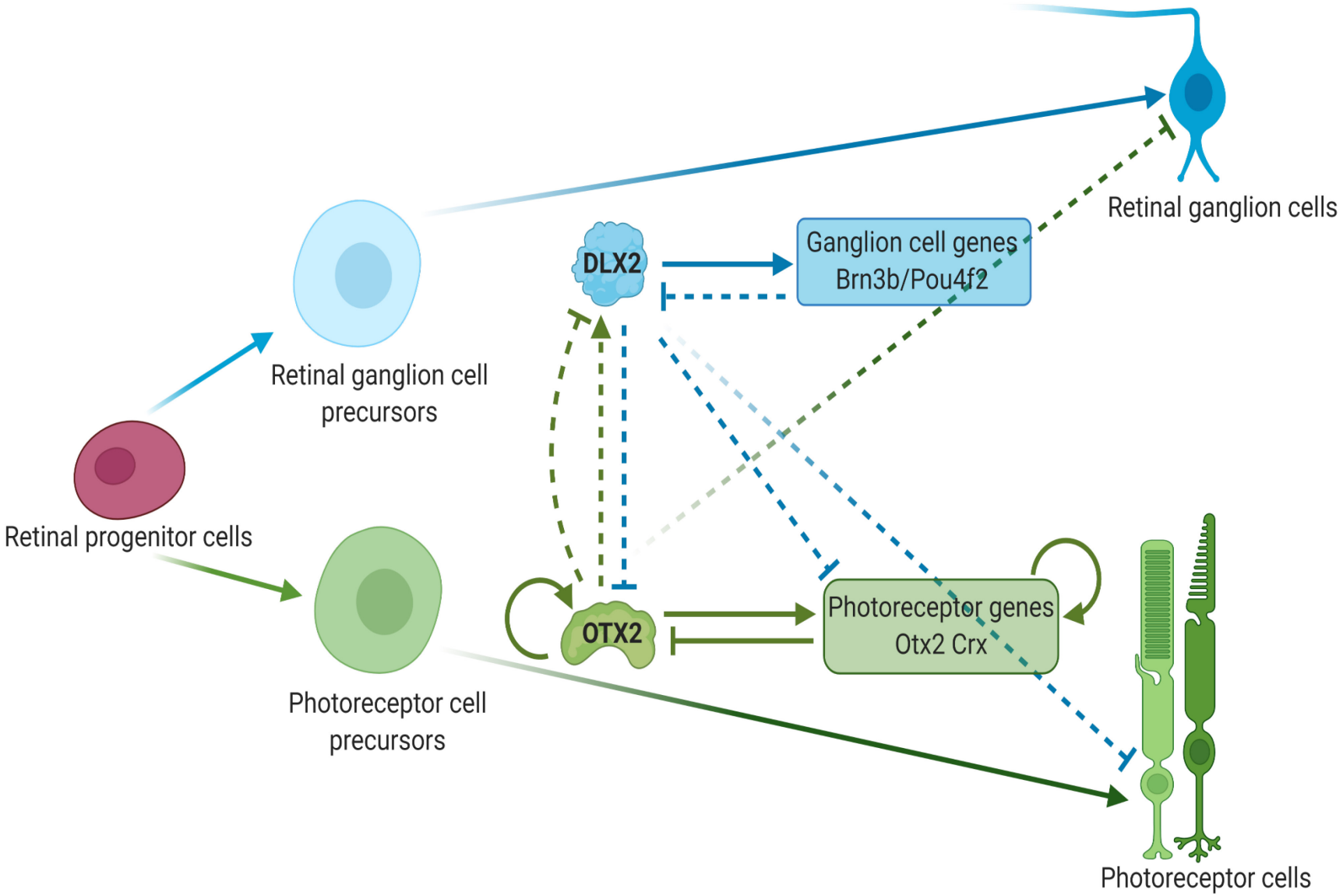
Retinal ganglion cells
DLX2
Ganglion cell genes
Brn3b/Pou4f2
Retinal ganglion cell
precursors
Retinal progenitor cells
OTX2
Photoreceptor genes
Otx2 Crx
Photoreceptor cell
precursors
Photoreceptor cells

Figure 6.1

Proposed model of OTX2 and DLX1/DLX2 regulation of retinal cell fate decisions

We propose that *Dlx1/Dlx2* plays a critical role in promoting retinal ganglion cell differentiation and survival by activating *Brn3b/Pou4f2* and other retinal ganglion cell genes required for RGC differentiation and survival. In addition to promoting RGC fate, DLX1/DLX2 also represses the expression of photoreceptor genes such as *Otx2* and *Crx* in order to restrict photoreceptor cell fate in retinal progenitor cells.

In photoreceptor differentiation, OTX2 activates *Crx* and other photoreceptor genes driving retinal progenitor cells to adopt photoreceptor cell fate. Concomitantly, cross-regulation of transcription factors occurs where OTX2 may have a dual function in regulating *Dlx1/Dlx2* expression in the developing retina. OTX2 may inhibit *Dlx1/Dlx2* expression thus inhibiting certain progenitor cells from adopting retinal ganglion cell fate. OTX2 may also activate the expression of *Dlx1/Dlx2* in other progenitor populations to establish the necessary developmental programming for the differentiation of other retinal cell types. This figure was created with Biorender.com.

Literature Cited

Acampora, D., Gulisano, M., & Simeone, A. (2000). Genetic and molecular roles of Otx homeodomain proteins in head development. *Gene*, *246*(1–2), 23–35.

Acampora, D., Mazan, S., Lallemand, Y., Avantaggiato, V., Maury, M., Simeone, A., & Brûlet, P. (1995). Forebrain and midbrain regions are deleted in Otx2-/- mutants due to a defective anterior neuroectoderm specification during gastrulation. *Development* , *121*(10), 3279–3290.

Akagi, T., Mandai, M., Ooto, S., Hirami, Y., Osakada, F., Kageyama, R., … Takahashi, M. (2004). Otx2 homeobox gene induces photoreceptor-specific phenotypes in cells derived from adult iris and ciliary tissue. *Investigative Ophthalmology & Visual Science*, *45*(12), 4570–4575.

Baddam, P., Kung, T., Adesida, A. B., & Graf, D. (2021). Histological and molecular characterization of the growing nasal septum in mice. *Journal of Anatomy*, *238*(3), 751–764.

Badea, T. C., Cahill, H., Ecker, J., Hattar, S., & Nathans, J. (2009). Distinct roles of transcription factors brn3a and brn3b in controlling the development, morphology, and function of retinal ganglion cells. *Neuron*, *61*(6), 852–864.

Barbieri, A. M., Lupo, G., Bulfone, A., Andreazzoli, M., Mariani, M., Fougerousse, F., … Banfi, S. (1999). A homeobox gene, vax2, controls the patterning of the eye dorsoventral axis. *Proceedings of the National Academy of Sciences of the United States of America*, *96*(19), 10729–10734.

Bauer, P. (2011). Luciferase Reporter Gene Assays. In M. Schwab (Ed.), *Encyclopedia of Cancer* (pp. 2077–2081). Berlin, Heidelberg: Springer Berlin Heidelberg.

Bäumer, N., Marquardt, T., Stoykova, A., Spieler, D., Treichel, D., Ashery-Padan, R., & Gruss, P. (2003). Retinal pigmented epithelium determination requires the redundant activities of Pax2 and Pax6. *Development* , *130*(13), 2903–2915.

Béby, F., Housset, M., Fossat, N., Le Greneur, C., Flamant, F., Godement, P., & Lamonerie, T. (2010). Otx2 gene deletion in adult mouse retina induces rapid RPE dystrophy and slow photoreceptor degeneration. *PloS One*, *5*(7), e11673.

Beby, F., & Lamonerie, T. (2013). The homeobox gene Otx2 in development and disease. *Experimental Eye Research*, *111*, 9–16.

Bernard, C., Kim, H.-T., Torero Ibad, R., Lee, E. J., Simonutti, M., Picaud, S., … Kim, J. W. (2014). Graded Otx2 activities demonstrate dose-sensitive eye and retina phenotypes. *Human Molecular Genetics*, *23*(7), 1742–1753.

Bosze, B., Hufnagel, R. B., & Brown, N. L. (2020). Chapter 21 - Specification of retinal cell types. In J. Rubenstein, P. Rakic, B. Chen, & K. Y. Kwan (Eds.), *Patterning and Cell Type Specification in the Developing CNS and PNS (Second Edition)* (pp. 481–504). Academic Press.

Bovolenta, P., Mallamaci, A., Briata, P., Corte, G., & Boncinelli, E. (1997). Implication of OTX2 in pigment epithelium determination and neural retina differentiation. *The Journal of Neuroscience: The Official Journal of the Society for Neuroscience*, *17*(11), 4243–4252.

Boyl, P. P., Signore, M., Annino, A., Barbera, J. P., Acampora, D., & Simeone, A. (2001). Otx genes in the development and evolution of the vertebrate brain. *International Journal of Developmental Neuroscience: The Official Journal of the International Society for Developmental Neuroscience*, *19*(4), 353–363.

Boyle, P., & Després, C. (2010). Dual-function transcription factors and their entourage: unique and unifying themes governing two pathogenesis-related genes. *Plant Signaling & Behavior*, *5*(6), 629–634.

Bringmann, A., Pannicke, T., Grosche, J., Francke, M., Wiedemann, P., Skatchkov, S. N., … Reichenbach, A. (2006). Müller cells in the healthy and diseased retina. *Progress in Retinal and Eye Research*, *25*(4), 397–424.

Brown, N. L., Patel, S., Brzezinski, J., & Glaser, T. (2001). Math5 is required for retinal ganglion cell and optic nerve formation. *Development* , *128*(13), 2497–2508.

Brzezinski, J. A., 4th, Lamba, D. A., & Reh, T. A. (2010). Blimp1 controls photoreceptor versus bipolar cell fate choice during retinal development. *Development* , *137*(4), 619–629.

Brzezinski, J. A., 4th, Uoon Park, K., & Reh, T. A. (2013). Blimp1 (Prdm1) prevents re-specification of photoreceptors into retinal bipolar cells by restricting competence. *Developmental Biology*, *384*(2), 194–204.

Brzezinski, J. A., & Reh, T. A. (2015). Photoreceptor cell fate specification in vertebrates. *Development* , *142*(19), 3263–3273.

Buch, P. K., Bainbridge, J. W., & Ali, R. R. (2008). AAV-mediated gene therapy for retinal disorders: from mouse to man. *Gene Therapy*, *15*(11), 849–857.

Buenaventura, D. F., Ghinia-Tegla, M. G., & Emerson, M. M. (2018). Fate-restricted retinal progenitor cells adopt a molecular profile and spatial position distinct from multipotent progenitor cells. *Developmental Biology*, *443*(1), 35–49.

Bunt, J., Hasselt, N. A., Zwijnenburg, D. A., Koster, J., Versteeg, R., & Kool, M. (2013). OTX2 sustains a bivalent-like state of OTX2-bound promoters in medulloblastoma by maintaining their H3K27me3 levels. *Acta Neuropathologica*, *125*(3), 385–394.

Burmeister, M., Novak, J., Liang, M. Y., Basu, S., Ploder, L., Hawes, N. L., … McInnes, R. R. (1996). Ocular retardation mouse caused by Chx10 homeobox null allele: impaired retinal progenitor proliferation and bipolar cell differentiation. *Nature Genetics*, *12*(4), 376–384.

Casares, F., & Mann, R. S. (1998). Control of antennal versus leg development in Drosophila. *Nature*, *392*(6677), 723–726.

Cepko, C. (2014). Intrinsically different retinal progenitor cells produce specific types of progeny. *Nature Reviews. Neuroscience*, *15*(9), 615–627.

Chan, C., Lonfat, N., Zhao, R., Davis, A., Li, L., Wu, M.-R., … Wang, S. (2019). Cell type- and stage-specific expression of Otx2 is coordinated by a cohort of transcription factors and multiple cis-regulatory modules in the retina (p. 2019.12.19.882969). doi:10.1101/2019.12.19.882969

Chan, C. S. Y., Lonfat, N., Zhao, R., Davis, A. E., Li, L., Wu, M.-R., … Wang, S. (2020). Cell type- and stage-specific expression of Otx2 is regulated by multiple transcription factors and cis-regulatory modules in the retina. *Development* , *147*(14). doi:10.1242/dev.187922

Chen, H., Bagri, A., Zupicich, J. A., Zou, Y., Stoeckli, E., Pleasure, S. J., … Tessier-Lavigne, M. (2000). Neuropilin-2 regulates the development of selective cranial and sensory nerves and hippocampal mossy fiber projections. *Neuron*, *25*(1), 43–56.

Chen, S., Wang, Q. L., Nie, Z., Sun, H., Lennon, G., Copeland, N. G., … Zack, D. J. (1997). Crx, a novel Otx-like paired-homeodomain protein, binds to and transactivates photoreceptor cell-specific genes. *Neuron*, *19*(5), 1017–1030.

Cheng, H., Aleman, T. S., Cideciyan, A. V., Khanna, R., Jacobson, S. G., & Swaroop, A. (2006). In vivo function of the orphan nuclear receptor NR2E3 in establishing photoreceptor identity during mammalian retinal development. *Human Molecular Genetics*, *15*(17), 2588–2602.

Chow, R. L., Volgyi, B., Szilard, R. K., Ng, D., McKerlie, C., Bloomfield, S. A., … McInnes, R. R. (2004). Control of late off-center cone bipolar cell differentiation and visual signaling by the homeobox gene Vsx1. *Proceedings of the National Academy of Sciences of the United States of America*, *101*(6), 1754–1759.

Courtois, V., Chatelain, G., Han, Z.-Y., Le Novère, N., Brun, G., & Lamonerie, T. (2003). New Otx2 mRNA isoforms expressed in the mouse brain. *Journal of Neurochemistry*, *84*(4), 840–853.

Das, P. M., Ramachandran, K., vanWert, J., & Singal, R. (2004). Chromatin immunoprecipitation assay. *BioTechniques*, *37*(6), 961–969.

Dateki, S., Fukami, M., Sato, N., Muroya, K., Adachi, M., & Ogata, T. (2008). OTX2 mutation in a patient with anophthalmia, short stature, and partial growth hormone deficiency: functional studies using the IRBP, HESX1, and POU1F1 promoters. *The Journal of Clinical Endocrinology and Metabolism*, *93*(10), 3697–3702.

Dateki, S., Kosaka, K., Hasegawa, K., Tanaka, H., Azuma, N., Yokoya, S., … Ogata, T. (2010). Heterozygous orthodenticle homeobox 2 mutations are associated with variable pituitary phenotype. *The Journal of Clinical Endocrinology and Metabolism*, *95*(2), 756–764.

de Melo, J., & Blackshaw, S. (2011). In vivo electroporation of developing mouse retina. *Journal of Visualized Experiments: JoVE*, (52). doi:10.3791/2847

de Melo, J., Du, G., Fonseca, M., Gillespie, L.-A., Turk, W. J., Rubenstein, J. L. R., & Eisenstat, D. D. (2005). Dlx1 and Dlx2 function is necessary for terminal differentiation and survival of late-born retinal ganglion cells in the developing mouse retina. *Development* , *132*(2), 311–322.

de Melo, J., Miki, K., Rattner, A., Smallwood, P., Zibetti, C., Hirokawa, K., … Blackshaw, S. (2012). Injury-independent induction of reactive gliosis in retina by loss of function of

the LIM homeodomain transcription factor Lhx2. *Proceedings of the National Academy of Sciences of the United States of America*, *109*(12), 4657–4662.

de Melo, J., Peng, G.-H., Chen, S., & Blackshaw, S. (2011). The Spalt family transcription factor Sall3 regulates the development of cone photoreceptors and retinal horizontal interneurons. *Development* , *138*(11), 2325–2336.

de Melo, J., Qiu, X., Du, G., Cristante, L., & Eisenstat, D. D. (2003). Dlx1, Dlx2, Pax6, Brn3b, and Chx10 homeobox gene expression defines the retinal ganglion and inner nuclear layers of the developing and adult mouse retina. *The Journal of Comparative Neurology*, *461*(2), 187–204.

de Melo, J., Zhou, Q.-P., Zhang, Q., Zhang, S., Fonseca, M., Wigle, J. T., & Eisenstat, D. D. (2008). Dlx2 homeobox gene transcriptional regulation of Trkb neurotrophin receptor expression during mouse retinal development. *Nucleic Acids Research*, *36*(3), 872–884.

de Melo, J., Zibetti, C., Clark, B. S., Hwang, W., Miranda-Angulo, A. L., Qian, J., & Blackshaw, S. (2016). Lhx2 Is an Essential Factor for Retinal Gliogenesis and Notch Signaling. *The Journal of Neuroscience: The Official Journal of the Society for Neuroscience*, *36*(8), 2391–2405.

Deml, B., Reis, L. M., Lemyre, E., Clark, R. D., Kariminejad, A., & Semina, E. V. (2016). Novel mutations in PAX6, OTX2 and NDP in anophthalmia, microphthalmia and coloboma. *European Journal of Human Genetics: EJHG*, *24*(4), 535–541.

Di Giovannantonio, L. G., Di Salvio, M., Omodei, D., Prakash, N., Wurst, W., Pierani, A., … Simeone, A. (2014). Otx2 cell-autonomously determines dorsal mesencephalon versus cerebellum fate independently of isthmic organizing activity. *Development* , *141*(2), 377–388.

Dimova, D. K., & Dyson, N. J. (2005). The E2F transcriptional network: old acquaintances with new faces. *Oncogene*, *24*(17), 2810–2826.

Dorsky, R. I., Chang, W. S., Rapaport, D. H., & Harris, W. A. (1997). Regulation of neuronal diversity in the Xenopus retina by Delta signalling. *Nature*, *385*(6611), 67–70.

Dyer, M. A., Livesey, F. J., Cepko, C. L., & Oliver, G. (2003). Prox1 function controls progenitor cell proliferation and horizontal cell genesis in the mammalian retina. *Nature Genetics*, *34*(1), 53–58.

Eisenstat, D. D., Liu, J. K., Mione, M., Zhong, W., Yu, G., Anderson, S. A., … Rubenstein, J. L. (1999). DLX-1, DLX-2, and DLX-5 expression define distinct stages of basal forebrain differentiation. *The Journal of Comparative Neurology*, *414*(2), 217–237.

Elliott, J., Jolicoeur, C., Ramamurthy, V., & Cayouette, M. (2008). Ikaros confers early temporal competence to mouse retinal progenitor cells. *Neuron*, *60*(1), 26–39.

Emerson, M. M., Surzenko, N., Goetz, J. J., Trimarchi, J., & Cepko, C. L. (2013). Otx2 and Onecut1 promote the fates of cone photoreceptors and horizontal cells and repress rod photoreceptors. *Developmental Cell*, *26*(1), 59–72.

Feng, L., Xie, Z.-H., Ding, Q., Xie, X., Libby, R. T., & Gan, L. (2010). MATH5 controls the acquisition of multiple retinal cell fates. *Molecular Brain*, *3*, 36.

Fischer, A. J., & Reh, T. A. (2003). Potential of Müller glia to become neurogenic retinal progenitor cells. *Glia*, *43*(1), 70–76.

Fuhrmann, S., Levine, E. M., & Reh, T. A. (2000). Extraocular mesenchyme patterns the optic vesicle during early eye development in the embryonic chick. *Development* , *127*(21), 4599–4609.

Fuhrmann, Sabine. (2008). Wnt signaling in eye organogenesis. *Organogenesis*, *4*(2), 60–67.

Fujitani, Y., Fujitani, S., Luo, H., Qiu, F., Burlison, J., Long, Q., … Wright, C. V. E. (2006). Ptf1a determines horizontal and amacrine cell fates during mouse retinal development. *Development* , *133*(22), 4439–4450.

Furukawa, T., Morrow, E. M., & Cepko, C. L. (1997). Crx, a novel otx-like homeobox gene, shows photoreceptor-specific expression and regulates photoreceptor differentiation. *Cell*, *91*(4), 531–541.

Furukawa, T., Morrow, E. M., Li, T., Davis, F. C., & Cepko, C. L. (1999). Retinopathy and attenuated circadian entrainment in Crx-deficient mice. *Nature Genetics*, *23*(4), 466–470.

Furukawa, T., Mukherjee, S., Bao, Z. Z., Morrow, E. M., & Cepko, C. L. (2000). rax, Hes1, and notch1 promote the formation of Müller glia by postnatal retinal progenitor cells. *Neuron*, *26*(2), 383–394.

Gat-Yablonski, G. (2011). Brain development is a multi-level regulated process--the case of the OTX2 gene. *Pediatric Endocrinology Reviews: PER*, *9*(1), 422–430.

Geng, X., Speirs, C., Lagutin, O., Inbal, A., Liu, W., Solnica-Krezel, L., … Oliver, G. (2008). Haploinsufficiency of Six3 fails to activate Sonic hedgehog expression in the ventral forebrain and causes holoprosencephaly. *Developmental Cell*, *15*(2), 236–247.

Ghanem, N., Andrusiak, M. G., Svoboda, D., Al Lafi, S. M., Julian, L. M., McClellan, K. A., … Slack, R. S. (2012). The Rb/E2F pathway modulates neurogenesis through direct regulation of the Dlx1/Dlx2 bigene cluster. *The Journal of Neuroscience: The Official Journal of the Society for Neuroscience*, *32*(24), 8219–8230.

Ghanem, N., Yu, M., Long, J., Hatch, G., Rubenstein, J. L. R., & Ekker, M. (2007). Distinct cis-regulatory elements from the Dlx1/Dlx2 locus mark different progenitor cell populations in the ganglionic eminences and different subtypes of adult cortical interneurons. *The Journal of Neuroscience: The Official Journal of the Society for Neuroscience*, *27*(19), 5012–5022.

Ghinia Tegla, M. G., Buenaventura, D. F., Kim, D. Y., Thakurdin, C., Gonzalez, K. C., & Emerson, M. M. (2020). OTX2 represses sister cell fate choices in the developing retina to promote photoreceptor specification. *ELife*, *9*. doi:10.7554/eLife.54279

Goldman, D. (2014). Müller glial cell reprogramming and retina regeneration. *Nature Reviews. Neuroscience*, *15*(7), 431–442.

Gordân, R., Narlikar, L., & Hartemink, A. J. (2010). Finding regulatory DNA motifs using alignment-free evolutionary conservation information. *Nucleic Acids Research*, *38*(6), e90.

Graw, J. (2010). Chapter Ten - Eye Development. In P. Koopman (Ed.), *Current Topics in Developmental Biology* (Vol. 90, pp. 343–386). Academic Press.

Gu, Y.-N., Lee, E.-S., & Jeon, C.-J. (2016). Types and density of calbindin D28k-immunoreactive ganglion cells in mouse retina. *Experimental Eye Research*, *145*, 327–336.

Heavner, W., & Pevny, L. (2012). Eye development and retinogenesis. *Cold Spring Harbor Perspectives in Biology*, *4*(12). doi:10.1101/cshperspect.a008391

Hennig, A. K., Peng, G.-H., & Chen, S. (2008). Regulation of photoreceptor gene expression by Crx-associated transcription factor network. *Brain Research*, *1192*, 114–133.

Hojo, M., Ohtsuka, T., Hashimoto, N., Gradwohl, G., Guillemot, F., & Kageyama, R. (2000). Glial cell fate specification modulated by the bHLH gene Hes5 in mouse retina. *Development* , *127*(12), 2515–2522.

Horsford, D. J., Nguyen, M.-T. T., Sellar, G. C., Kothary, R., Arnheiter, H., & McInnes, R. R. (2005). Chx10 repression of Mitf is required for the maintenance of mammalian neuroretinal identity. *Development* , *132*(1), 177–187.

Hufnagel, R. B., & Brown, N. L. (2013). Chapter 27 - Specification of Retinal Cell Types. In J. L. R. Rubenstein & P. Rakic (Eds.), *Patterning and Cell Type Specification in the Developing CNS and PNS* (pp. 519–536). Oxford: Academic Press.

Inoue, T., Hojo, M., Bessho, Y., Tano, Y., Lee, J. E., & Kageyama, R. (2002). Math3 and NeuroD regulate amacrine cell fate specification in the retina. *Development* , *129*(4), 831–842.

Ip, C. K., Fossat, N., Jones, V., Lamonerie, T., & Tam, P. P. L. (2014). Head formation: OTX2 regulates Dkk1 and Lhx1 activity in the anterior mesendoderm. *Development* , *141*(20), 3859–3867.

Jadhav, A. P., Mason, H. A., & Cepko, C. L. (2006). Notch 1 inhibits photoreceptor production in the developing mammalian retina. *Development* , *133*(5), 913–923.

Javed, A., & Cayouette, M. (2017). Temporal Progression of Retinal Progenitor Cell Identity: Implications in Cell Replacement Therapies. *Frontiers in Neural Circuits*, *11*, 105.

Jiang, Y., Ding, Q., Xie, X., Libby, R. T., Lefebvre, V., & Gan, L. (2013). Transcription factors SOX4 and SOX11 function redundantly to regulate the development of mouse retinal ganglion cells. *The Journal of Biological Chemistry*, *288*(25), 18429–18438.

Jin, K., Jiang, H., Xiao, D., Zou, M., Zhu, J., & Xiang, M. (2015). Tfap2a and 2b act downstream of Ptf1a to promote amacrine cell differentiation during retinogenesis. *Molecular Brain*, *8*, 28.

Katoh, K., Omori, Y., Onishi, A., Sato, S., Kondo, M., & Furukawa, T. (2010). Blimp1 suppresses Chx10 expression in differentiating retinal photoreceptor precursors to ensure

proper photoreceptor development. *The Journal of Neuroscience: The Official Journal of the Society for Neuroscience*, *30*(19), 6515–6526.

Kheradpour, P., Stark, A., Roy, S., & Kellis, M. (2007). Reliable prediction of regulator targets using 12 Drosophila genomes. *Genome Research*, *17*(12), 1919–1931.

Kimura-Yoshida, C., Nakano, H., Okamura, D., Nakao, K., Yonemura, S., Belo, J. A., … Matsuo, I. (2005). Canonical Wnt signaling and its antagonist regulate anterior-posterior axis polarization by guiding cell migration in mouse visceral endoderm. *Developmental Cell*, *9*(5), 639–650.

Klimova, L., Antosova, B., Kuzelova, A., Strnad, H., & Kozmik, Z. (2015). Onecut1 and Onecut2 transcription factors operate downstream of Pax6 to regulate horizontal cell development. *Developmental Biology*, *402*(1), 48–60.

Koike, C., Nishida, A., Ueno, S., Saito, H., Sanuki, R., Sato, S., … Furukawa, T. (2007). Functional roles of Otx2 transcription factor in postnatal mouse retinal development. *Molecular and Cellular Biology*, *27*(23), 8318–8329.

Lamba, P., Khivansara, V., D'Alessio, A. C., Santos, M. M., & Bernard, D. J. (2008). Paired-like homeodomain transcription factors 1 and 2 regulate follicle-stimulating hormone beta-subunit transcription through a conserved cis-element. *Endocrinology*, *149*(6), 3095–3108.

Li, S., Mo, Z., Yang, X., Price, S. M., Shen, M. M., & Xiang, M. (2004). Foxn4 controls the genesis of amacrine and horizontal cells by retinal progenitors. *Neuron*, *43*(6), 795–807.

Liu, H., Etter, P., Hayes, S., Jones, I., Nelson, B., Hartman, B., … Reh, T. A. (2008). NeuroD1 regulates expression of thyroid hormone receptor 2 and cone opsins in the developing mouse retina. *The Journal of Neuroscience: The Official Journal of the Society for Neuroscience*, *28*(3), 749–756.

Liu, I. S., Chen, J. D., Ploder, L., Vidgen, D., van der Kooy, D., Kalnins, V. I., & McInnes, R. R. (1994). Developmental expression of a novel murine homeobox gene (Chx10): evidence for roles in determination of the neuroretina and inner nuclear layer. *Neuron*, *13*(2), 377–393.

Liu, J. K., Ghattas, I., Liu, S., Chen, S., & Rubenstein, J. L. (1997). Dlx genes encode DNA-binding proteins that are expressed in an overlapping and sequential pattern during basal

ganglia differentiation. *Developmental Dynamics: An Official Publication of the American Association of Anatomists*, *210*(4), 498–512.

Liu, S., Liu, X., Li, S., Huang, X., Qian, H., Jin, K., & Xiang, M. (2020). Foxn4 is a temporal identity factor conferring mid/late-early retinal competence and involved in retinal synaptogenesis. *Proceedings of the National Academy of Sciences of the United States of America*, *117*(9), 5016–5027.

Mark, M., Rijli, F. M., & Chambon, P. (1997). Homeobox genes in embryogenesis and pathogenesis. *Pediatric Research*, *42*(4), 421–429.

Markitantova, Y., & Simirskii, V. (2020). Inherited Eye Diseases with Retinal Manifestations through the Eyes of Homeobox Genes. *International Journal of Molecular Sciences*, *21*(5). doi:10.3390/ijms21051602

Marquardt, T., Ashery-Padan, R., Andrejewski, N., Scardigli, R., Guillemot, F., & Gruss, P. (2001). Pax6 is required for the multipotent state of retinal progenitor cells. *Cell*, *105*(1), 43–55.

Martinez-Morales, J. R., Signore, M., Acampora, D., Simeone, A., & Bovolenta, P. (2001). Otx genes are required for tissue specification in the developing eye. *Development* , *128*(11), 2019–2030.

Matsuo, I., Kuratani, S., Kimura, C., Takeda, N., & Aizawa, S. (1995). Mouse Otx2 functions in the formation and patterning of rostral head. *Genes & Development*, *9*(21), 2646–2658.

Mears, A. J., Kondo, M., Swain, P. K., Takada, Y., Bush, R. A., Saunders, T. L., … Swaroop, A. (2001). Nrl is required for rod photoreceptor development. *Nature Genetics*, *29*(4), 447–452.

Merlo, G. R., Zerega, B., Paleari, L., Trombino, S., Mantero, S., & Levi, G. (2000). Multiple functions of Dlx genes. *The International Journal of Developmental Biology*, *44*(6), 619–626.

Mukhopadhyay, A., Deplancke, B., Walhout, A. J. M., & Tissenbaum, H. A. (2008). Chromatin immunoprecipitation (ChIP) coupled to detection by quantitative real-time PCR to study transcription factor binding to DNA in Caenorhabditis elegans. *Nature Protocols*, *3*(4), 698–709.

Muranishi, Y., Terada, K., Inoue, T., Katoh, K., Tsujii, T., Sanuki, R., … Furukawa, T. (2011). An essential role for RAX homeoprotein and NOTCH-HES signaling in Otx2 expression in embryonic retinal photoreceptor cell fate determination. *The Journal of Neuroscience: The Official Journal of the Society for Neuroscience*, *31*(46), 16792–16807.

Muto, A., Iida, A., Satoh, S., & Watanabe, S. (2009). The group E Sox genes Sox8 and Sox9 are regulated by Notch signaling and are required for Müller glial cell development in mouse retina. *Experimental Eye Research*, *89*(4), 549–558.

Nayak, A., Glöckner-Pagel, J., Vaeth, M., Schumann, J. E., Buttmann, M., Bopp, T., … Berberich-Siebelt, F. (2009). Sumoylation of the transcription factor NFATc1 leads to its subnuclear relocalization and interleukin-2 repression by histone deacetylase. *The Journal of Biological Chemistry*, *284*(16), 10935–10946.

Neitz, M., & Neitz, J. (2001). The uncommon retina of the common house mouse. *Trends in Neurosciences*, *24*(5), 248–250.

Nishida, A., Furukawa, A., Koike, C., Tano, Y., Aizawa, S., Matsuo, I., & Furukawa, T. (2003). Otx2 homeobox gene controls retinal photoreceptor cell fate and pineal gland development. *Nature Neuroscience*, *6*(12), 1255–1263.

Nishihara, D., Yajima, I., Tabata, H., Nakai, M., Tsukiji, N., Katahira, T., … Yamamoto, H. (2012). Otx2 is involved in the regional specification of the developing retinal pigment epithelium by preventing the expression of sox2 and fgf8, factors that induce neural retina differentiation. *PloS One*, *7*(11), e48879.

Nitta, K. R., Jolma, A., Yin, Y., Morgunova, E., Kivioja, T., Akhtar, J., … Taipale, J. (2015). Conservation of transcription factor binding specificities across 600 million years of bilateria evolution. *ELife*, *4*. doi:10.7554/eLife.04837

Ohsawa, R., & Kageyama, R. (2008). Regulation of retinal cell fate specification by multiple transcription factors. *Brain Research*, *1192*, 90–98.

Omori, Y., Katoh, K., Sato, S., Muranishi, Y., Chaya, T., Onishi, A., … Furukawa, T. (2011). Analysis of transcriptional regulatory pathways of photoreceptor genes by expression profiling of the Otx2-deficient retina. *PloS One*, *6*(5), e19685.

Oron-Karni, V., Farhy, C., Elgart, M., Marquardt, T., Remizova, L., Yaron, O., … Ashery-Padan, R. (2008). Dual requirement for Pax6 in retinal progenitor cells. *Development* , *135*(24), 4037–4047.

Ozawa, Y., Nakao, K., Kurihara, T., Shimazaki, T., Shimmura, S., Ishida, S., … Okano, H. (2008). Roles of STAT3/SOCS3 pathway in regulating the visual function and ubiquitin-proteasome-dependent degradation of rhodopsin during retinal inflammation. *The Journal of Biological Chemistry*, *283*(36), 24561–24570.

Panganiban, G., & Rubenstein, J. L. R. (2002). Developmental functions of the Distal-less/Dlx homeobox genes. *Development* , *129*(19), 4371–4386.

Parras, C. M., Hunt, C., Sugimori, M., Nakafuku, M., Rowitch, D., & Guillemot, F. (2007). The proneural gene Mash1 specifies an early population of telencephalic oligodendrocytes. *The Journal of Neuroscience: The Official Journal of the Society for Neuroscience*, *27*(16), 4233–4242.

Peng, G.-H., & Chen, S. (2005). Chromatin immunoprecipitation identifies photoreceptor transcription factor targets in mouse models of retinal degeneration: new findings and challenges. *Visual Neuroscience*, *22*(5), 575–586.

Pensieri, P. (2019). *Role of Otx2 in mature retinal photoreceptors*. COMUE Université Côte d'Azur.

Petryniak, M. A., Potter, G. B., Rowitch, D. H., & Rubenstein, J. L. R. (2007). Dlx1 and Dlx2 control neuronal versus oligodendroglial cell fate acquisition in the developing forebrain. *Neuron*, *55*(3), 417–433.

Pinto, V. I. (2010). *DLX HOMEOBOX TRANSCRIPTIONAL REGULATION OF CRX AND OTX2 GENE EXPRESSION DURING VERTEBRATE RETINAL DEVELOPMENT* (Master of Science; D. Eisenstat, Ed.). University of Manitoba.

Poché, R. A., Kwan, K. M., Raven, M. A., Furuta, Y., Reese, B. E., & Behringer, R. R. (2007). Lim1 is essential for the correct laminar positioning of retinal horizontal cells. *The Journal of Neuroscience: The Official Journal of the Society for Neuroscience*, *27*(51), 14099–14107.

Ragge, N. K., Brown, A. G., Poloschek, C. M., Lorenz, B., Henderson, R. A., Clarke, M. P., … Hanson, I. M. (2005). Heterozygous mutations of OTX2 cause severe ocular malformations. *American Journal of Human Genetics*, *76*(6), 1008–1022.

Raymond, S. M., & Jackson, I. J. (1995). The retinal pigmented epithelium is required for development and maintenance of the mouse neural retina. *Current Biology: CB*, *5*(11), 1286–1295.

Roberts, M. R., Hendrickson, A., McGuire, C. R., & Reh, T. A. (2005). Retinoid X receptor (gamma) is necessary to establish the S-opsin gradient in cone photoreceptors of the developing mouse retina. *Investigative Ophthalmology & Visual Science*, *46*(8), 2897–2904.

Sakai, A., Nakato, R., Ling, Y., Hou, X., Hara, N., Iijima, T., … Sugiyama, S. (2017). Genome-Wide Target Analyses of Otx2 Homeoprotein in Postnatal Cortex. *Frontiers in Neuroscience*, *11*, 307.

Sampath, A. P., Strissel, K. J., Elias, R., Arshavsky, V. Y., McGinnis, J. F., Chen, J., … Hurley, J. B. (2005). Recoverin improves rod-mediated vision by enhancing signal transmission in the mouse retina. *Neuron*, *46*(3), 413–420.

Samuel, A., Housset, M., Fant, B., & Lamonerie, T. (2014). Otx2 ChIP-seq reveals unique and redundant functions in the mature mouse retina. *PloS One*, *9*(2), e89110.

Sato, S., Inoue, T., Terada, K., Matsuo, I., Aizawa, S., Tano, Y., … Furukawa, T. (2007). Dkk3-Cre BAC transgenic mouse line: a tool for highly efficient gene deletion in retinal progenitor cells. *Genesis* , *45*(8), 502–507.

Saxena, M., Roman, A. K. S., O'Neill, N. K., Sulahian, R., Jadhav, U., & Shivdasani, R. A. (2017). Transcription factor-dependent "anti-repressive" mammalian enhancers exclude H3K27me3 from extended genomic domains. *Genes & Development*, *31*(23–24), 2391–2404.

Smale, S. T. (2011). Hierarchies of NF-κB target-gene regulation. *Nature Immunology*, *12*(8), 689–694.

Swaroop, A., Kim, D., & Forrest, D. (2010). Transcriptional regulation of photoreceptor development and homeostasis in the mammalian retina. *Nature Reviews. Neuroscience*, *11*(8), 563–576.

Szatko, K. P., Korympidou, M. M., Ran, Y., Berens, P., Dalkara, D., Schubert, T., … Franke, K. (2020). Neural circuits in the mouse retina support color vision in the upper visual field. *Nature Communications*, *11*(1), 3481.

Tomita, K., Moriyoshi, K., Nakanishi, S., Guillemot, F., & Kageyama, R. (2000). Mammalian achaete-scute and atonal homologs regulate neuronal versus glial fate determination in the central nervous system. *The EMBO Journal*, *19*(20), 5460–5472.

Torero Ibad, R., Rheey, J., Mrejen, S., Forster, V., Picaud, S., Prochiantz, A., & Moya, K. L. (2011). Otx2 promotes the survival of damaged adult retinal ganglion cells and protects against excitotoxic loss of visual acuity in vivo. *The Journal of Neuroscience: The Official Journal of the Society for Neuroscience*, *31*(14), 5495–5503.

Torres, M., Gómez-Pardo, E., & Gruss, P. (1996). Pax2 contributes to inner ear patterning and optic nerve trajectory. *Development* , *122*(11), 3381–3391.

Vinckevicius, A., & Chakravarti, D. (2012). Chromatin immunoprecipitation: advancing analysis of nuclear hormone signaling. *Journal of Molecular Endocrinology*, *49*(2), R113-23.

Wang, S., Sengel, C., Emerson, M. M., & Cepko, C. L. (2014). A gene regulatory network controls the binary fate decision of rod and bipolar cells in the vertebrate retina. *Developmental Cell*, *30*(5), 513–527.

Wu, F., Li, R., Umino, Y., Kaczynski, T. J., Sapkota, D., Li, S., … Mu, X. (2013). Onecut1 Is Essential for Horizontal Cell Genesis and Retinal Integrity. *The Journal of Neuroscience: The Official Journal of the Society for Neuroscience*, *33*(32), 13053–13065.

Wu, S., Chang, K.-C., & Goldberg, J. L. (2018). Retinal Cell Fate Specification. *Trends in Neurosciences*, *41*(4), 165–167.

Xiang, M. (2013). Intrinsic control of mammalian retinogenesis. *Cellular and Molecular Life Sciences: CMLS*, *70*(14), 2519–2532.

Yamamoto, H., Kon, T., Omori, Y., & Furukawa, T. (2020). Functional and Evolutionary Diversification of Otx2 and Crx in Vertebrate Retinal Photoreceptor and Bipolar Cell Development. *Cell Reports*, *30*(3), 658-671.e5.

Yang, X.-J. (2004). Roles of cell-extrinsic growth factors in vertebrate eye pattern formation and retinogenesis. *Seminars in Cell & Developmental Biology*, *15*(1), 91–103.

Yoshida, S., Mears, A. J., Friedman, J. S., Carter, T., He, S., Oh, E., … Swaroop, A. (2004). Expression profiling of the developing and mature Nrl-/- mouse retina: identification of retinal disease candidates and transcriptional regulatory targets of Nrl. *Human Molecular Genetics*, *13*(14), 1487–1503.

Zagozewski, Jamie L., Zhang, Q., Pinto, V. I., Wigle, J. T., & Eisenstat, D. D. (2014). The role of homeobox genes in retinal development and disease. *Developmental Biology*, *393*(2), 195–208.

Zagozewski, Jamie Lauren. (2017). *Genetic Regulation of Vertebrate Retinal Development* (Doctor of Philosophy; D. Eisenstat, Ed.). University of Alberta.

Zanotti, S., Smerdel-Ramoya, A., & Canalis, E. (2011). Reciprocal Regulation of Notch and Nuclear Factor of Activated T-cells (NFAT) c1 Transactivation in Osteoblasts*. *The Journal of Biological Chemistry*, *286*(6), 4576–4588.

Zhang, Q., Zagozewski, J., Cheng, S., Dixit, R., Zhang, S., de Melo, J., … Eisenstat, D. D. (2017). Regulation of Brn3b by DLX1 and DLX2 is required for retinal ganglion cell differentiation in the vertebrate retina. *Development* , *144*(9), 1698–1711.

Zhou, Q.-P., Le, T. N., Qiu, X., Spencer, V., de Melo, J., Du, G., … Eisenstat, D. D. (2004). Identification of a direct Dlx homeodomain target in the developing mouse forebrain and retina by optimization of chromatin immunoprecipitation. *Nucleic Acids Research*, *32*(3), 884–892.

Zuber, M. E., Gestri, G., Viczian, A. S., Barsacchi, G., & Harris, W. A. (2003). Specification of the vertebrate eye by a network of eye field transcription factors. *Development* , *130*(21), 5155–5167.

Appendix

Characterizing the *Nrp2* Single Knockout Mouse Eye Phenotype as a Model for Persistent Fetal Vasculature

7.1 Rationale for gene expression studies and results

Given the importance of *Neuropilins* in angiogenesis and RGC axon migration, we proposed that *Nrp2* is involved in the developing neural retinal and embryonic retinal vasculature. We have observed that *Nrp2* mutation leads to morphological changes in the mouse eye such as microphthalmia, development of cataracts, and retinal folding at postnatal day 7 and day 28. Furthermore, functional tests, such as Optical Coherence Tomography (OCT) and electroretinography (ERG) carried out in our lab and in collaboration with other investigators demonstrate aberration in retinal cell layers and inner retinal malfunction (Hejazi et al, in preparation). Given that *Nrp2* mutation leads to these severe phenotypic changes in the mouse eye, we hypothesized that it would affect the expression of key retinal genes. To characterize gene expression level changes of various retinal cell type markers between the wildtype and *Nrp2* single knockout mouse retina, real-time PCR (qRT-PCR) was conducted in wildtype and *Nrp2* SKO dissected retina tissues at two postnatal timepoints, P7 and P28. Genes representing each retina layer as well as vasculature and neuronal cells were investigated. Specifically, *Syntaxin* (*Stx1*), *Calbindin*, *Prox1*, *Recoverin*, *Rhodopsin*, *M-opsin*, *S-opsin* (cones), *Vsx2/Chx10*, *Brn3a*, and *Brn3b* expression levels were compared relative to internal control *36b4* (a ribosomal phosphoprotein) using the ΔΔCt method.

Brn3a and *Brn3b* demarcate ganglion cell layer (GCL) and are markers of retinal ganglion cells. *Syntaxin* demarcates the inner plexiform layer (IPL) and is a marker of amacrine cells. *Recoverin* demarcates the outer plexiform layer (OPL) and the outer nuclear layer (ONL) and is a marker of bipolar cells. *Prox1* and *Calbindin* are markers of amacrine and horizontal cells. *Chx10/Vsx2* is a marker of bipolar cells. *Rhodopsin* is a marker of rod photoreceptors. *M*

Opsins and *S Opsins* are markers of cone photoreceptors. Ribosomal phosphoprotein (*36b4*) was used as an internal control.

At P7, all retinal genes tested were increased in the *Nrp2* KO mouse retina; however, only *Calbindin*, *Recoverin*, *S-opsin* and *Vsx2* (*Chx10*) were increased greatly but not significantly (**Figure 7.1 upper panel**). At P28, it was interesting to observe that the expression of these retinal genes investigated downregulated slightly but not significantly in the mutant retina when compared to the wildtype (**Figure 7.1 lower panel**).

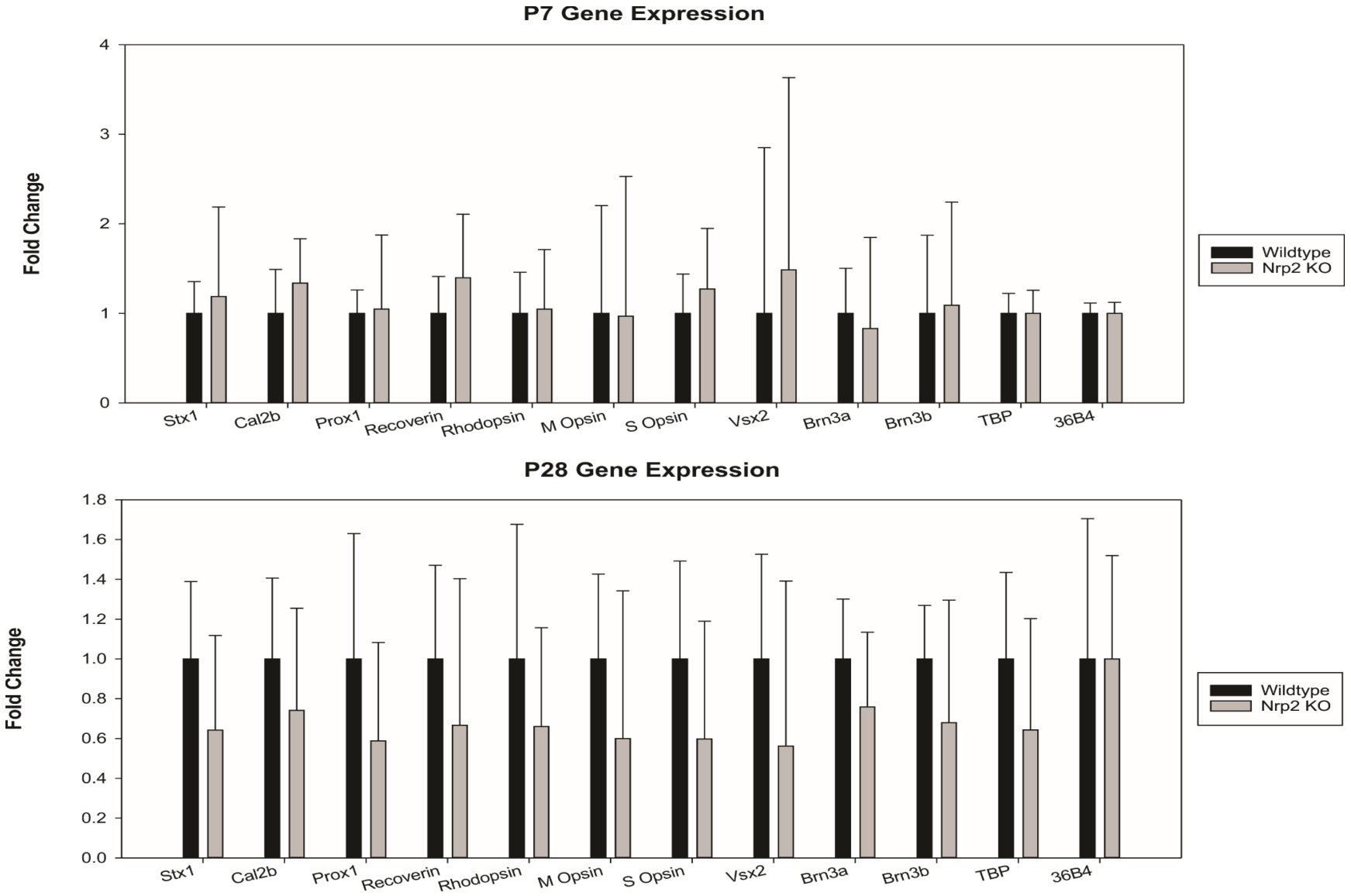
P7 Gene Expression
Fold Change
4
3
2
1
0
Stx1
Cal2b
Prox1
Recoverin
Rhodopsin
M Opsin
S Opsin
Vsx2
Brn3a
Brn3b
TBP
36B4
Wildtype
Nrp2 KO
P28 Gene Expression
Fold Change
1.8
1.6
1.4
1.2
1.0
0.8
0.6
0.4
0.2
0.0
Stx1
Cal2b
Prox1
Recoverin
Rhodopsin
M Opsin
S Opsin
Vsx2
Brn3a
Brn3b
TBP
36B4
Wildtype
Nrp2 KO

Figure 7.1

Gene expression fold changes of vasculature and neural retina cell type genes in Nrp2 single knockout mouse retina compared to the wildtype at time points P7 and P28

The transcript expression level of markers of the neural retina layers, retinal cell types and vasculature was quantified at P7 and P28 in the wildtype and *Nrp2* knockout mouse retinal tissues. Fold changes were calculated using the ΔΔCt method using reference gene expression level *36b4*. At P7, increase was observed for *Calbindin* (*Cal2b*), *Recoverin*, *S-Opsin* (A) and *Vsx2(Chx10)*, although it was not statistically significant. At P28, retina neuronal marker expressions were quantified, and fold changes were calculated in a similar fashion, and the expression level was decreased slightly, although it was not statistically significant.

Stx1 (amacrine, IPL), *Cal2b* (ganglion/horizontal), *Prox1* (horizontal), *Recoverin* (bipolar, OPL and ONL), *Rhodopsin* (rod photoreceptors), *M-opsin* (cone photoreceptors), *S-opsin* (cone photoreceptors), *Vsx2/Chx10* (bipolar), *Brn3a* (RGC, GCL), *Brn3b* (RGC, GCL) expression levels were compared relative to internal control *36b4* (ribosomal phosphoprotein).

4 biological replicates were conducted at P7. 5 biological replicates were conducted at P28. Paired Student's t-test, $p<0.05$, were conducted.

7.2 Discussion

Figure 7.1 (upper panel) revealed that *Calbindin 2*, *Recoverin*, *S Opsin* and *Vsx2* (*Chx10*) have increased expression in the *Nrp2* mutant compared to wildtype at P7 (not statistically significant). However, at P28, all genes examined decreased their expression slightly in the mutant compared to the wildtype (**Figure 7.1 lower panel**). *Calbindin 2* is expressed in horizontal cells and retinal ganglion cells to regulate presynaptic cytosolic calcium ion concentration (Gu, Lee, & Jeon, 2016). *Recoverin* is expressed in rod photoreceptors and plays

an important role in calcium signaling during retinal phototransduction (Sampath et al., 2005). *Recoverin* improves rod-driven vision by enhancing signal transmission in the retina (Sampath et al., 2005). *S-Opsin* in mice is sensitive to UV-light and these UV-sensitive *S opsins* make a major contribution to the electrical response generated during ERG (Neitz & Neitz, 2001). *Vsx2* (*Chx10*) is a major bipolar cell gene. Functionally, in the *Nrp2* null mouse retina, ERG data indicate that for both scotopic (rod-driven) and photopic (cone-driven) responses, there seems to be earlier hyperpolarization of the photoreceptors from the outer retina layer (measured by the a-wave). There also seems to be decreased amplitude of depolarization response of the post-synaptic bipolar cells in both the photopic and scotopic responses (measured by the b wave), which measures response of cone bipolar cells.

Taken together, these data support that the *Nrp2* mutation may affect both dark-adapted (scotopic, mediated mostly by rods) and light adapted (photopic, mediated mostly by cones) vision such that several genes of photoreceptors and bipolar cells as well as genes involved in the synaptic connection of the retinal neurons are aberrantly expressed in the mutant. These results suggest that the loss of *Nrp2* leads to alterations during development, which likely affects postnatal eye development and vision in *Nrp2* KO mice. . It also suggests changes to hyaloid vasculature during embryonic stages may affect retina patterning and development postnatally. Hence, these genes may upregulate their expression to compensate and possibly correct for such vision impairment at an early age